

PREPARED FOR SUBMISSION TO JHEP

Polarized fragmenting jet functions in Inclusive and Exclusive Jet Production

Zhong-Bo Kang^{a,b,c}, Hongxi Xing^{d,e,f}, Fanyi Zhao^g and Yiyu Zhou^{d,e,a}

^a*Department of Physics and Astronomy, University of California, Los Angeles, California 90095, USA*

^b*Mani L. Bhaumik Institute for Theoretical Physics, University of California, Los Angeles, California 90095, USA*

^c*Center for Frontiers in Nuclear Science, Stony Brook University, Stony Brook, New York 11794, USA*

^d*Key Laboratory of Atomic and Subatomic Structure and Quantum Control (MOE), Guangdong Basic Research Center of Excellence for Structure and Fundamental Interactions of Matter, Institute of Quantum Matter, South China Normal University, Guangzhou 510006, China*

^e*Guangdong-Hong Kong Joint Laboratory of Quantum Matter, Guangdong Provincial Key Laboratory of Nuclear Science, Southern Nuclear Science Computing Center, South China Normal University, Guangzhou 510006, China*

^f*Southern Center for Nuclear-Science Theory (SCNT), Institute of Modern Physics, Chinese Academy of Sciences, Huizhou 516000, China*

^g*Center for Theoretical Physics, Massachusetts Institute of Technology, Cambridge, MA 02139, USA*

E-mail: zkang@ucla.edu, hxing@m.scnu.edu.cn, fanyi@mit.edu, zyiyu@m.scnu.edu.cn

ABSTRACT: In this work, we present a complete theoretical framework for analyzing the distribution of polarized hadrons within jets, with and without measuring the transverse momentum relative to the standard jet axis. Using soft-collinear effective theory (SCET), we derive the factorization and provide the theoretical calculation of both semi-inclusive and exclusive fragmenting jet functions (FJFs) under longitudinal and transverse polarization. With the polarized FJFs, one gains access to a variety of new observables that can be used for extracting both collinear and transverse momentum dependent parton distribution functions (PDFs) and fragmentation functions (FFs). As examples, we provide numerical results for the spin asymmetry $A_{TU,T}^{\cos(\phi_S - \hat{\phi}_{S_h})}$ from polarized semi-inclusive hadron-in-jet production in polarized pp collisions at RHIC kinematics, where a transversely polarized quark would lead to the transverse spin of the final-state hadron inside the jet and is thus sensitive to the transversity fragmentation functions. Similarly, another spin asymmetry, $A_{TU,L}^{\cos(\phi_q - \phi_S)}$ from polarized exclusive hadron-in-jet production in polarized ep collisions at EIC kinematics would allow us to access the helicity fragmentation functions. These observables demonstrate promising potential in investigating transverse momentum dependent PDFs and FFs and are worthwhile for further measurements.

Contents

1	Introduction	1
2	The collinear fragmenting jet functions (FJFs)	3
2.1	Collinear FJFs in semi-inclusive jet productions	3
2.1.1	NLO calculation	5
2.1.2	Renormalization and matching onto collinear FFs	9
2.2	Collinear FJFs in exclusive jet productions	11
3	The transverse momentum dependent FJFs (TMD FJFs)	14
3.1	TMD FJFs in semi-inclusive jet productions	14
3.1.1	TMD Factorization	16
3.1.2	Hard matching functions	21
3.2	TMD FJFs in exclusive jet production	24
4	Phenomenology	25
4.1	Transverse spin transfer to Λ in jet in polarized pp collisions	26
4.2	Back-to-back electron-jet production with longitudinally polarized Λ in jet	31
5	Conclusion	34
A	Perturbative NLO semi-inclusive FJFs	35
B	Calculation of collinear exclusive FJFs	36
C	Separation of hard matching functions	41

1 Introduction

Jet substructure, originally developed to exploit the flow of energy within jets of particles at the Large Hadron Collider (LHC) to enhance new physics searches [1], has since emerged as a primary tool for studying Quantum Chromodynamics (QCD). Not only has jet substructure been vastly studied in ongoing experiments at the Relativistic Heavy Ion Collider (RHIC) and the LHC [2–7], but also in future facilities such as the Electron-Ion Collider (EIC) [8, 9]. For example, at the LHC, the jet substructure has been successfully used to tag the origin of jets in precision measurements and searches for new physics. At both the RHIC and the LHC, the jet substructure has been an important tool for studying the properties of the hot and dense quark-gluon plasma. On the other hand, at the EIC, as a good proxy of

parton-level dynamics, jet allows for a clean factorization between the target and current-fragmentation regions, which is generally difficult in hadron productions [10–12] in deep inelastic scatterings (DIS).

Most recently, one particular set of jet substructure observables, the distribution of hadrons inside the jet, has received a lot of attention [13–19]. Studying hadron distribution inside the jet enables us to pinpoint fragmentation functions of various kinds and to explore the elusive hadronization process. They are complementary to the more standard processes, such as semi-inclusive hadron production in deep inelastic scattering and hadron production in e^+e^- collisions, and allow us to study QCD factorization and to test the universality properties of the associated fragmentation functions in different processes [20]. For example, one can measure the distribution of hadrons inside the jet as a function of the hadron momentum fraction z_h , where z_h is the ratio of the transverse momentum of the hadron (p_{hT}) to that of the jet (p_{JT}), both relative to the beam axis. Such a z_h dependence can be used for extracting the z_h -dependence of the collinear fragmentation functions (FFs) [21, 22]. On the other hand, if one measures both z_h and the transverse momentum \mathbf{j}_\perp distribution of the hadrons with respect to the jet axis, one would be able to study the transverse momentum-dependent fragmentation functions (TMD FFs) [23].

The theoretical object which describes the momentum distribution of hadrons inside a fully reconstructed jet is called fragmenting jet functions (FJFs). For the z_h -dependence while integrating over the hadron’s transverse momentum with respect to the jet axis, we would have collinear FJFs, which can be matched onto the standard collinear FFs. These collinear FJFs have been studied in the so-called semi-inclusive jet production, as well as the exclusive jet production. For semi-inclusive jet production, one measures the signal jet while completely inclusive on other particles in the final state, see the studies in *e.g.*, [21, 24–29]. On the other hand, in the context being discussed, “exclusive” jet production refers to situations where a fixed number of jets are produced in the final state but one vetoes additional jets. For example, in the back-to-back electron-jet production in electron-proton collisions, our factorization would depend on the exclusive FJFs, where we have an electron and a single signal jet in the final state. See the studies along this line [30–34]. On the other hand, measuring both z_h and \mathbf{j}_\perp distribution of the hadrons with respect to the standard jet axis would give us the transverse momentum dependent fragmenting jet functions (TMD FJFs). There are close relationships [23, 27, 35–37] between these TMD FJFs and the standard TMD FFs [38–40]. More recently, studies have been advanced to the polarized sector, including the polarization of both the parton initiating the jet and the hadron produced within the jet [34, 41–43]. For a recent study exploring dihadron fragmentation functions (or two hadrons) inside the jet, see [44, 45]. For the TMD study of the hadron with respect to the Winner-Take-All jet axis, see [37, 46–48]. As for the TMD study inside the groomed jet, see [36, 49, 50]. More recently, exploring the connections between TMD physics and the energy-energy correlators has seen a lot of progress [51–53].

For the polarized collinear FJFs and TMD FJFs, we have performed studies in previous publications, mainly in [34, 41] for semi-inclusive and exclusive jet productions. Even though we provided theoretical formalism and illustrated some phenomenological studies there, for the computations of FJFs, only partial results were available in those previous

publications, but not the complete full results. This is the goal of our current paper. We will perform all the relevant computations and give all associated matching coefficients that allow us to connect these FJFs to the standard FFs. In doing so, we also update our formalism using the more recent approach outlined in the TMD Handbook [13]. We provide additional phenomenological studies at the RHIC and the future EIC.

The rest of the paper is organized as follows: In Section 2, we establish the theoretical foundation for collinear FJFs, elucidate a number of correlations between the polarization of the hadrons and fragmenting partons, and illuminate their physical significance and connections to standard fragmentation functions. In Section 3, we introduce the semi-inclusive and exclusive TMD FJFs. We discuss their factorization and evolution properties, as well as their relations to the standard TMD FFs. In Section 4, we employ this framework to predict the spin asymmetry $A_{TU,T}^{\cos(\phi_S-\hat{\phi}_{S_h})}$ for the semi-inclusive production of transversely polarized Λ baryons inside jet in transversely polarized pp collisions at RHIC kinematics, and $A_{TU,L}^{\cos(\phi_q-\phi_S)}$ for the exclusive production of longitudinally polarized $\Lambda/\bar{\Lambda}$ inside jet in polarized ep collisions at EIC kinematics. Finally, we provide a summary of our findings in Section 5. We collect a few additional details in the Appendix.

2 The collinear fragmenting jet functions (FJFs)

In this section, we introduce the definition of the semi-inclusive and exclusive fragmenting jet functions (FJFs) in soft-collinear effective theory (SCET) [54–58] with both unpolarized and polarized fragmenting hadron. Such FJFs are used to describe the longitudinal momentum fraction distribution of hadrons within jets. We first provide the operator definitions of FJFs, then perform the calculation to NLO, and lastly derive and solve the RG evolution equations.

2.1 Collinear FJFs in semi-inclusive jet productions

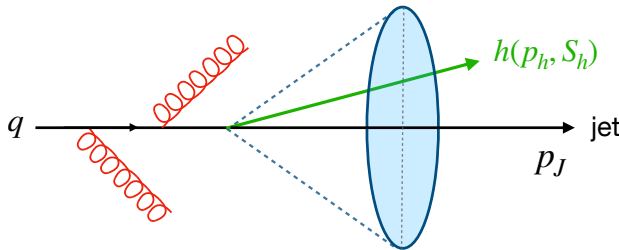


Figure 1: Illustration for the distribution of hadrons h inside a jet that is initiated by a parton q . The hadron has a momentum p_h and spin S_h , while the jet has a momentum p_J .

We can construct the semi-inclusive fragmenting quark and gluon jet functions using the corresponding gauge invariant quark and gluon fields in SCET which are given by:

$$\chi_n = W_n^\dagger \xi_n, \quad \mathcal{B}_{n\perp}^\mu = \frac{1}{g} [W_n^\dagger i D_{n\perp}^\mu W_n], \quad (2.1)$$

where the subscript n indicates that the field is along the n -collinear direction, and $n^\mu = (1, 0, 0, 1)$ is the light-cone vector whose spatial component is aligned with the jet axis. In Eq. (2.1), the covariant derivative is $iD_{n\perp}^\mu = \mathcal{P}_{n\perp}^\mu + gA_{n\perp}^\mu$, where \mathcal{P}^μ is the label momentum operator. Moreover, W_n is the Wilson line of collinear gluons:

$$W_n(x) = \sum_{\text{perms}} \exp\left(-g \frac{1}{\bar{n} \cdot \mathcal{P}} \bar{n} \cdot A_n(x)\right). \quad (2.2)$$

It is also useful to define the conjugate light-cone vector $\bar{n}^\mu = (1, 0, 0, -1)$, such that $n^2 = \bar{n}^2 = 0$ and $n \cdot \bar{n} = 2$. Thus, any four-vector p^μ can be decomposed as $p^\mu = [p^+, p^-, \mathbf{p}_\perp]^1$, where $p^+ = n \cdot p$ and $p^- = \bar{n} \cdot p$, namely:

$$p^\mu = p^- \frac{n^\mu}{2} + p^+ \frac{\bar{n}^\mu}{2} + p_\perp^\mu. \quad (2.3)$$

For a hadron in the reference frame where it has no transverse momentum and moves along the $+z$ -direction, it will have a large p_h^- component and a small p_h^+ component, *i.e.*, $p_h^+ \ll p_h^-$. Thus the momentum p_h and spin S_h of the hadron inside the jet can be parameterized as:

$$p_h = \left[\frac{M_h^2}{p_h^-}, p_h^-, \mathbf{0} \right], \quad S_h = \left[-\lambda_h \frac{M_h}{p_h^-}, \lambda_h \frac{p_h^-}{M_h}, \mathbf{S}_{h\perp} \right]. \quad (2.4)$$

Here λ_h is the helicity of the hadron with mass M_h , and $\mathbf{S}_{h\perp}$ is the transverse polarization of the hadron inside the jet.

Having these collinear quark and gluon fields readily available, we can formulate the correlator definitions for the quark and gluon semi-inclusive FJFs, each with different polarizations [21, 30, 32, 59]:

$$\mathcal{G}_q^h(z, z_h, p_T R, \mu) = \frac{z}{2N_c} \delta\left(z_h - \frac{\omega_h}{\omega_J}\right) \text{Tr} \left[\frac{\not{n}}{2} \langle 0 | \delta(\omega - \bar{n} \cdot \mathcal{P}) \chi_n(0) | (Jh) X \rangle \right. \\ \left. \times \langle (Jh) X | \bar{\chi}_n(0) | 0 \rangle \right], \quad (2.5)$$

$$\Delta \mathcal{G}_q^h(z, z_h, p_T R, \mu) = \frac{z}{2N_c} \delta\left(z_h - \frac{\omega_h}{\omega_J}\right) \text{Tr} \left[\frac{\not{n}}{2} \gamma_5 \langle 0 | \delta(\omega - \bar{n} \cdot \mathcal{P}) \chi_n(0) | (Jh) X \rangle \right. \\ \left. \times \langle (Jh) X | \bar{\chi}_n(0) | 0 \rangle \right], \quad (2.6)$$

$$\mathbf{S}_{h\perp}^i \Delta_T \mathcal{G}_q^h(z, z_h, p_T R, \mu) = \frac{z}{2N_c} \delta\left(z_h - \frac{\omega_h}{\omega_J}\right) \text{Tr} \left[\frac{\not{n}}{2} \gamma_1^i \gamma_5 \langle 0 | \delta(\omega - \bar{n} \cdot \mathcal{P}) \chi_n(0) | (Jh) X \rangle \right. \\ \left. \times \langle (Jh) X | \bar{\chi}_n(0) | 0 \rangle \right], \quad (2.7)$$

$$\mathcal{G}_g^h(z, z_h, p_T R, \mu) = -\frac{z\omega}{(d-2)(N_c^2-1)} \delta\left(z_h - \frac{\omega_h}{\omega_J}\right) \\ \times \langle 0 | \delta(\omega - \bar{n} \cdot \mathcal{P}) \mathcal{B}_{n\perp, \mu}(0) | (Jh) X \rangle \langle (Jh) X | \mathcal{B}_{n\perp}^\mu(0) | 0 \rangle, \quad (2.8)$$

$$\Delta \mathcal{G}_g^h(z, z_h, p_T R, \mu) = \frac{\epsilon^{\mu\nu\alpha\beta} \bar{n}_\alpha n_\beta}{2} \frac{z\omega}{(d-2)(N_c^2-1)} \delta\left(z_h - \frac{\omega_h}{\omega_J}\right)$$

¹We use square bracket for vectors written in light cone coordinates.

$$\times \langle 0 | \delta(\omega - \bar{n} \cdot \mathcal{P}) \mathcal{B}_{n\perp, \mu}(0) | (Jh)X \rangle \langle (Jh)X | \mathcal{B}_{n\perp, \nu}(0) | 0 \rangle, \quad (2.9)$$

where N_c is the number of colors for quarks and $(d-2)$ is the number of polarizations for gluons in d dimensional space-time. Note that we only consider massless quark flavors. For studies about heavy meson, see *e.g.*, Refs. [22, 49, 60, 61]. The state $| (Jh)X \rangle$ denotes the final state, encompassing both unobserved particles labeled as X , and the observed jet J containing an identified hadron h , which is collectively referred to as (Jh) . Additionally, ω represents the large light-cone component for the momentum of the quark or gluon initiating the jet, whereas $\omega_J = p_J^-$ and $\omega_h = p_h^-$ correspond respectively to the large light-cone component for the momentum of the jet itself and the identified hadron within the jet, as shown in Fig. 1. In our convention and the perturbative calculations performed below, we choose a frame where the jet has no transverse momentum and $\omega_J \simeq 2E_J$ with E_J the jet energy. However, in the actual experimental measurements at the collider experiments such as proton-proton collisions at the LHC, the jet has a transverse momentum p_T with a jet radius R [62] in the lab frame. Since we will perform phenomenological studies for the relevant collider experiments, we include $p_T R$ as an argument in our collinear FJFs in Eqs. (2.5) to (2.9).

At the same time, the energy fractions z and z_h are defined as:

$$z = \frac{\omega_J}{\omega}, \quad z_h = \frac{\omega_h}{\omega_J}. \quad (2.10)$$

As given in Eqs. (2.5) to (2.7), to obtain the helicity and transversity distributions of the hadron in quark FJFs, namely $\Delta \mathcal{G}_q^h$ and $\Delta_T \mathcal{G}_q^h$, we replace the \not{n} in Eq. (2.5) by $\not{n} \gamma_5$ and $\not{n} \gamma_\perp^i \gamma_5$. The unpolarized collinear FJF $\mathcal{G}_{q,g}^h$ represents the situation where an unpolarized quark or gluon initiates a jet that carries a momentum fraction z of the parent parton, and we further observe an unpolarized hadron h inside the jet which carries the momentum fraction z_h of the jet. Similarly, $\Delta \mathcal{G}_{q,g}^h$ stands for the case where a longitudinally polarized parton initiates a jet in which a longitudinally polarized hadron h is observed. Finally, $\Delta_T \mathcal{G}_q^h$ is the case for a transversely polarized quark going into a jet in which a transversely polarized hadron is observed. Note that we do not have the corresponding $\Delta_T \mathcal{G}_g^h$ for gluons when hadron h is a spin-1/2 particle, due to the helicity-conservation constraint. This is the same reason why the gluon transversity does not exist for the spin-1/2 nucleon [63].

2.1.1 NLO calculation

Although the semi-inclusive FJFs $\mathcal{G}_i^h(z, z_h, p_T R, \mu)$ are not perturbatively calculable, they can be matched onto the standard collinear fragmentation functions as long as $p_T R \gg \Lambda_{\text{QCD}}$ [21]. The matching coefficients can be computed by replacing the hadron h by a parton j and then computing $\mathcal{G}_i^j(z, z_h, p_T R, \mu)$ perturbatively. Prior to describing the process of computing the semi-inclusive FJFs, it is important to emphasize that the outcomes are influenced by the choice of jet algorithms. To streamline our explanation, however, we solely concentrate on the anti- k_T algorithm [62] in this study.

We will now compute the bare partonic semi-inclusive FJFs $\mathcal{G}_i^j(z, z_h, p_T R)$ in order to determine the UV counter terms. At the leading order (LO), one has a single parton. It is

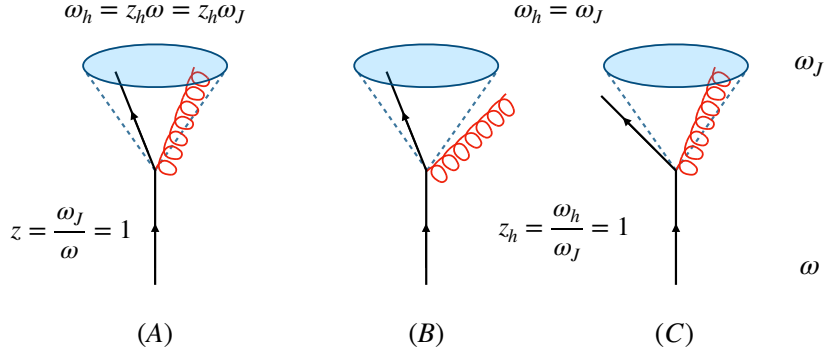


Figure 2: Contributions required for studying semi-inclusive FJFs. In (A), both the quark and the gluon are inside the jet, while in (B) and (C) only the quark or gluon is inside the jet.

this parton i that forms the jet as well as presenting the parton j inside the jet. Thus we have $z = 1$ and $z_h = 1$ at LO and bare polarized semi-inclusive FJFs are given by:

$$\Delta_{(T)} \mathcal{G}_i^{j,(0)}(z, z_h, p_T R) = \delta_{ij} \delta(1-z) \delta(1-z_h). \quad (2.11)$$

Here and throughout the rest of the paper, we use the symbol $\Delta_{(T)}$ to collectively represent both the longitudinally (Δ) and transversely (T) polarized cases.

At the next-to-leading order (NLO), we have to consider the $1 \rightarrow 2$ splitting process in the real emission diagrams as shown in Fig. 2, as well as virtual diagrams. In dimensional regularization, since virtual diagrams become scaleless integrals and vanish, we thus only consider the real diagrams. Following the discussion in [21], we consider the cases of both partons in the jet and only one parton in the jet as shown in Fig. 2. They are given by the same integrals over the transverse momentum q_\perp of the parton j , but are constrained by different Heaviside functions. Working in pure dimensional regularization with $d = 4 - 2\epsilon$ dimensions, we have:

$$\begin{aligned} \Delta_{(T)} \mathcal{G}_i^{j,(1)}(z, z_h, \omega_J) = & \frac{\alpha_s (e^{\gamma_E} \mu^2)^\epsilon}{2\pi \Gamma(1-\epsilon)} \left(\delta(1-z) \Delta_{(T)} \hat{P}_{ji}(z_h, \epsilon) \int \frac{dq_\perp^2}{(q_\perp^2)^{1+\epsilon}} \Theta_{\text{both}}^{\text{anti-}k_T} \right. \\ & \left. + \delta(1-z_h) \Delta_{(T)} \hat{P}_{ji}(z, \epsilon) \int \frac{dq_\perp^2}{(q_\perp^2)^{1+\epsilon}} \Theta_j^{\text{anti-}k_T} \right), \quad (2.12) \end{aligned}$$

where the $\Theta_{\text{both}}^{\text{anti-}k_T}$ and $\Theta_j^{\text{anti-}k_T}$ are the jet algorithm constraints with both partons in jet (Fig. 2A) and only one parton in jet (Fig. 2B, 2C), respectively, and the superscript “anti- k_T ” indicates that anti- k_T algorithm is used. The form of $\Theta_{\text{both}}^{\text{anti-}k_T}$ and $\Theta_j^{\text{anti-}k_T}$ are given by the Heaviside functions [21, 64, 65]:

$$\Theta_{\text{both}}^{\text{anti-}k_T} = \theta \left(z_h (1-z_h) \omega_J \tan \frac{\mathcal{R}}{2} - q_\perp \right), \quad (2.13)$$

$$\Theta_j^{\text{anti-}k_T} = \theta \left(q_\perp - (1-z) \omega_J \tan \frac{\mathcal{R}}{2} \right), \quad (2.14)$$

where \mathcal{R} is the angular separation between three vector momenta inside the jet [64]. This is to be compared with the jet radius R in the hadron collider that specifies the separation in pseudo-rapidity and azimuthal angle as in $\sqrt{(\Delta\eta)^2 + (\Delta\phi)^2}$. For jets with a small jet radius $R \ll 1$, we have

$$\mathcal{R} = \frac{R}{\cosh(\eta)}, \quad (2.15)$$

where η is the jet pseudo-rapidity. Note that

$$\omega_J \tan \frac{\mathcal{R}}{2} \approx 2E_J \frac{\mathcal{R}}{2} = p_T \cosh(\eta) \frac{R}{\cosh(\eta)} = p_T R, \quad (2.16)$$

and we will thus include the argument $p_T R$ in the FJFs.

The longitudinally polarized functions $\Delta\hat{P}_{ji}(z, \epsilon)$ in Eq. (2.12) are given in [66]:

$$\Delta\hat{P}_{qq}(z, \epsilon) = C_F \left[\frac{1+z^2}{1-z} - \epsilon(1-z) \right], \quad (2.17)$$

$$\Delta\hat{P}_{gq}(z, \epsilon) = C_F [2-z+2\epsilon(1-z)], \quad (2.18)$$

$$\Delta\hat{P}_{qg}(z, \epsilon) = T_F [2z-1-2\epsilon(1-z)], \quad (2.19)$$

$$\Delta\hat{P}_{gg}(z, \epsilon) = 2C_A \left[\frac{1}{1-z} - 2z + 1 + 2\epsilon(1-z) \right]. \quad (2.20)$$

The transversely polarized splitting functions $\Delta_T\hat{P}_{ji}(z, \epsilon)$ only exist for $\Delta_T\hat{P}_{qq}$ because there is no gluon transversity fragmentation function for spin-1/2 hadron as we mentioned above. We have the following expression for $\Delta_T\hat{P}_{qq}(z, \epsilon)$ [67]

$$\Delta_T\hat{P}_{qq}(z, \epsilon) = C_F \left[\frac{2z}{1-z} \right]. \quad (2.21)$$

By inserting the Θ functions for anti- k_T algorithm and carrying out the integration in Eq. (2.12), we obtain the bare results² for longitudinally polarized semi-inclusive FJFs $\Delta\mathcal{G}_{i,\text{bare}}^j(z, z_h, p_T R)$ with $i, j \in \{q, g\}$:

$$\begin{aligned} \Delta\mathcal{G}_{q,\text{bare}}^q(z, z_h, p_T R) &= \delta(1-z)\delta(1-z_h) \\ &+ \frac{\alpha_s}{2\pi} \left[\left(\frac{1}{\epsilon} + L \right) \Delta P_{qq}(z) \delta(1-z_h) - \left(\frac{1}{\epsilon} + L \right) \Delta P_{qq}(z_h) \delta(1-z) \right] \\ &+ \delta(1-z) \frac{\alpha_s}{2\pi} \left[2C_F(1+z_h^2) \left(\frac{\ln(1-z_h)}{1-z_h} \right)_+ + C_F(1-z_h) + 2\Delta P_{qq}(z_h) \ln(z_h) \right] \\ &- \delta(1-z_h) \frac{\alpha_s}{2\pi} \left[2C_F(1+z^2) \left(\frac{\ln(1-z)}{1-z} \right)_+ + C_F(1-z) \right], \quad (2.22) \\ \Delta\mathcal{G}_{q,\text{bare}}^g(z, z_h, p_T R) &= \frac{\alpha_s}{2\pi} \left[\left(\frac{1}{\epsilon} + L \right) \Delta P_{gq}(z) \delta(1-z_h) - \left(\frac{1}{\epsilon} + L \right) \Delta P_{gq}(z_h) \delta(1-z) \right] \\ &+ \delta(1-z) \frac{\alpha_s}{2\pi} \left[2\Delta P_{gq}(z_h) \ln(z_h(1-z_h)) - 2C_F(1-z_h) \right] \end{aligned}$$

²More details on the q_\perp integral and relevant expansions as $\epsilon \rightarrow 0$ can be found in Appendix A.

$$-\delta(1-z_h)\frac{\alpha_s}{2\pi}\left[2\Delta P_{gq}(z)\ln(1-z)-2C_F(1-z)\right], \quad (2.23)$$

$$\begin{aligned} \Delta\mathcal{G}_{g,\text{bare}}^q(z, z_h, p_T R) &= \frac{\alpha_s}{2\pi}\left[\left(\frac{1}{\epsilon}+L\right)\Delta P_{gq}(z)\delta(1-z_h)-\left(\frac{1}{\epsilon}+L\right)\Delta P_{gq}(z_h)\delta(1-z)\right] \\ &+ \delta(1-z)\frac{\alpha_s}{2\pi}\left[2\Delta P_{gq}(z_h)\ln(z_h(1-z_h))+2T_F(1-z_h)\right] \\ &- \delta(1-z_h)\frac{\alpha_s}{2\pi}\left[2\Delta P_{gq}(z)\ln(1-z)+2T_F(1-z)\right], \end{aligned} \quad (2.24)$$

$$\begin{aligned} \Delta\mathcal{G}_{g,\text{bare}}^g(z, z_h, p_T R) &= \delta(1-z)\delta(1-z_h) \\ &+ \frac{\alpha_s}{2\pi}\left[\left(\frac{1}{\epsilon}+L\right)\Delta P_{gg}(z)\delta(1-z_h)-\left(\frac{1}{\epsilon}+L\right)\Delta P_{gg}(z_h)\delta(1-z)\right] \\ &+ \delta(1-z)\frac{\alpha_s}{2\pi}\left[4C_A(2(1-z_h)^2+z_h)\left(\frac{\ln(1-z_h)}{1-z_h}\right)_+\right] \\ &+ \delta(1-z)\frac{\alpha_s}{2\pi}\left[2\Delta P_{gg}(z_h)\ln(z_h)-4C_A(1-z_h)\right] \\ &- \delta(1-z_h)\frac{\alpha_s}{2\pi}\left[4C_A(2(1-z)^2+z)\left(\frac{\ln(1-z)}{1-z}\right)_+-4C_A(1-z)\right], \end{aligned} \quad (2.25)$$

where the logarithm

$$L \equiv \ln\left(\frac{\mu^2}{(p_T R)^2}\right). \quad (2.26)$$

This indicates that the natural scale for the collinear FJFs is given by $\mu_g \sim p_T R$. As for the transversely polarized semi-inclusive FJFs, we obtain:

$$\begin{aligned} \Delta_T\mathcal{G}_{q,\text{bare}}^q(z, z_h, p_T R) &= \delta(1-z)\delta(1-z_h) \\ &+ \frac{\alpha_s}{2\pi}\left[\left(\frac{1}{\epsilon}+L\right)\Delta_T P_{qq}(z)\delta(1-z_h)-\left(\frac{1}{\epsilon}+L\right)\Delta_T P_{qq}(z_h)\delta(1-z)\right] \\ &+ \delta(1-z)\frac{\alpha_s}{2\pi}\left[4C_F z_h\left(\frac{\ln(1-z_h)}{1-z_h}\right)_++2\Delta_T P_{qq}(z_h)\ln(z_h)\right] \\ &- \delta(1-z_h)\frac{\alpha_s}{2\pi}\left[4C_F z\left(\frac{\ln(1-z)}{1-z}\right)_+\right]. \end{aligned} \quad (2.27)$$

Here the functions $\Delta_{(T)}P_{ji}(z)$ are the longitudinally (transversely) polarized Altarelli-Parisi splitting kernels:

$$\Delta P_{qq}(z) = C_F\left[\frac{1+z^2}{(1-z)_+} + \frac{3}{2}\delta(1-z)\right], \quad (2.28)$$

$$\Delta P_{gq}(z) = C_F[2-z], \quad (2.29)$$

$$\Delta P_{qg}(z) = T_F[2z-1], \quad (2.30)$$

$$\Delta P_{gg}(z) = 2C_A\left[\frac{1}{(1-z)_+} - 2z + 1\right] + \frac{\beta_0}{2}\delta(1-z), \quad (2.31)$$

$$\Delta_T P_{qq}(z) = C_F\left[\frac{2z}{(1-z)_+} + \frac{3}{2}\delta(1-z)\right], \quad (2.32)$$

where $\beta_0 \equiv \frac{11}{3}C_A - \frac{4}{3}T_F n_f$ and n_f is number of flavors. The “plus” distributions are defined as usual by:

$$\int_0^1 dz f(z)[g(z)]_+ = \int_0^1 dz (f(z) - f(1))g(z). \quad (2.33)$$

2.1.2 Renormalization and matching onto collinear FFs

In this section, we will renormalize the bare semi-inclusive FJFs obtained in the previous section, and then match the results to the standard collinear FFs. In doing so, it is important to point out that the $1/\epsilon$ poles with a factor of $\Delta_{(T)}P_{ij}(z_h)\delta(1-z)$ in Eqs. (2.22) to (2.25) and (2.27) are the infrared (IR) poles, that would be matched onto the standard longitudinally (transversely) polarized collinear FFs. On the other hand, the poles with a factor of $\Delta_{(T)}P_{ij}(z)\delta(1-z_h)$ are the ultraviolet (UV) poles which will be taken care of by renormalization. Since the UV poles do not involve the variable z_h , we should expect that z_h is merely a parameter in renormalization. This is exactly the same as the unpolarized situation studied in [21]. With this in mind, the relationship between the bare and renormalized semi-inclusive FJFs is given by

$$\Delta_{(T)}\mathcal{G}_{i,\text{bare}}^j(z, z_h, p_T R) = \sum_k \int_z^1 \frac{dz'}{z'} \Delta_{(T)}Z_{ik}\left(\frac{z}{z'}, \mu\right) \Delta_{(T)}\mathcal{G}_k^j(z', z_h, p_T R, \mu), \quad (2.34)$$

where $\Delta_{(T)}Z_{ik}\left(\frac{z}{z'}, \mu\right)$ is the renormalization matrix and $\Delta_{(T)}\mathcal{G}_k^j(z', z_h, p_T R, \mu)$ are the renormalized semi-inclusive FJFs. For the aforementioned reason, the convolution only involves the variable z . The renormalized semi-inclusive FJFs satisfy the following RG evolution equations:

$$\mu \frac{d}{d\mu} \Delta_{(T)}\mathcal{G}_i^j(z, z_h, p_T R, \mu) = \sum_k \int_z^1 \frac{dz'}{z'} \Delta_{(T)}\gamma_{ik}^{\mathcal{G}}\left(\frac{z}{z'}, \mu\right) \Delta_{(T)}\mathcal{G}_k^j(z', z_h, p_T R, \mu), \quad (2.35)$$

with the anomalous dimension matrix given by:

$$\Delta_{(T)}\gamma_{ik}^{\mathcal{G}}\left(\frac{z}{z'}, \mu\right) = - \sum_k \int_z^1 \frac{dz'}{z'} (\Delta_{(T)}Z)_{il}^{-1}\left(\frac{z}{z'}, \mu\right) \mu \frac{d}{d\mu} \Delta_{(T)}Z_{lk}(z', \mu), \quad (2.36)$$

and $(\Delta_{(T)}Z)_{il}^{-1}$ is the inverse of the renormalization matrix that is defined such that:

$$\sum_k \int_z^1 \frac{dz'}{z'} (\Delta_{(T)}Z)_{il}^{-1}\left(\frac{z}{z'}, \mu\right) \Delta_{(T)}Z_{kj}(z', \mu) = \delta_{ij}\delta(1-z). \quad (2.37)$$

Up to $\mathcal{O}(\alpha_s)$, the renormalization matrix is

$$\Delta_{(T)}Z_{ij}(z, \mu) = \delta_{ij}\delta(1-z) + \frac{\alpha_s(\mu)}{2\pi} \frac{1}{\epsilon} \Delta_{(T)}P_{ji}(z), \quad (2.38)$$

and therefore the anomalous dimension matrix is given by:

$$\Delta_{(T)}\gamma_{ij}^{\mathcal{G}}(z, \mu) = \frac{\alpha_s(\mu)}{\pi} \Delta_{(T)}P_{ji}(z). \quad (2.39)$$

We therefore observe that the evolution of the renormalized polarized semi-inclusive FJFs conforms to the time-like DGLAP equation for collinear polarized FFs [68]:

$$\mu \frac{d}{d\mu} \Delta_{(T)} \mathcal{G}_i^h(z, z_h, p_T R, \mu) = \frac{\alpha_s(\mu)}{\pi} \sum_k \int_z^1 \frac{dz'}{z'} \Delta_{(T)} P_{ji} \left(\frac{z}{z'} \right) \Delta_{(T)} \mathcal{G}_j^h(z', z_h, p_T R, \mu), \quad (2.40)$$

where the leading order splitting kernels are given in Eqs. (2.28) to (2.32). Notice that the hadronic FJFs have been reinstated since the hadronic and partonic FJFs would contain the same UV counter terms and thus follow the same RG evolution equations. As we mentioned in the previous section that the natural scale for the collinear FJFs is given by $\mu_g = p_T R$, thus one would use the above renormalization group equations to evolve these FJFs from their natural scale $p_T R$ to the hard scale p_T for the jet production. The effect of this would be to resum the logarithms of the jet radius R for narrow jets with $R \ll 1$. Analogous behaviors were observed in the context of the semi-inclusive unpolarized FJFs in [21].

With the UV poles eliminated by renormalization, we can proceed to dealing with the IR poles, which can be addressed by matching onto the collinear polarized FFs. Such matching can be done at a scale $\mu \gg \Lambda_{\text{QCD}}$ as follows:

$$\Delta_{(T)} \mathcal{G}_i^h(z, z_h, p_T R, \mu) = \sum_j \int_{z_h}^1 \frac{dz'_h}{z'_h} \Delta_{(T)} \mathcal{J}_{ij}(z, z'_h, p_T R, \mu) \Delta_{(T)} D_{h/j} \left(\frac{z_h}{z'_h}, \mu \right), \quad (2.41)$$

where again, the hadronic semi-inclusive FJFs and collinear FFs are reinstated. Here, $\Delta_{(T)} D_{h/j}(z_h, \mu)$ is the collinear fragmentation function characterizing a parton j fragmenting into a hadron h . Specifically, $\Delta D_{h/j}$ ($\Delta_T D_{h/j}$) is the helicity (transversity) fragmentation function describing a longitudinally (transversely) polarized parton fragmenting into a longitudinally (transversely) polarized hadron. And the matching relation above holds, with a power correction of order $\mathcal{O}(\Lambda_{\text{QCD}}^2/(p_T R)^2)$ [21, 31, 33]. In this case, however, different from the renormalization procedure, z_h is being convoluted and z is merely a parameter. This process is similar to the approach used for unpolarized FJFs described in [21], except that instead of the unpolarized FFs, collinear polarized FFs are used in this case. The perturbative results at the parton level for the polarized collinear FFs are given by:

$$\Delta_{(T)} D_{j/i}(z_h, \mu) = \delta_{ij} \delta(1 - z_h) + \frac{\alpha_s}{2\pi} \Delta_{(T)} P_{ji}(z_h) \left(-\frac{1}{\epsilon} \right). \quad (2.42)$$

Finally, the matching coefficients $\Delta_{(T)} \mathcal{J}_{ij}$ for anti- k_T jet algorithm are as follows

$$\begin{aligned} \Delta \mathcal{J}_{qq}(z, z_h, p_T R, \mu) &= \delta(1 - z) \delta(1 - z_h) + \frac{\alpha_s}{2\pi} \left\{ L \left[\Delta P_{qq}(z) \delta(1 - z_h) - \Delta P_{qq}(z_h) \delta(1 - z) \right] \right. \\ &\quad + \delta(1 - z) \left[2C_F(1 + z_h^2) \left(\frac{\ln(1 - z_h)}{1 - z_h} \right)_+ + C_F(1 - z_h) + \Delta \mathcal{I}_{qq}^{\text{anti-}k_T}(z_h) \right] \\ &\quad \left. - \delta(1 - z_h) \left[2C_F(1 + z^2) \left(\frac{\ln(1 - z)}{1 - z} \right)_+ + C_F(1 - z) \right] \right\}, \quad (2.43) \\ \Delta \mathcal{J}_{qg}(z, z_h, p_T R, \mu) &= \frac{\alpha_s}{2\pi} \left\{ L \left[\Delta P_{qg}(z) \delta(1 - z_h) - \Delta P_{qg}(z_h) \delta(1 - z) \right] \right\} \end{aligned}$$

$$\begin{aligned}
& + \delta(1-z) \left[2\Delta P_{gq}(z_h) \ln(1-z_h) - 2C_F(1-z_h) + \Delta \mathcal{I}_{gq}^{\text{anti-}k_T}(z_h) \right] \\
& - \delta(1-z_h) \left[2\Delta P_{gq}(z) \ln(1-z) - 2C_F(1-z) \right] \Bigg\}, \tag{2.44}
\end{aligned}$$

$$\begin{aligned}
\Delta \mathcal{J}_{gq}(z, z_h, p_T R, \mu) &= \frac{\alpha_s}{2\pi} \left\{ L \left[\Delta P_{gq}(z) \delta(1-z_h) - \Delta P_{gq}(z_h) \delta(1-z) \right] \right. \\
& + \delta(1-z) \left[2\Delta P_{gq}(z_h) \ln(1-z_h) + 2T_F(1-z_h) + \Delta \mathcal{I}_{gq}^{\text{anti-}k_T}(z_h) \right] \\
& \left. - \delta(1-z_h) \left[2\Delta P_{gq}(z) \ln(1-z) + 2T_F(1-z) \right] \right\}, \tag{2.45}
\end{aligned}$$

$$\begin{aligned}
\Delta \mathcal{J}_{gg}(z, z_h, p_T R, \mu) &= \delta(1-z) \delta(1-z_h) + \frac{\alpha_s}{2\pi} \left\{ L \left[\Delta P_{gg}(z) \delta(1-z_h) - \Delta P_{gg}(z_h) \delta(1-z) \right] \right. \\
& + \delta(1-z) \left[4C_A(2(1-z_h)^2 + z_h) \left(\frac{\ln(1-z_h)}{1-z_h} \right)_+ \right. \\
& \quad \left. - 4C_A(1-z_h) + \Delta \mathcal{I}_{gg}^{\text{anti-}k_T}(z_h) \right] \\
& \left. - \delta(1-z_h) \left[4C_A(2(1-z)^2 + z) \left(\frac{\ln(1-z)}{1-z} \right)_+ - 4C_A(1-z) \right] \right\}, \tag{2.46}
\end{aligned}$$

$$\begin{aligned}
\Delta_T \mathcal{J}_{qq}(z, z_h, p_T R, \mu) &= \delta(1-z) \delta(1-z_h) + \frac{\alpha_s}{2\pi} \left\{ L \left[\Delta_T P_{qq}(z) \delta(1-z_h) - \Delta_T P_{qq}(z_h) \delta(1-z) \right] \right. \\
& + \delta(1-z) \left[4C_F z_h \left(\frac{\ln(1-z_h)}{1-z_h} \right)_+ + \Delta_T \mathcal{I}_{qq}^{\text{anti-}k_T}(z_h) \right] \\
& \left. - \delta(1-z_h) \left[4C_F z \left(\frac{\ln(1-z)}{1-z} \right)_+ \right] \right\}, \tag{2.47}
\end{aligned}$$

where we have defined $\Delta_{(T)} \mathcal{I}_{ij}^{\text{anti-}k_T}$ as:

$$\begin{aligned}
\Delta \mathcal{I}_{ij}^{\text{anti-}k_T}(z_h) &= 2\Delta P_{ji}(z_h) \ln(z_h), \\
\Delta_T \mathcal{I}_{ij}^{\text{anti-}k_T}(z_h) &= 2\Delta_T P_{ji}(z_h) \ln(z_h). \tag{2.48}
\end{aligned}$$

The matching coefficient functions $\Delta \mathcal{J}_{ij}$ for the longitudinally polarized case have been given in the previous publication [34] with a different notation \mathcal{J}_{ij}^L . Here, we provide the detailed steps of how such matching coefficients are derived. At the same time, the matching coefficient for the transversely polarized case $\Delta_T \mathcal{J}_{qq}$ is presented here for the first time.

2.2 Collinear FJFs in exclusive jet productions

Exclusive jet production, such as back-to-back dijet production in proton-proton collisions [69, 70] or back-to-back electron-jet production in electron-proton collisions [71], can provide valuable insight into the understanding of the fundamental dynamics of hadron structure and interactions. However, in such situations, typically the radiation outside the jet is restricted. For example, in back-to-back dijet production, one usually restricts the

transverse momentum imbalance q_T to be much smaller than the average transverse momentum of the jets. In this case, the hard/collinear gluon emission outside the jet would move the imbalance q_T away from the back-to-back region. Because of that, the collinear radiation can only happen inside the jet. Consequently, for jet function calculations in exclusive jet production, we only have to consider Fig. 2A while B and C would not contribute. We refer to the corresponding FJFs as exclusive FJFs below, which are key ingredients in the factorization formalism for these processes. They describe the probability distribution for a parton in the jet to fragment into a hadron with a given collinear momentum fraction in exclusive jet production.

The perturbative computations for exclusive FJFs $\Delta_{(T)}\mathcal{G}_i^j(z_h, p_T R, \mu)$ are identical to those for the semi-inclusive FJFs, except that we keep only the contributions from Fig. 2A. Since both partons are always inside the jet, we always have $z = 1$, *i.e.*, the jet carries all the energy of the parton that initiates the jet in this case. Because of this, we no longer keep the variable z in the FJFs and thus the exclusive FJFs only depend on z_h . The RG equations for exclusive FJFs can also be derived in the same manner as above, and we find that they satisfy the following equation

$$\mu \frac{d}{d\mu} \Delta_{(T)}\mathcal{G}_i^h(z_h, p_T R, \mu) = \gamma_{\mathcal{G}}^i(\mu) \Delta_{(T)}\mathcal{G}_i^h(z_h, p_T R, \mu), \quad (2.49)$$

where the index i is not summed over, and the anomalous dimensions $\gamma_{\mathcal{G}}^i(\mu)$ with $i = q, g$ at this order are given by:

$$\gamma_{\mathcal{G}}^q(\mu) = \frac{\alpha_s(\mu)}{\pi} \left(C_F L + \frac{3}{2} C_F \right), \quad (2.50)$$

$$\gamma_{\mathcal{G}}^g(\mu) = \frac{\alpha_s(\mu)}{\pi} \left(C_A L + \frac{\beta_0}{2} \right). \quad (2.51)$$

A few comments are in order. First of all, it is important to emphasize that the RG equation for exclusive FJFs is a multiplicative renormalization, instead of a convolution over z as in the semi-inclusive FJFs given in the previous section. Secondly, the anomalous dimension $\gamma_{\mathcal{G}}^i(\mu)$ is the same as that of the exclusive jet functions in [64] and exclusive unpolarized FJFs [27, 33, 72]. Since in the factorization formalism, one simply replaces the exclusive jet function with the exclusive FJFs, thus they should have the same anomalous dimensions simply because of the RG consistency. At the same time, we find that the UV divergent terms are all proportional to $\delta(1 - z_h)$ where the radiated gluon becomes soft, and thus the result should be independent of the polarization of the partons. This explains the anomalous dimensions for both longitudinally and transversely polarized FJFs are the same as the unpolarized FJFs. The solution to the RG equation for the exclusive FJFs is then:

$$\Delta_{(T)}\mathcal{G}_i^h(z_h, p_T R, \mu) = \Delta_{(T)}\mathcal{G}_i^h(z_h, p_T R, \mu_{\mathcal{G}}) \exp \left[\int_{\mu_{\mathcal{G}}}^{\mu} \frac{d\mu'}{\mu'} \gamma_{\mathcal{G}}^i(\mu') \right], \quad (2.52)$$

where the scale $\mu_{\mathcal{G}}$ is the characteristic scale that eliminates the large logarithms in the fixed-order perturbative calculations. The logarithm L indicates that the natural scale for the exclusive FJFs is also given by $\mu_{\mathcal{G}} = p_T R$, the same as for the semi-inclusive FJFs. One

would thus evolve the FJFs from the natural scale $\mu_g \sim p_T R$ to the hard scale of the process $\mu \sim p_T$ and effectively resum the logarithm of jet radius, $\ln R$.

Finishing the discussion on the RG equation for the exclusive FJFs, let us now turn to their matching to the standard collinear FFs. Similar to the semi-inclusive FJFs, the exclusive fragmenting jet functions $\Delta_{(T)} \mathcal{G}_i^h(z_h, p_T R, \mu)$ are also closely related to the fragmentation functions $\Delta_{(T)} D_{h/j}$ and in this work we label the corresponding matching coefficients as $\Delta_{(T)} \mathcal{J}_{ij}$. Following [27, 31, 33, 72], one has the following expansion for exclusive FJFs:

$$\Delta_{(T)} \mathcal{G}_i^h(z_h, p_T R, \mu) = \sum_j \int_{z_h}^1 \frac{dz'_h}{z'_h} \Delta_{(T)} \mathcal{J}_{ij}(z'_h, p_T R, \mu) \Delta_{(T)} D_{h/j} \left(\frac{z_h}{z'_h}, \mu \right). \quad (2.53)$$

Again this equation is valid up to power corrections of order $\mathcal{O}(\Lambda_{\text{QCD}}^2/(p_T R)^2)$ for light hadrons. For heavy meson fragmenting jet functions, Λ_{QCD} should be replaced by the heavy quark mass m_Q in the above equation [33, 73]. We provide the NLO results of matching coefficients $\Delta_{(T)} \mathcal{J}_{ij}$, which depend on the jet algorithm. The results for unpolarized FJFs with cone algorithm were given in [74], while those for anti- k_T jets were first written down in [72]. While the results for the unpolarized FJFs are available in the literature, the coefficients for the polarized FJFs are given for the first time in our current paper. We provide the detailed derivations of exclusive FJFs with polarizations for anti- k_T jets in Appendix B. Here we only list the final results:

$$\Delta \mathcal{J}_{qq}(z_h, p_T R, \mu) = \delta(1 - z_h) + \frac{\alpha_s C_F}{2\pi} \left[\delta(1 - z_h) \left(\frac{L^2}{2} - \frac{\pi^2}{12} \right) - \Delta P_{qq}(z_h) L + 1 - z_h + \Delta \hat{\mathcal{J}}_{qq}^{\text{anti-}k_T}(z_h) \right], \quad (2.54)$$

$$\Delta \mathcal{J}_{qg}(z_h, p_T R, \mu) = \frac{\alpha_s C_F}{2\pi} \left[-\Delta P_{gq}(z_h) L - 2(1 - z_h) + \Delta \hat{\mathcal{J}}_{qg}^{\text{anti-}k_T}(z_h) \right], \quad (2.55)$$

$$\Delta \mathcal{J}_{gq}(z_h, p_T R, \mu) = \frac{\alpha_s T_F}{2\pi} \left[-\Delta P_{qg}(z_h) L + 2(1 - z_h) + \Delta \hat{\mathcal{J}}_{gq}^{\text{anti-}k_T}(z_h) \right], \quad (2.56)$$

$$\Delta \mathcal{J}_{gg}(z_h, p_T R, \mu) = \delta(1 - z_h) + \frac{\alpha_s C_A}{2\pi} \left[\delta(1 - z_h) \left(\frac{L^2}{2} - \frac{\pi^2}{12} \right) - \Delta P_{gg}(z_h) L - 4(1 - z_h) + \Delta \hat{\mathcal{J}}_{gg}^{\text{anti-}k_T}(z_h) \right], \quad (2.57)$$

$$\Delta_T \mathcal{J}_{qq}(z_h, p_T R, \mu) = \delta(1 - z_h) + \frac{\alpha_s C_F}{2\pi} \left[\delta(1 - z_h) \left(\frac{L^2}{2} - \frac{\pi^2}{12} \right) - \Delta_T P_{qq}(z_h) L + \Delta_T \hat{\mathcal{J}}_q^{\text{anti-}k_T}(z_h) \right], \quad (2.58)$$

where for anti- k_T jets, the jet-algorithm dependent pieces, $\Delta_{(T)} \hat{\mathcal{J}}_{ij}^{\text{anti-}k_T}(z_h)$, are given by

$$\Delta \hat{\mathcal{J}}_{qq}^{\text{anti-}k_T}(z_h) = 2\Delta P_{qq}(z_h) \ln(z_h) + 2(1 + z_h^2) \left(\frac{\ln(1 - z_h)}{1 - z_h} \right)_+, \quad (2.59)$$

$$\Delta \hat{\mathcal{J}}_{qg}^{\text{anti-}k_T}(z_h) = 2\Delta P_{gq}(z_h) \ln(z_h(1 - z_h)), \quad (2.60)$$

$$\Delta_{\mathcal{F}_{gg}^{\text{anti-}k_T}}(z_h) = 2\Delta P_{gg}(z_h) \ln(z_h(1-z_h)), \quad (2.61)$$

$$\Delta_{\mathcal{F}_{gg}^{\text{anti-}k_T}}(z_h) = 2\Delta P_{gg}(z_h) \ln(z_h) + 4\left(2(1-z_h)^2 + z_h\right) \left(\frac{\ln(1-z_h)}{1-z_h}\right)_+, \quad (2.62)$$

$$\Delta_T \mathcal{F}_{qq}^{\text{anti-}k_T}(z_h) = 2\Delta_T P_{qq}(z_h) \ln(z_h) + 4z_h \left(\frac{\ln(1-z_h)}{1-z_h}\right)_+, \quad (2.63)$$

where the splitting kernels $\Delta_{(T)}P_{ji}(z_h)$ [66, 67] have been introduced in Eqs. (2.28) to (2.32).

3 The transverse momentum dependent FJFs (TMD FJFs)

In this section, we study TMD FJFs in both the semi-inclusive jet production and the exclusive jet production, including polarizations of the initiating parton and the final observed hadron inside the jet. They are termed as polarized TMD FJFs [34]. Some partial results are available in the previous publications [34, 41], but never the complete results. For example, the hard matching functions for both longitudinally and transversely polarized cases are presented for the first time. Below, we provide the complete results for all the relevant polarized semi-inclusive and exclusive TMD FJFs. The operator definitions of these functions in SCET are presented, followed by their factorization formalism, which involves hard functions, soft functions, and TMD FFs.

The kinematics is set up as in Fig. 3, a hadron h is observed inside the jet, carrying a fraction z_h of the jet longitudinal momentum (not labeled in the figure), a transverse momentum \mathbf{j}_\perp with azimuthal angle $\hat{\phi}_h$, and a transverse spin $\mathbf{S}_{h\perp}$ with azimuthal angle $\hat{\phi}_{S_h}$. Both \mathbf{j}_\perp and $\mathbf{S}_{h\perp}$ are measured with respect to the jet axis z_J , while both azimuthal angles $\hat{\phi}_h$ and $\hat{\phi}_{S_h}$ are measured within the jet transverse plane and with respect to x_J , the x -axis that is rotated into jet coordinates³.

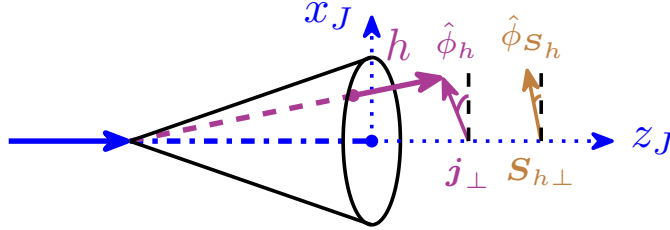


Figure 3: Illustration for the distribution of hadrons inside a jet with transverse momentum \mathbf{j}_\perp and azimuthal angle $\hat{\phi}_h$, and transverse spin $\mathbf{S}_{h\perp}$ and azimuthal angle $\hat{\phi}_{S_h}$. Both azimuthal angles are measured with respect to the jet coordinate x_J and within the jet transverse plane.

3.1 TMD FJFs in semi-inclusive jet productions

Again we start with the semi-inclusive TMD FJFs, which is an essential ingredient for studying the transverse momentum distribution of hadrons inside a jet in *e.g.*, single inclusive jet production in proton-proton collisions ($p+p \rightarrow \text{jet}(h) + X$) or in electron-proton

³Please see Eqs. (4.8) and (4.9) for the parameterization of \mathbf{j}_\perp and $\mathbf{S}_{h\perp}$.

collisions ($e + p \rightarrow \text{jet}(h) + X$). Following the previous publication [34], we define the general correlators for TMD FJFs initiated by quark or gluon as:

$$\Delta^{h/q}(z, z_h, \mathbf{j}_\perp, S_h) = \frac{z}{2N_c} \delta\left(z_h - \frac{\omega_h}{\omega_J}\right) \langle 0 | \delta(\omega - \bar{n} \cdot \mathcal{P}) \delta^2(\mathcal{P}_\perp / z_h + \mathbf{j}_\perp) \chi_n(0) | (Jh)X \rangle \quad (3.1)$$

$$\times \langle (Jh)X | \bar{\chi}_n(0) | 0 \rangle,$$

$$\Delta^{h/g, \mu\nu}(z, z_h, \mathbf{j}_\perp, S_h) = \frac{z\omega}{(d-2)(N_c^2-1)} \delta\left(z_h - \frac{\omega_h}{\omega_J}\right) \quad (3.2)$$

$$\times \langle 0 | \delta(\omega - \bar{n} \cdot \mathcal{P}) \delta^2(\mathcal{P}_\perp / z_h + \mathbf{j}_\perp) \mathcal{B}_{n_\perp}^\mu(0) | (Jh)X \rangle \langle (Jh)X | \mathcal{B}_{n_\perp}^\nu(0) | 0 \rangle,$$

where we have the energy fractions z and z_h defined the same as in Eq. (2.10). One can parameterize these correlators at the leading power [34, 40]:

$$\Delta^{h/q}(z, z_h, \mathbf{j}_\perp, S_h) = \Delta^{h/q[\not{\psi}]} \frac{\not{\psi}}{2} - \Delta^{h/q[\not{\psi}\gamma_5]} \frac{\not{\psi}\gamma_5}{2} + \Delta^{h/q[in_\nu\sigma^{k\nu}\gamma_5]} \frac{i\bar{n}_\mu\sigma^{k\mu}\gamma_5}{2}, \quad (3.3)$$

$$\Delta^{h/g, kl}(z, z_h, \mathbf{j}_\perp, S_h) = \frac{1}{2} \delta_T^{kl} (\delta_T^{mn} \Delta^{h/g, mn}) - \frac{i}{2} \epsilon_T^{kl} (i\epsilon_T^{mn} \Delta^{h/g, mn}) + \hat{S} \Delta^{h/g, kl}. \quad (3.4)$$

Here we have defined $\Delta^{h/q[\Gamma]} \equiv \frac{1}{4} \text{Tr}(\Delta^{h/q}\Gamma)$, and we have $\hat{S}O^{kl} = \frac{1}{2}(O^{kl} + O^{lk} - \delta_T^{kl}O^{\rho\rho})$ and $\delta_T^{kl} = -g_T^{kl}$. The three terms on the right-hand side of Eq. (3.3) correspond (in order) to the TMD FJFs with unpolarized, longitudinally polarized, and transversely polarized initial quarks. On the other hand, the three terms on the right-hand side of Eq. (3.4) correspond to unpolarized, circularly polarized, and linearly polarized gluons. More details have been presented in the previous work [34]. For completeness, here we provide the parameterization of quark TMD FJFs:

$$\Delta^{h/q[\not{\psi}]} = \mathcal{D}_1^{h/q}(z, z_h, \mathbf{j}_\perp) - \frac{\epsilon_T^{kl} j_\perp^k S_{h_\perp}^l}{z_h M_h} \mathcal{D}_{1T}^{\perp h/q}(z, z_h, \mathbf{j}_\perp), \quad (3.5)$$

$$\Delta^{h/q[\not{\psi}\gamma_5]} = \lambda_h \mathcal{G}_{1L}^{h/q}(z, z_h, \mathbf{j}_\perp) - \frac{\mathbf{j}_\perp \cdot \mathbf{S}_{h_\perp}}{z_h M_h} \mathcal{G}_{1T}^{h/q}(z, z_h, \mathbf{j}_\perp), \quad (3.6)$$

$$\Delta^{h/q[in_\nu\sigma^{k\nu}\gamma_5]} = S_{h_\perp}^k \mathcal{H}_1^{h/q}(z, z_h, \mathbf{j}_\perp) - \frac{\epsilon_T^{kl} j_\perp^l}{z_h M_h} \mathcal{H}_1^{\perp h/q}(z, z_h, \mathbf{j}_\perp) - \frac{j_\perp^k}{z_h M_h} \lambda_h \mathcal{H}_{1L}^{\perp h/q}(z, z_h, \mathbf{j}_\perp)$$

$$+ \frac{j_\perp^k \mathbf{j}_\perp \cdot \mathbf{S}_{h_\perp} - \frac{1}{2} \mathbf{j}_\perp^2 S_{h_\perp}^k}{z_h^2 M_h^2} \mathcal{H}_{1T}^{\perp h/q}(z, z_h, \mathbf{j}_\perp), \quad (3.7)$$

The functions \mathcal{D} , \mathcal{G} and \mathcal{H} on the right-hand side of Eqs. (3.5) to (3.7) represent the TMD FJFs initiated by unpolarized, longitudinally polarized, and transversely polarized initial quark respectively. The parameterization for gluon TMD FJFs is given by

$$\delta_T^{kl} \Delta^{h/g, kl} = \mathcal{D}_1^{h/g}(z, z_h, \mathbf{j}_\perp) - \frac{\epsilon_T^{ij} j_\perp^i S_{h_\perp}^j}{z_h M_h} \mathcal{D}_1^{\perp h/g}(z, z_h, \mathbf{j}_\perp), \quad (3.8)$$

$$i\epsilon_T^{kl} \Delta^{h/g, kl} = \lambda_h \mathcal{G}_{1L}^{h/g}(z, z_h, \mathbf{j}_\perp) - \frac{\mathbf{j}_\perp \cdot \mathbf{S}_{h_\perp}}{z_h M_h} \mathcal{G}_{1T}^{h/g}(z, z_h, \mathbf{j}_\perp), \quad (3.9)$$

$$\hat{S} \Delta^{h/g, kl} = \frac{j_\perp^k j_\perp^l}{2z_h^2 M_h^2} \mathcal{H}_1^{\perp h/g}(z, z_h, \mathbf{j}_\perp) - \frac{\epsilon_T^{j_1\{k} S_{h_\perp}^{l\}} + \epsilon_T^{S_{h_\perp}\{k} j_\perp^{l\}}}{8z_h M_h} \mathcal{H}_{1T}^{h/g}(z, z_h, \mathbf{j}_\perp)$$

$$+ \frac{\epsilon_T^{j_\perp \{k, l\}} j_\perp}{4z_h^2 M_h^2} \left(\lambda_h \mathcal{H}_{1L}^{\perp, h/g}(z, z_h, \mathbf{j}_\perp) - \frac{\mathbf{j}_\perp \cdot \mathbf{S}_{h\perp}}{z_h M_h} \mathcal{H}_{1T}^{\perp, h/g}(z, z_h, \mathbf{j}_\perp) \right), \quad (3.10)$$

where the functions \mathcal{D} , \mathcal{G} and \mathcal{H} represent the TMD FJFs initiated by unpolarized, circularly polarized, and linearly polarized gluons, respectively. The two \mathcal{G} functions with circularly polarized gluons are anti-symmetric of indices $k, l = 1, 2$, and the four \mathcal{H} functions related to linearly polarized gluons are symmetric and traceless combinations of $k, l = 1, 2$. We have adopted the notation $v_T^{\{k} w_T^{l\}} = v_T^k w_T^l + v_T^l w_T^k$ as in [13, 39].

Since TMD FJFs represent the hadron fragmentation inside a fully reconstructed jet, their physical meaning is similar to that of standard TMD FFs as reviewed in [40]. Naturally, we adopt the calligraphic font of the letters used by the corresponding TMD FFs as the notations of TMD FJFs. For example, $\mathcal{H}_1^{h/q}$ in Eq. (3.7) is the so-called quark transversity TMD FJFs, *i.e.*, a transversely polarized quark initiates a jet, in which a transversely polarized hadron is observed. On the other hand, $\mathcal{G}_{1L}^{h/g}$ in Eq. (3.9) is the helicity gluon TMD FJFs, *i.e.*, a longitudinally polarized gluon initiates a jet, in which a longitudinally polarized hadron is observed.

In this study, we focus on the kinematic region $\Lambda_{\text{QCD}} \lesssim j_\perp \ll p_T R$, necessitating the adoption of the TMD factorization [20]. In the previous work [23], the TMD factorization for transverse momentum distribution of unpolarized hadrons inside the jet was derived. Over there, the evolution equations are based on the separate rapidity renormalization group equations for the so-called “unsubtracted” TMD FFs and soft functions. Below, in the process of reviewing the TMD factorization, we update the formalism with the more recent language outlined in the TMD Handbook [13]. This new formalism makes the evolution of the in-jet TMD FJFs simpler and more transparent than before. We then present the hard matching functions, where the expressions for longitudinally and transversely polarized cases are provided here for the first time.

3.1.1 TMD Factorization

In the kinematic region under consideration, the radiation relevant at leading power is restricted to collinear radiation within the jet, characterized by the momentum that scales as $p_c = [p_c^+, p_c^-, p_{c\perp}] \sim p_c^- [\lambda^2, 1, \lambda]$, where the power counting parameter $\lambda \sim j_\perp/p_T$. Additionally, soft radiation of order j_\perp is also relevant. It is worth noting that harder emissions are only permitted outside the jet cone and will thus only impact the determination of the jet axis. Consequently, the hadron transverse momentum j_\perp , which is defined with respect to the jet axis, remains intact from the radiations external to the jet. Taking the unpolarized case as an example, a factorized formalism for the unpolarized TMD FJFs within SCET can be formulated [23]:

$$\begin{aligned} \mathcal{D}_1^{h/c}(z, z_h, \mathbf{j}_\perp, p_T R, \mu, \zeta_J) &= \hat{H}_{c \rightarrow i}^U(z, p_T R, \mu) \int d^2 \mathbf{k}_\perp d^2 \boldsymbol{\lambda}_\perp \delta^2(z_h \boldsymbol{\lambda}_\perp + \mathbf{k}_\perp - \mathbf{j}_\perp) \\ &\quad \times D_1^{h/i(u)}(z_h, \mathbf{k}_\perp, \mu, \zeta/\nu^2) S_i(\boldsymbol{\lambda}_\perp, \mu, \nu \mathcal{R}/2), \end{aligned} \quad (3.11)$$

where $S_i(\boldsymbol{\lambda}_\perp, \mu, \nu \mathcal{R}/2)$ is the in-jet soft function, and $D_1^{h/i(u)}(z_h, \mathbf{k}_\perp, \mu, \zeta/\nu^2)$ is the “unsubtracted” TMD FFs with the superscript “(u)” to emphasize this fact. Here μ is the

standard renormalization scale as above while ν is a rapidity scale associated with the rapidity divergence [75, 76], and ζ is the so-called Collins-Soper scale [20]. We also have a scale ζ_J to be defined below. The δ function establishes a relationship between the hadron transverse momentum \mathbf{j}_\perp , relative to the jet axis, and two other momenta: the transverse momentum $\boldsymbol{\lambda}_\perp$ of soft radiation, and the hadron transverse momentum \mathbf{k}_\perp with respect to the fragmenting parton. Notice that $\boldsymbol{\lambda}_\perp$ is multiplied by z_h to adjust for the dissimilarity between the fragmenting parton and the observed hadron. The relationship among the three aforementioned transverse momenta is illustrated in Fig. 4.

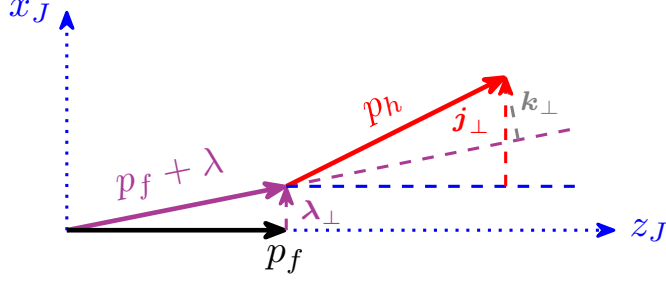


Figure 4: Illustration of the soft radiation (purple) and fragmentation process (red). The initial fragmenting quark carries a momentum p_f along the jet axis z_J . It undergoes a soft radiation of $\boldsymbol{\lambda}_\perp$, and then fragments into a hadron with momentum p_h . The momentum p_h has a transverse component of \mathbf{k}_\perp with respect to the quark after soft radiation, or a transverse component of \mathbf{j}_\perp with respect to the jet axis.

As is common practice in TMD physics, we convert the aforementioned expression from the transverse momentum space to the coordinate b -space with the following transformation:

$$\begin{aligned} \mathcal{D}_1^{h/c}(z, z_h, \mathbf{j}_\perp, p_T R, \mu, \zeta_J) &= \hat{H}_{c \rightarrow i}^U(z, p_T R, \mu) \\ &\times \int \frac{d^2 \mathbf{b}}{(2\pi)^2} e^{i \mathbf{j}_\perp \cdot \mathbf{b} / z_h} \tilde{D}_1^{h/i(u)}(z_h, \mathbf{b}, \mu, \zeta / \nu^2) \tilde{S}_i(\mathbf{b}, \mu, \nu \mathcal{R} / 2), \end{aligned} \quad (3.12)$$

where we have defined the $\tilde{D}_1^{h/i(u)}(z_h, \mathbf{b}, \mu, \zeta / \nu^2)$ and $\tilde{S}_i(\mathbf{b}, \mu, \nu \mathcal{R} / 2)$ in Fourier b -space with $i = q, g$ as:

$$\begin{aligned} \tilde{D}_1^{h/i(u)}(z_h, \mathbf{b}, \mu, \zeta / \nu^2) &= \frac{1}{z_h^2} \int d^2 \mathbf{k}_\perp e^{-i \mathbf{k}_\perp \cdot \mathbf{b} / z_h} D_1^{h/i(u)}(z_h, k_\perp, \mu, \zeta / \nu^2) \\ &= \frac{1}{z_h^2} \int dk_\perp k_\perp 2\pi J_0\left(\frac{b k_\perp}{z_h}\right) D_1^{h/i(u)}(z_h, k_\perp, \mu, \zeta / \nu^2), \end{aligned} \quad (3.13)$$

$$\tilde{S}_i(\mathbf{b}, \mu, \nu \mathcal{R} / 2) = \int d^2 \boldsymbol{\lambda}_\perp e^{-i \boldsymbol{\lambda}_\perp \cdot \mathbf{b}} S_i(\boldsymbol{\lambda}_\perp, \mu, \nu \mathcal{R} / 2), \quad (3.14)$$

where $J_0(b k_\perp / z_h)$ is the Bessel function of the first kind. The μ - and ν -renormalization group equations for the “unsubtracted” TMD FFs $D_1^{h/i(u)}$ are well known:

$$\mu \frac{d}{d\mu} \ln \tilde{D}_1^{h/i(u)}(z_h, \mathbf{b}, \mu, \zeta / \nu^2) = \gamma_{\mu, i}^D(\mu, \zeta / \nu^2), \quad (3.15)$$

$$\nu \frac{d}{d\nu} \ln \tilde{D}_1^{h/i(u)}(z_h, \mathbf{b}, \mu, \zeta/\nu^2) = \gamma_{\nu,i}^D(b, \mu), \quad (3.16)$$

where the leading order μ - and ν -anomalous dimensions are given by:

$$\gamma_{\mu,q}^D(\mu, \zeta/\nu^2) = \frac{\alpha_s}{\pi} C_F \left(\ln \left(\frac{\nu^2}{\zeta} \right) + \frac{3}{2} \right), \quad (3.17)$$

$$\gamma_{\mu,g}^D(\mu, \zeta/\nu^2) = \frac{\alpha_s}{\pi} C_A \left(\ln \left(\frac{\nu^2}{\zeta} \right) + \frac{\beta_0}{2C_A} \right), \quad (3.18)$$

$$\gamma_{\nu,i}^D(b, \mu) = \frac{\alpha_s}{\pi} C_i \ln \left(\frac{\mu^2}{\mu_b^2} \right), \quad (3.19)$$

with $C_q = C_F$, $C_g = C_A$, and $\mu_b \equiv 2e^{-\gamma_E}/b$.

On the other hand, the in-jet soft function up to the NLO is given by [23, 41, 77]:

$$\tilde{S}_i(\mathbf{b}, \mu, \nu \mathcal{R}/2) = 1 + \frac{\alpha_s}{2\pi} C_i \left[-\frac{1}{2} \ln^2 \left(\frac{\mu^2}{\mu_b^2} \right) - \ln \left(\frac{\mu^2}{\mu_b^2} \right) \ln \left(\frac{\nu^2 \tan^2(\mathcal{R}/2)}{\mu^2} \right) - \frac{\pi^2}{12} \right]. \quad (3.20)$$

The corresponding μ - and ν -renormalization group equations are given by:

$$\mu \frac{d}{d\mu} \ln \tilde{S}_i(\mathbf{b}, \mu, \nu \mathcal{R}/2) = \gamma_{\mu,i}^S(b, \mu, \nu \mathcal{R}/2), \quad (3.21)$$

$$\nu \frac{d}{d\nu} \ln \tilde{S}_i(\mathbf{b}, \mu, \nu \mathcal{R}/2) = \gamma_{\nu,i}^S(b, \mu), \quad (3.22)$$

where the anomalous dimensions are given by:

$$\gamma_{\mu,i}^S(b, \mu, \nu \mathcal{R}/2) = -\frac{\alpha_s}{\pi} C_i \ln \left(\frac{\nu^2 \tan^2(\mathcal{R}/2)}{\mu^2} \right), \quad (3.23)$$

$$\gamma_{\nu,i}^S(b, \mu) = -\frac{\alpha_s}{\pi} C_i \ln \left(\frac{\mu^2}{\mu_b^2} \right). \quad (3.24)$$

It is instructive to compare this in-jet soft function \tilde{S}_i with the standard soft function $\tilde{S}_{n\bar{n},i}(\mathbf{b}, \mu, \nu)$, which arises in the TMD factorization for the semi-inclusive deep inelastic scattering (SIDIS) and Drell-Yan production (involving quarks) or for the Higgs production in proton-proton collisions (involving gluons), whose expression is given by:

$$\tilde{S}_{n\bar{n},i}(\mathbf{b}, \mu, \nu) = 1 + \frac{\alpha_s}{\pi} C_i \left[-\frac{1}{2} \ln^2 \left(\frac{\mu^2}{\mu_b^2} \right) - \ln \left(\frac{\mu^2}{\mu_b^2} \right) \ln \left(\frac{\nu^2}{\mu^2} \right) - \frac{\pi^2}{12} \right]. \quad (3.25)$$

After replacing $\nu \rightarrow \nu \tan(\mathcal{R}/2)$, the in-jet soft function \tilde{S}_i is exactly equal to $\sqrt{\tilde{S}_{n\bar{n},i}}$ at the NLO:

$$\tilde{S}_i(\mathbf{b}, \mu, \nu \mathcal{R}/2) = \sqrt{\tilde{S}_{n\bar{n},i}(\mathbf{b}, \mu, \nu)} \Big|_{\nu \rightarrow \nu \tan(\mathcal{R}/2)}. \quad (3.26)$$

Now since the standard ‘‘subtracted’’ TMD FFs are defined as a combination of ‘‘unsubtracted’’ TMD FFs $\tilde{D}_1^{h/i(u)}$ and \tilde{S}_i [13], we would define the ‘‘subtracted’’ in-jet TMD FFs as a product of $\tilde{D}_1^{h/i(u)}$ and \tilde{S}_i as follows:

$$\tilde{D}_1^{h/i}(z_h, \mathbf{b}, \mu, \zeta_J) \equiv \tilde{D}_1^{h/i(u)}(z_h, \mathbf{b}, \mu, \zeta/\nu^2) \tilde{S}_i(\mathbf{b}, \mu, \nu \mathcal{R}/2), \quad (3.27)$$

where the rapidity divergences cancel out between $D_1^{h/i(u)}$ and \tilde{S}_i due to the sign difference shown in Eqs. (3.19) and (3.24). At the same time, we find that a slightly different Collins-Soper scale ζ_J arises in the in-jet “subtracted” TMD FFs, which is related to the Collins-Soper scale ζ for the standard TMD FFs,

$$\sqrt{\zeta_J} \equiv \sqrt{\zeta} \mathcal{R}/2 = p_T R, \quad (3.28)$$

where we have used $\tan(\mathcal{R}/2) \approx \mathcal{R}/2$ for narrow jets with $\mathcal{R} \ll 1$. Note that in our regularization scheme, the natural Collins-Soper scale for TMD FFs is $\sqrt{\zeta} = \omega_J = 2E_J = 2p_T \cosh \eta$ and using $\mathcal{R} = R/\cosh \eta$, we obtain the natural scale $\sqrt{\zeta_J}$ for the unpolarized TMD FJFs, which is simply $p_T R$. With this newly defined Collins-Soper scale ζ_J , following [13, 78], we can thus convert the ν -RG equations above as:

$$\frac{d}{d \ln \sqrt{\zeta_J}} \ln \tilde{D}_1^{h/i}(z_h, \mathbf{b}, \mu, \zeta_J) = \tilde{K}(b, \mu), \quad (3.29)$$

where $\tilde{K}(b, \mu) = -\gamma_{\nu,i}^D(b, \mu)$ in Eq. (3.19) is the so-called Collins-Soper evolution kernel. In the small- b region where $1/b \gg \Lambda_{\text{QCD}}$, it can be computed perturbatively and the four-loop expressions are available in [79, 80]. Notice that $\tilde{K}(b, \mu)$ would become non-perturbative in the large- b region, see recent numerical computations in lattice QCD [81–85]. On the other hand, the standard μ -RG equation is given by:

$$\frac{d}{d \ln \mu} \ln \tilde{D}_1^{h/i}(z_h, \mathbf{b}, \mu, \zeta_J) = \gamma_\mu^i[\alpha_s(\mu), \zeta_J/\mu^2], \quad (3.30)$$

where the anomalous dimension $\gamma_\mu^i[\alpha_s(\mu), \zeta_J/\mu^2]$ are given by:

$$\gamma_\mu^i[\alpha_s(\mu), \zeta_J/\mu^2] = -\Gamma_{\text{cusp}}^i[\alpha_s(\mu)] \ln\left(\frac{\zeta_J}{\mu^2}\right) + \gamma_\mu^i[\alpha_s(\mu)], \quad (3.31)$$

where we have written the more general form [13] with Γ_{cusp}^i and γ_μ^i the cusp and non-cusp anomalous dimensions. They are perturbatively expanded as $\Gamma_{\text{cusp}}^i[\alpha_s] = \sum_{n=1} \Gamma_{n-1}^i \left(\frac{\alpha_s}{4\pi}\right)^n$ and $\gamma_\mu^i[\alpha_s] = \sum_{n=1} \gamma_n^i \left(\frac{\alpha_s}{4\pi}\right)^n$ and at the next-to-leading logarithmic (NLL) order, they are given by [31, 86]:

$$\Gamma_0^q = 4C_F, \quad \Gamma_1^q = 4C_F \left[\left(\frac{67}{9} - \frac{\pi^2}{3} \right) C_A - \frac{20}{9} T_F n_f \right], \quad \gamma_0^q = 6C_F, \quad (3.32)$$

$$\Gamma_{0,1}^g = \frac{C_A}{C_F} \Gamma_{0,1}^q, \quad \gamma_0^g = 2\beta_0. \quad (3.33)$$

One can solve the ζ_J - and μ -RG evolution equation to obtain the “subtracted” in-jet TMD FFs:

$$\begin{aligned} \tilde{D}_1^{h/i}(z_h, \mathbf{b}, \mu, \zeta_J) &= \tilde{D}_1^{h/i}(z_h, \mathbf{b}, \mu_0, \zeta_0) \exp \left[\int_{\mu_0}^{\mu} \frac{d\mu'}{\mu'} \gamma_\mu^i[\alpha_s(\mu), \zeta_J/\mu^2] \right] \\ &\quad \times \exp \left[\tilde{K}(b, \mu_0) \ln \left(\frac{\sqrt{\zeta_J}}{\sqrt{\zeta_0}} \right) \right]. \end{aligned} \quad (3.34)$$

One typically evolves the in-jet TMD FFs $\tilde{D}_1^{h/i}$ from the initial scale $\mu_0 = \sqrt{\zeta_0} = \mu_b$ to the final scale $\mu \sim p_T$ of the jet and $\sqrt{\zeta_J} = p_T R$ as mentioned above. On the other hand, at the initial scale $\mu_0 = \sqrt{\zeta_0} = \mu_b$, one can expand $\tilde{D}_1^{h/i}(z_h, \mathbf{b}, \mu_0, \zeta_0)$ in terms of the corresponding collinear FFs when $\mu_b \gg \Lambda_{\text{QCD}}$.

To generalize the above TMD factorization to the polarized TMD FJFs, let us define the following operator \mathcal{C} :

$$\mathcal{C}[\tilde{D}^{h/i,(n)}] \equiv \int \frac{b^{n+1} db}{2\pi n!} \left(\frac{z_h^2 M_h^2}{j_\perp} \right)^n J_n \left(\frac{j_\perp b}{z_h} \right) \tilde{D}^{h/i,(n)}(z_h, \mathbf{b}, \mu, \zeta_J), \quad (3.35)$$

where $\tilde{D}^{h/i,(n)}$ is n -th moment of the TMD FFs in the Fourier b -space:

$$\tilde{D}^{h/i,(n)}(z_h, \mathbf{b}, \mu, \zeta_J) = \frac{1}{z_h^2} \frac{2\pi n!}{(z_h^2 M_h^2)^n} \int dk_\perp k_\perp \left(\frac{k_\perp}{b} \right)^n J_n \left(\frac{bk_\perp}{z_h} \right) D^{h/i}(z_h, \mathbf{k}_\perp, \mu, \zeta_J). \quad (3.36)$$

In addition, we suppress the superscript (0) when $n = 0$. One can easily verify that with $n = 0$ and $D = D_1$, the combination of Eqs. (3.13) and (3.27) would lead to Eq. (3.36). It is important to realize that each in-jet TMD FF $\tilde{D}^{h/i,(n)}(z_h, \mathbf{b}, \mu, \zeta_J)$ would follow the same Collins-Soper evolution equation as in Eq. (3.29), as well as the same μ -RG equation as in Eq. (3.30). They are identical to the standard TMD FFs with the replacement ζ by ζ_J . Thus, their evolved results would be given exactly by Eq. (3.34), except one replaces $\tilde{D}_1^{h/i}(z_h, \mathbf{b}, \mu, \zeta_J)$ by the corresponding TMD FFs $\tilde{D}^{h/i,(n)}(z_h, \mathbf{b}, \mu, \zeta_J)$ defined above and given below for specific TMD FFs. Note that the evolved in-jet unpolarized TMD FFs $\tilde{D}_1^{h/i}(z_h, \mathbf{b}, \mu, \zeta_J)$ is given by Eq. (3.34), which depends on the TMD FFs $\tilde{D}_1^{h/i}(z_h, \mathbf{b}, \mu_0, \zeta_0)$ at the initial scale μ_0 and ζ_0 . Often, one further matches the TMD FFs at the initial scales onto collinear FFs. For example, the matching coefficients for the unpolarized TMD FFs are known up to N³LO [87, 88]. On the other hand, the matching coefficients for $\tilde{H}_1^{h/q}$ are known up to NNLO [89]. We can now write down the factorization for all the TMD FJFs as:

$$\mathcal{D}_1^{h/c}(z, z_h, \mathbf{j}_\perp, p_T R, \mu, \zeta_J) = \hat{H}_{c \rightarrow i}^U(z, p_T R, \mu) \mathcal{C} \left[\tilde{D}_1^{h/i} \right], \quad (3.37)$$

$$\mathcal{D}_{1T}^{\perp,h/c}(z, z_h, \mathbf{j}_\perp, p_T R, \mu, \zeta_J) = \hat{H}_{c \rightarrow i}^U(z, p_T R, \mu) \mathcal{C} \left[\tilde{D}_{1T}^{\perp,h/i,(1)} \right], \quad (3.38)$$

$$\mathcal{G}_{1L}^{h/c}(z, z_h, \mathbf{j}_\perp, p_T R, \mu, \zeta_J) = \hat{H}_{c \rightarrow i}^L(z, p_T R, \mu) \mathcal{C} \left[\tilde{G}_{1L}^{h/i} \right], \quad (3.39)$$

$$\mathcal{G}_{1T}^{h/c}(z, z_h, \mathbf{j}_\perp, p_T R, \mu, \zeta_J) = \hat{H}_{c \rightarrow i}^L(z, p_T R, \mu) \mathcal{C} \left[\tilde{G}_{1T}^{h/i,(1)} \right], \quad (3.40)$$

$$\mathcal{H}_1^{h/c}(z, z_h, \mathbf{j}_\perp, p_T R, \mu, \zeta_J) = \hat{H}_{c \rightarrow i}^T(z, p_T R, \mu) \mathcal{C} \left[\tilde{H}_1^{h/i} \right], \quad (3.41)$$

$$\mathcal{H}_1^{\perp,h/c}(z, z_h, \mathbf{j}_\perp, p_T R, \mu, \zeta_J) = \hat{H}_{c \rightarrow i}^T(z, p_T R, \mu) \mathcal{C} \left[\tilde{H}_1^{\perp,h/i,(1)} \right], \quad (3.42)$$

$$\mathcal{H}_{1L}^{\perp,h/c}(z, z_h, \mathbf{j}_\perp, p_T R, \mu, \zeta_J) = \hat{H}_{c \rightarrow i}^T(z, p_T R, \mu) \mathcal{C} \left[\tilde{H}_{1L}^{\perp,h/i,(1)} \right], \quad (3.43)$$

$$\mathcal{H}_{1T}^{\perp,h/c}(z, z_h, \mathbf{j}_\perp, p_T R, \mu, \zeta_J) = \hat{H}_{c \rightarrow i}^T(z, p_T R, \mu) \mathcal{C} \left[\tilde{H}_{1T}^{\perp,h/i,(2)} \right]. \quad (3.44)$$

Here the superscripts U , L and T of $\hat{H}_{c \rightarrow i}$ represent unpolarized, longitudinally polarized and transversely polarized hard matching functions, respectively. The hard matching functions will be provided in the next subsection. The above equations also show how various

		Quark polarization		
		U	L	T
Hadron polarization	U	$\mathcal{D}_1 = \text{---} \langle \text{---} \rangle$		$\mathcal{H}_1^\perp = \text{---} \langle \text{---} \rangle - \text{---} \langle \text{---} \rangle$
	L		$\mathcal{G}_{1L} = \text{---} \langle \text{---} \rangle - \text{---} \langle \text{---} \rangle$	$\mathcal{H}_{1L}^\perp = \text{---} \langle \text{---} \rangle - \text{---} \langle \text{---} \rangle$
	T	$\mathcal{D}_{1T}^\perp = \text{---} \langle \text{---} \rangle - \text{---} \langle \text{---} \rangle$	$\mathcal{G}_{1T} = \text{---} \langle \text{---} \rangle - \text{---} \langle \text{---} \rangle$	$\mathcal{H}_1 = \text{---} \langle \text{---} \rangle - \text{---} \langle \text{---} \rangle$ $\mathcal{H}_{1T}^\perp = \text{---} \langle \text{---} \rangle - \text{---} \langle \text{---} \rangle$

Table 1: Summary of the semi-inclusive TMD FJFs. The header row represents the polarization of the quark (indicated by the blue line) that initiates the jet, while the header column indicates the corresponding polarizations of produced hadrons (indicated by the red arrow from the red dot). Shown here is for quark TMD FJFs, with U , L , T representing the unpolarized case, and longitudinal and transverse polarization. For gluon TMD FJFs, one would interpret L , T , as circular and linear polarization [40].

TMD FJFs are matched onto their corresponding TMD FFs, with which the matching of the scenarios listed in Table 1 can be performed.

3.1.2 Hard matching functions

The hard matching functions $\hat{H}_{c \rightarrow i}^{U,L,T}$ describe the out-of-jet radiation during which an energetic parton c , generated in a hard scattering event, undergoes a splitting into a parton i , which subsequently initiates a jet with energy ω_J and radius R . The hard matching functions for the unpolarized case $\hat{H}_{c \rightarrow i}^U$ are available previously [21, 59, 65, 90]. They describe the splitting from an unpolarized initial parton c to an unpolarized parton i , irrespective of the polarization of the final-state hadron inside the jet. Because of that, we would have the same hard matching functions for both unpolarized TMD FJFs $\mathcal{D}_1^{h/c}$ and the polarized TMD FJFs $\mathcal{D}_{1T}^{\perp,h/c}$, as indicated in Eqs. (3.37) and (3.38). We remind the reader that $\mathcal{D}_{1T}^{\perp,h/c}$ stands for the situation where an unpolarized parton c splits into an unpolarized parton i that fragments into a transversely polarized hadron h . This arises from the correlation between the hadron's transverse momentum with respect to the jet axis and the transverse spin of the hadron itself. For the same reasons, we have the same longitudinally polarized hard matching functions $\hat{H}_{c \rightarrow i}^L$ for the TMD FJFs $\mathcal{G}_{1L}^{h/c}$ and $\mathcal{G}_{1T}^{h/c}$, as indicated in Eqs. (3.39) and (3.40). Likewise, we have the same transversely polarized hard matching functions $\hat{H}_{c \rightarrow i}^T$ for the TMD FJFs $\mathcal{H}_1^{h/c}$, $\mathcal{H}_1^{\perp,h/c}$, $\mathcal{H}_{1L}^{\perp,h/c}$, and $\mathcal{H}_{1T}^{\perp,h/c}$, as indicated in Eqs. (3.41) to (3.44). Looking at Table 1, the FJFs listed in the same column possess identical hard matching functions, due to the fact that the parton polarization is the same in the same column.

For completeness, we list the unpolarized results $\hat{H}_{c \rightarrow i}^U$ here. We then provide in addition the results $\hat{H}_{c \rightarrow i}^{L,T}$ for the polarized cases.

$$\begin{aligned} \hat{H}_{q \rightarrow q'}^U(z, p_T R, \mu) &= \delta_{qq'} \delta(1-z) + \delta_{qq'} \frac{\alpha_s}{2\pi} \left[C_F \delta(1-z) \left(-\frac{L^2}{2} - \frac{3}{2}L + \frac{\pi^2}{12} \right) \right. \\ &\quad \left. + P_{qq}(z)L - 2C_F(1+z^2) \left(\frac{\ln(1-z)}{1-z} \right)_+ - C_F(1-z) \right], \end{aligned} \quad (3.45)$$

$$\hat{H}_{q \rightarrow g}^U(z, p_T R, \mu) = \frac{\alpha_s}{2\pi} \left[(L - 2\ln(1-z)) P_{gq}(z) - C_F z \right], \quad (3.46)$$

$$\begin{aligned} \hat{H}_{g \rightarrow g}^U(z, p_T R, \mu) &= \delta(1-z) + \frac{\alpha_s}{2\pi} \left[\delta(1-z) \left(-C_A \frac{L^2}{2} - \frac{\beta_0}{2}L + C_A \frac{\pi^2}{12} \right) \right. \\ &\quad \left. + P_{gg}(z)L - \frac{4C_A(1-z+z^2)^2}{z} \left(\frac{\ln(1-z)}{1-z} \right)_+ \right], \end{aligned} \quad (3.47)$$

$$\hat{H}_{g \rightarrow q}^U(z, p_T R, \mu) = \frac{\alpha_s}{2\pi} \left[(L - 2\ln(1-z)) P_{gq}(z) - 2T_F z(1-z) \right], \quad (3.48)$$

where the leading splitting kernels are given by:

$$P_{qq}(z) = C_F \left[\frac{1+z^2}{(1-z)_+} + \frac{3}{2} \delta(1-z) \right], \quad (3.49)$$

$$P_{gq}(z) = C_F \frac{1+(1-z)^2}{z}, \quad (3.50)$$

$$P_{qg}(z) = T_F [z^2 + (1-z)^2], \quad (3.51)$$

$$P_{gg}(z) = 2C_A \left[\frac{z}{(1-z)_+} + \frac{1-z}{z} + z(1-z) \right] + \frac{\beta_0}{2} \delta(1-z). \quad (3.52)$$

The hard matching functions for the longitudinally polarized parton case are given here for the first time:

$$\begin{aligned} \hat{H}_{q \rightarrow q'}^L(z, p_T R, \mu) &= \delta_{qq'} \delta(1-z) + \delta_{qq'} \frac{\alpha_s}{2\pi} \left[C_F \delta(1-z) \left(-\frac{L^2}{2} - \frac{3}{2}L + \frac{\pi^2}{12} \right) \right. \\ &\quad \left. + \Delta P_{qq}(z)L - 2C_F(1+z^2) \left(\frac{\ln(1-z)}{1-z} \right)_+ - C_F(1-z) \right], \end{aligned} \quad (3.53)$$

$$\hat{H}_{q \rightarrow g}^L(z, p_T R, \mu) = \frac{\alpha_s}{2\pi} \left[(L - 2\ln(1-z)) \Delta P_{gq}(z) + 2C_F(1-z) \right], \quad (3.54)$$

$$\begin{aligned} \hat{H}_{g \rightarrow g}^L(z, p_T R, \mu) &= \delta(1-z) + \frac{\alpha_s}{2\pi} \left[\delta(1-z) \left(-C_A \frac{L^2}{2} - \frac{\beta_0}{2}L + C_A \frac{\pi^2}{12} \right) \right. \\ &\quad \left. + \Delta P_{gg}(z)L + 4C_A(1-z) - 4C_A(2(1-z)^2 + z) \left(\frac{\ln(1-z)}{1-z} \right)_+ \right], \end{aligned} \quad (3.55)$$

$$\hat{H}_{g \rightarrow q}^L(z, p_T R, \mu) = \frac{\alpha_s}{2\pi} \left[(L - 2\ln(1-z)) \Delta P_{gq}(z) - 2T_F(1-z) \right], \quad (3.56)$$

Finally, for the transversely polarized case, we only have contributions from the $q \rightarrow q$ channel, for the same reason mentioned before: gluon transversity FFs do not exist for

spin-1/2 hadron. The transversely polarized hard matching function is then given by:

$$\begin{aligned} \hat{H}_{q \rightarrow q'}^T(z, p_T R, \mu) = & \delta_{qq'} \delta(1-z) + \delta_{qq'} \frac{\alpha_s}{2\pi} \left\{ \Delta_T P_{qq}(z) L + C_F \left[-4z \left(\frac{\ln(1-z)}{1-z} \right)_+ \right. \right. \\ & \left. \left. + \left(-\frac{3}{2}L - \frac{L^2}{2} + \frac{\pi^2}{12} \right) \delta(1-z) \right] \right\}. \end{aligned} \quad (3.57)$$

Note that the leading order splitting kernels for the polarized cases are given in Eqs. (2.28) to (2.32).

The hard matching functions $\hat{H}_{i \rightarrow j}^{U,L,T}(z, p_T R, \mu)$ follow the RG equations below:

$$\mu \frac{d}{d\mu} \hat{H}_{i \rightarrow j}^U(z, p_T R, \mu) = \sum_k \int_z^1 \frac{dz'}{z'} \gamma_{ik}^U \left(\frac{z}{z'}, p_T R, \mu \right) \hat{H}_{k \rightarrow j}^U(z', p_T R, \mu), \quad (3.58)$$

$$\mu \frac{d}{d\mu} \hat{H}_{i \rightarrow j}^L(z, p_T R, \mu) = \sum_k \int_z^1 \frac{dz'}{z'} \gamma_{ik}^L \left(\frac{z}{z'}, p_T R, \mu \right) \hat{H}_{k \rightarrow j}^L(z', p_T R, \mu), \quad (3.59)$$

$$\mu \frac{d}{d\mu} \hat{H}_{q \rightarrow q'}^T(z, p_T R, \mu) = \int_z^1 \frac{dz'}{z'} \gamma_{qq}^T \left(\frac{z}{z'}, p_T R, \mu \right) \hat{H}_{q \rightarrow q'}^T(z', p_T R, \mu), \quad (3.60)$$

where indices i, j and k all represent partons q or g . For the unpolarized hard matching functions, their anomalous dimensions $\gamma_{ij}^U(z, p_T R, \mu)$ are given by:

$$\gamma_{qq}^U(z, p_T R, \mu) = \frac{\alpha_s}{\pi} \left(P_{qq}(z) - C_F L \delta(1-z) - \frac{3C_F}{2} \delta(1-z) \right), \quad (3.61)$$

$$\gamma_{qg}^U(z, p_T R, \mu) = \frac{\alpha_s}{\pi} P_{gq}(z), \quad (3.62)$$

$$\gamma_{gg}^U(z, p_T R, \mu) = \frac{\alpha_s}{\pi} \left(P_{gg}(z) - C_A L \delta(1-z) - \frac{\beta_0}{2} \delta(1-z) \right), \quad (3.63)$$

$$\gamma_{gq}^U(z, p_T R, \mu) = \frac{\alpha_s}{\pi} P_{qg}(z). \quad (3.64)$$

On the other hand, the anomalous dimensions for the polarized cases, $\gamma_{ij}^{L(T)}(z, p_T R, \mu)$ are given by:

$$\gamma_{qq}^L(z, p_T R, \mu) = \frac{\alpha_s}{\pi} \left(\Delta P_{qq}(z) - C_F L \delta(1-z) - \frac{3C_F}{2} \delta(1-z) \right), \quad (3.65)$$

$$\gamma_{qg}^L(z, p_T R, \mu) = \frac{\alpha_s}{\pi} \Delta P_{gq}(z), \quad (3.66)$$

$$\gamma_{gg}^L(z, p_T R, \mu) = \frac{\alpha_s}{\pi} \left(\Delta P_{gg}(z) - C_A L \delta(1-z) - \frac{\beta_0}{2} \delta(1-z) \right), \quad (3.67)$$

$$\gamma_{gq}^L(z, p_T R, \mu) = \frac{\alpha_s}{\pi} \Delta P_{qg}(z), \quad (3.68)$$

$$\gamma_{qq}^T(z, p_T R, \mu) = \frac{\alpha_s}{\pi} \left(\Delta_T P_{qq}(z) - C_F L \delta(1-z) - \frac{3C_F}{2} \delta(1-z) \right). \quad (3.69)$$

Obviously, the natural scale for the hard matching functions is $\mu \sim p_T R$ as indicated in the logarithm L in the perturbative results. Therefore, we can resum the large logarithms of jet radius $\ln R$ by evolving the hard matching functions from scale $\mu \sim p_T R$ to the hard

scattering scale $\mu \sim p_T$ with the RG equations. We notice that similar to the unpolarized case studied in [23]:

$$\gamma_{ij}^U(z, p_T R, \mu) = \delta_{ij} \delta(1-z) \Gamma_i(p_T R, \mu) + \frac{\alpha_s}{\pi} P_{ji}(z), \quad (3.70)$$

where Γ_i are given by:

$$\Gamma_q(p_T R, \mu) = \frac{\alpha_s}{\pi} C_F \left(-L - \frac{3}{2} \right), \quad \Gamma_g(p_T R, \mu) = \frac{\alpha_s}{\pi} C_A \left(-L - \frac{\beta_0}{2C_A} \right). \quad (3.71)$$

Following the same exercise, we can express the anomalous dimensions $\gamma_{ij}^{L(T)}(z, p_T R, \mu)$ in Eqs. (3.65) to (3.69) into a general form:

$$\gamma_{ij}^{L(T)}(z, p_T R, \mu) = \delta_{ij} \delta(1-z) \Gamma_i(p_T R, \mu) + \frac{\alpha_s}{\pi} \Delta_{(T)} P_{ji}(z), \quad (3.72)$$

where the functions $\Gamma_i(p_T R, \mu)$ in the first term are independent of polarization and are therefore the same as the unpolarized Γ_i in Eq. (3.71).

3.2 TMD FJFs in exclusive jet production

For the exclusive jet production, exclusive TMD FJFs $\tilde{\mathcal{D}}_1^{h/i}(z_h, \mathbf{j}_\perp, p_T R, \mu, \zeta_J)$ arises in the factorization formalism. Since one cannot have out-of-jet hard radiation as explained in Section 2.2, the factorization formalism in the $j_\perp \ll p_T R$ region would be given by

$$\begin{aligned} \tilde{\mathcal{D}}_1^{h/i}(z_h, \mathbf{j}_\perp, p_T R, \mu, \zeta_J) &= \int d^2 \mathbf{k}_\perp d^2 \boldsymbol{\lambda}_\perp \delta^2(z_h \boldsymbol{\lambda}_\perp + \mathbf{k}_\perp - \mathbf{j}_\perp) D_1^{h/i(u)} \left(z_h, \mathbf{k}_\perp, \mu, \frac{\zeta}{\nu^2} \right) S_i \left(\boldsymbol{\lambda}_\perp, \mu, \frac{\nu \mathcal{R}}{2} \right) \\ &= \int \frac{d^2 \mathbf{b}}{(2\pi)^2} e^{i \mathbf{j}_\perp \cdot \mathbf{b} / z_h} \tilde{D}_1^{h/i}(z_h, \mathbf{b}, \mu, \zeta_J), \end{aligned} \quad (3.73)$$

where we have used Eq. (3.27). Again for exclusive jet production, we no longer have the dependence on z as in the semi-inclusive TMD FJFs. Following the same procedure as before, we can generalize this to the polarized exclusive TMD FJFs. With the operator \mathcal{C} defined in Eq. (3.35), the unpolarized exclusive TMD FJFs are given by:

$$\tilde{\mathcal{D}}_1^{h/i}(z_h, p_T R, \mathbf{j}_\perp, \mu, \zeta_J) = \mathcal{C} \left[\tilde{D}_1^{h/i} \right], \quad (3.74)$$

Similarly for exclusive TMD FJFs with different polarizations, we have:

$$\tilde{\mathcal{D}}_{1T}^{\perp, h/i}(z_h, \mathbf{j}_\perp, p_T R, \mu, \zeta_J) = \mathcal{C} \left[\tilde{D}_{1T}^{\perp, h/i, (1)} \right], \quad (3.75)$$

$$\tilde{\mathcal{G}}_{1L}^{h/i}(z_h, \mathbf{j}_\perp, p_T R, \mu, \zeta_J) = \mathcal{C} \left[\tilde{G}_{1L}^{h/i} \right], \quad (3.76)$$

$$\tilde{\mathcal{G}}_{1T}^{\perp, h/i}(z_h, \mathbf{j}_\perp, p_T R, \mu, \zeta_J) = \mathcal{C} \left[\tilde{G}_{1T}^{\perp, h/i, (1)} \right], \quad (3.77)$$

$$\tilde{\mathcal{H}}_1^{h/i}(z_h, \mathbf{j}_\perp, p_T R, \mu, \zeta_J) = \mathcal{C} \left[\tilde{H}_1^{h/i} \right], \quad (3.78)$$

$$\tilde{\mathcal{H}}_1^{\perp, h/i}(z_h, \mathbf{j}_\perp, p_T R, \mu, \zeta_J) = \mathcal{C} \left[\tilde{H}_1^{\perp, h/i, (1)} \right], \quad (3.79)$$

$$\tilde{\mathcal{H}}_{1L}^{\perp, h/i}(z_h, \mathbf{j}_\perp, p_T R, \mu, \zeta_J) = \mathcal{C} \left[\tilde{H}_{1L}^{\perp, h/i, (1)} \right], \quad (3.80)$$

$$\tilde{\mathcal{H}}_{1T}^{\perp, h/i}(z_h, \mathbf{j}_\perp, p_T R, \mu, \zeta_J) = \mathcal{C} \left[\tilde{H}_{1T}^{\perp, h/i, (2)} \right]. \quad (3.81)$$

4 Phenomenology

There has been growing phenomenological work for studying hadron distribution inside the jet, in particular in connection with the 3D imaging of the hadrons. For example, for single inclusive jet production in proton-proton collisions as well as electron-proton scatterings, unpolarized and polarized collinear hadron distribution inside the jet have been studied [21, 25, 34, 43]. The TMD distribution of hadrons inside the jet produced in transversely polarized proton-proton collisions is sensitive to the Collins TMD FFs and has been studied in [91]. For exclusive jet production, such as back-to-back Z +jet production in proton-proton collisions and back-to-back lepton+jet production in DIS, TMD hadron distribution inside jets has been studied [27, 41, 42, 92, 93].

Before we present the phenomenology, we first provide more details on TMD FFs. In previous sections, we have discussed the evolution of FJFs in the perturbative region, *i.e.*, $1/b \gg \Lambda_{\text{QCD}}$. However, to do calculations for phenomenology, we must take care of the non-perturbative evolution of TMDs at the large- b region. In order to do this, we adopt the b_* -prescription [94]. Alternative approaches can be found in [95–99]. The b_* is defined as:

$$b_* \equiv \frac{b}{\sqrt{1 + b^2/b_{\text{max}}^2}}, \quad (4.1)$$

where we choose $b_{\text{max}} = 1.5 \text{ GeV}^{-1}$. With this definition, the magnitude of b_* approaches b when $b \ll b_{\text{max}}$, and approaches b_{max} in the large- b region. For the perturbative contribution, we work at the NLL order, where we keep $\Gamma_{0,1}^i$ and γ_0^i in Eqs. (3.31) and (3.34). For the non-perturbative contribution, we include the following non-perturbative Sudakov factor [100, 101]:

$$S_{\text{NP}}^q(b, Q_0, \sqrt{\zeta_J}) = \frac{g_2}{2} \ln\left(\frac{b}{b_*}\right) \ln\left(\frac{\sqrt{\zeta_J}}{Q_0}\right) + \frac{g_h}{z_h^2} b^2, \quad (4.2)$$

where $Q_0^2 = 2.4 \text{ GeV}^2$, $g_2 = 0.84$ and $g_h = 0.042$, and $\sqrt{\zeta_J} = p_T R$ following Eq. (3.28). For gluon TMD FFs, we use [23]:

$$S_{\text{NP}}^g(b, Q_0, \sqrt{\zeta_J}) = \frac{C_A}{C_F} \frac{g_2}{2} \ln\left(\frac{b}{b_*}\right) \ln\left(\frac{\sqrt{\zeta_J}}{Q_0}\right) + \frac{g_h}{z_h^2} b^2. \quad (4.3)$$

Now that we have properly addressed the non-perturbative evolution, we can proceed with predicting relevant observables. In this section, we provide two additional phenomenological examples. For the case of single inclusive jet production, we compute the transverse momentum distribution for hadrons inside the jet at RHIC kinematics, where a transversely polarized proton collides with an unpolarized proton, producing a jet with a transversely polarized Λ -baryon inside. This process will be sensitive to both transversity distributions h_1 and transversity TMD FJFs \mathcal{H}_1 . For the exclusive jet production, we study back-to-back lepton jet production in lepton-proton collisions, where the incoming proton is transversely polarized and the final hadron inside the jet is longitudinally polarized. This observable is sensitive to the “worm-gear” TMD PDFs g_{1T} and longitudinally polarized TMD FJFs \mathcal{G}_{1L} .

4.1 Transverse spin transfer to Λ in jet in polarized pp collisions

For semi-inclusive process, we consider the pp collision in its center-of-mass frame:

$$p(P_A, S_A) + p(P_B) \rightarrow [\text{jet}(p_J)h(z_h, \mathbf{j}_\perp, S_h)] + X, \quad (4.4)$$

where P_A and P_B are the momenta of the incident protons, S_A is the polarization of the proton A . They are defined as:

$$P_A = \frac{\sqrt{s}}{2}(1, 0, 0, 1), \quad P_B = \frac{\sqrt{s}}{2}(1, 0, 0, -1), \quad (4.5)$$

$$S_A = \left[-\lambda_A \frac{M_A}{p_A^-}, \lambda_A \frac{p_A^-}{M_A}, \mathbf{S}_T \right], \quad (4.6)$$

where s is the squared proton center of mass energy. Notice that S_A is written in light-cone coordinate defined in Eq. (2.3), and λ_A is the helicity of the incoming proton with mass M_A , p_A^- is the large light-cone momentum of the proton A , ϕ_S is the azimuthal angle between the transverse spin \mathbf{S}_T of the initial proton and the reaction plane, with the reaction plane defined by the incoming beam direction and jet axis direction (painted yellow in Fig. 5). For the jet production, p_J is the jet momentum, with p_T being the magnitude of its transverse component:

$$p_J = (p_T \cosh \eta, p_T, 0, p_T \sinh \eta). \quad (4.7)$$

Note here the y -component of p_J is zero because we put the jet within the reaction plane (xz -plane). The hadron inside the jet has a transverse momentum \mathbf{j}_\perp with respect to the jet axis, and collinear momentum fraction z_h of the jet momentum. Together with the hadron's transverse spin $\mathbf{S}_{h\perp}$, they are given by:

$$\mathbf{j}_\perp = |\mathbf{j}_\perp| (\cos \hat{\phi}_h \cos \theta_J, \sin \hat{\phi}_h, -\cos \hat{\phi}_h \sin \theta_J), \quad (4.8)$$

$$\mathbf{S}_{h\perp} = |\mathbf{S}_{h\perp}| (\cos \hat{\phi}_{S_h} \cos \theta_J, \sin \hat{\phi}_{S_h}, -\cos \hat{\phi}_{S_h} \sin \theta_J), \quad (4.9)$$

where θ_J is the angle between jet axis and z -axis, $\hat{\phi}_h$ is the azimuthal angle between the momentum p_h of the produced hadron and the reaction plane, and $\hat{\phi}_{S_h}$ is the azimuthal angle between the transverse spin $\mathbf{S}_{h\perp}$ and the reaction plane. The ‘‘hat’’ that decorates $\hat{\phi}_h$ and $\hat{\phi}_{S_h}$ indicates that these angles are measured in the jet coordinates.

For single inclusive jet production, the most general azimuthal dependence⁴ for the hadron z_h and \mathbf{j}_\perp distributions inside the jet is given by [34]:

$$\begin{aligned} \frac{d\sigma^{p(S_A)+p \rightarrow \text{jet}h(S_h)+X}}{d\eta d^2\mathbf{p}_T dz_h d^2\mathbf{j}_\perp} &= F_{UU,U} + |\mathbf{S}_T| \sin(\phi_S - \hat{\phi}_h) F_{TU,U}^{\sin(\phi_S - \hat{\phi}_h)} \\ &+ \lambda_h \left[\lambda_A F_{LU,L} + |\mathbf{S}_T| \cos(\phi_S - \hat{\phi}_h) F_{TU,L}^{\cos(\phi_S - \hat{\phi}_h)} \right] \\ &+ |\mathbf{S}_{h\perp}| \left[\sin(\hat{\phi}_h - \hat{\phi}_{S_h}) F_{UU,T}^{\sin(\hat{\phi}_h - \hat{\phi}_{S_h})} + \lambda_A \cos(\hat{\phi}_h - \hat{\phi}_{S_h}) F_{LU,T}^{\cos(\hat{\phi}_h - \hat{\phi}_{S_h})} \right] \end{aligned}$$

⁴Here we consider the situation where only one of the incoming hadrons could be polarized and the final-state hadron can be polarized.

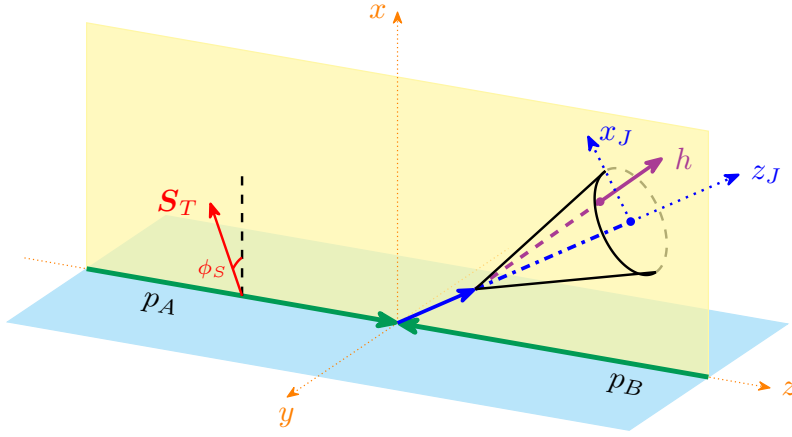


Figure 5: Illustration for the distribution of hadrons inside jets in the collisions of a polarized proton and an unpolarized proton or lepton. The reaction plane is painted yellow. For detailed illustration of jet cone and hadron kinematics, please see Fig. 3.

$$+ |\mathbf{S}_T| \left[\cos(\phi_S - \hat{\phi}_{S_h}) F_{TU,T}^{\cos(\phi_S - \hat{\phi}_{S_h})} + \cos(2\hat{\phi}_h - \phi_S - \hat{\phi}_{S_h}) F_{TU,T}^{\cos(2\hat{\phi}_h - \phi_S - \hat{\phi}_{S_h})} \right], \quad (4.10)$$

where $F_{AB,C}$ denotes the spin-dependent structure functions, with A , B and C indicating the polarization of incoming proton A , incoming proton B (or electron), and the fragmented hadron inside the jet. λ_A and $|\mathbf{S}_\perp|$ are the longitudinal and transverse spin of the initial polarized proton A , while λ_h and $|\mathbf{S}_{h_T}|$ are the longitudinal and transverse polarization of the hadron inside jet measured in the fragmenting parton helicity frame.

The structure function $F_{UU,U}(z_h, \mathbf{j}_\perp)$ is defined by:

$$\begin{aligned} F_{UU,U}(z_h, \mathbf{j}_\perp) &= \frac{\alpha_s^2}{s} \sum_{a,b,c} \int_{x_1^{\min}}^1 \frac{dx_1}{x_1} f_1^{a/A}(x_1, \mu) \int_{x_2^{\min}}^1 \frac{dx_2}{x_2} f_2^{b/B}(x_2, \mu) \\ &\quad \times \int_{z^{\min}}^1 \frac{dz}{z^2} \hat{\sigma}_{ab}^c(\hat{s}, \hat{p}_T, \hat{\eta}, \mu) \mathcal{D}_1^{h/c}(z, z_h, \mathbf{j}_\perp, p_T R, \mu, \zeta_J) \\ &\equiv \mathcal{C}[ff\mathcal{D}_1\hat{\sigma}], \end{aligned} \quad (4.11)$$

where $f_1^{a/A}(x_1, \mu)$ and $f_2^{b/B}(x_2, \mu)$ are the collinear unpolarized PDFs in the proton with corresponding momentum fractions x_1 and x_2 , and $\hat{\sigma}_{ab}^c$ is the hard function for unpolarized parton a , b to unpolarized parton c . On the other hand, $\mathcal{D}_1^{h/c}(z, z_h, \mathbf{j}_\perp, p_T R, \mu, \zeta_J)$ are the unpolarized TMD FJFs in Eq. (3.12) and we have studied extensively in the previous section. The lower integration limits x_1^{\min} , x_2^{\min} and z^{\min} can be found in [21, 25]. The variables \hat{s} , \hat{p}_T and $\hat{\eta}$ are the squared parton center of mass energy, transverse momentum and rapidity of parton c , respectively, and are related to their hadron analogues as:

$$\hat{s} = x_1 x_2 s, \quad \hat{p}_T = p_T / z, \quad \hat{\eta} = \eta - \frac{1}{2} \ln\left(\frac{x_1}{x_2}\right). \quad (4.12)$$

	a	U	L	T
c				
U	$\hat{\sigma}_{ab}^c$			
L		$\Delta\hat{\sigma}_{ab}^c$		
T				$\Delta_T\hat{\sigma}_{ab}^c$

Table 2: Hard functions for parton a , b to parton c . The header row represents the polarization of the parton a while the header column indicates the polarizations of the parton c . Parton b is always unpolarized.

In Eq. (4.11), we also defined the notation $\mathcal{C}[ff\mathcal{D}_1\hat{\sigma}]$, where parton flavors are summed for PDFs and FJFs along with their corresponding unpolarized hard functions. Using this notation, we can write down the expressions for all the polarized structure functions:

$$F_{TU,U}^{\sin(\phi_S-\hat{\phi}_h)}(z_h, j_\perp) = \mathcal{C}\left[\frac{j_\perp}{z_h M_h} h_1 f_1 \mathcal{H}_1^\perp \Delta_T \hat{\sigma}\right], \quad (4.13)$$

$$F_{LU,L}(z_h, j_\perp) = \mathcal{C}\left[g_{1L} f_1 \mathcal{G}_{1L} \Delta \hat{\sigma}\right], \quad (4.14)$$

$$F_{TU,L}^{\cos(\phi_S-\hat{\phi}_h)}(z_h, j_\perp) = -\mathcal{C}\left[\frac{j_\perp}{z_h M_h} h_1 f_1 \mathcal{H}_{1L}^\perp \Delta_T \hat{\sigma}\right], \quad (4.15)$$

$$F_{UU,T}^{\sin(\hat{\phi}_h-\hat{\phi}_{S_h})}(z_h, j_\perp) = -\mathcal{C}\left[\frac{j_\perp}{z_h M_h} f_1 f_1 \mathcal{D}_{1T}^\perp \hat{\sigma}\right], \quad (4.16)$$

$$F_{LU,T}^{\cos(\hat{\phi}_h-\hat{\phi}_{S_h})}(z_h, j_\perp) = -\mathcal{C}\left[\frac{j_\perp}{z_h M_h} g_{1L} f_1 \mathcal{G}_{1T} \Delta \hat{\sigma}\right], \quad (4.17)$$

$$F_{TU,T}^{\cos(\phi_S-\hat{\phi}_{S_h})}(z_h, j_\perp) = \mathcal{C}\left[h_1 f_1 \mathcal{H}_1 \Delta_T \hat{\sigma}\right], \quad (4.18)$$

$$F_{TU,T}^{\cos(2\hat{\phi}_h-\phi_S-\hat{\phi}_{S_h})}(z_h, j_\perp) = -\mathcal{C}\left[\frac{j_\perp^2}{2z_h^2 M_h^2} h_1 f_1 \mathcal{H}_{1T}^\perp \Delta_T \hat{\sigma}\right]. \quad (4.19)$$

The corresponding polarizations for hard functions $\hat{\sigma}_{ab}^c$, $\Delta\hat{\sigma}_{ab}^c$ and $\Delta_T\hat{\sigma}_{ab}^c$ are given in Table 2. The expressions for $F_{UU,U}$ and $F_{UU,T}^{\sin(\hat{\phi}_h-\hat{\phi}_{S_h})}$ were given in the previous publication [34] while [91] performed a phenomenological study for $F_{TU,U}^{\sin(\phi_S-\hat{\phi}_h)}$, that is related to the Collins TMD FFs. The detailed expressions for all the other structure functions are written down here for the first time.

Relevant measurements have been performed for the π^\pm -in-jet production in the case of Collins FFs [102]. More relevantly, a measurement of transverse spin transfer to $\Lambda/\bar{\Lambda}$ hyperons in polarized pp collisions (no jet is involved) was performed by the STAR collaboration at RHIC [103]. This suggests that measuring the transverse polarization of $\Lambda/\bar{\Lambda}$ hyperons inside the jet in transversely polarized pp collisions could be achieved at RHIC. This process would correspond to the structure function $F_{TU,T}^{\cos(\phi_S-\hat{\phi}_{S_h})}$, which is sensitive to both transversity PDFs h_1 and transversity TMD FJFs $\mathcal{H}_1^{h/q}$. Below, we focus on this structure function and define the following spin asymmetry for Λ -in-jet productions:

$$A_{TU,T}^{\cos(\phi_S-\hat{\phi}_{S_h})} \equiv F_{TU,T}^{\cos(\phi_S-\hat{\phi}_{S_h})} \Big/ F_{UU,U}. \quad (4.20)$$

In order to compute $F_{TU,T}^{\cos(\hat{\phi}_h - \hat{\phi}_{S_h})}$, we will need to parameterize the collinear transversity PDF $h_1(x, \mu)$, which appears in the initial state of $F_{TU,T}^{\cos(\phi_S - \hat{\phi}_{S_h})}$ in Eq. (4.18). For this, we follow the parameterization in [104] and write the quark transversity as:

$$h_1^q(x, Q_0) = N_q^h x^{a_q} (1-x)^{b_q} \frac{(a_q + b_q)^{a_q + b_q}}{a_q^{a_q} b_q^{b_q}} \frac{1}{2} (f_1^q(x, Q_0) + g_1^q(x, Q_0)), \quad (4.21)$$

at initial scale $Q_0 = 1.27$ GeV, for up and down quarks $q = u$ and d only. The f_1^q and g_1^q are the collinear unpolarized and helicity parton distributions respectively, for which we use the parameters from [105]. Lastly, in the generation of TMD FFs grids, we also need the transversity FFs. In this work we use the parameterization from [42], which assumes a simple normalization of the collinear unpolarized FFs:

$$H_{\Lambda/q}(z, Q) = N_q^H D_{\Lambda/q}(z, Q). \quad (4.22)$$

Here $H_{\Lambda/q}$ and $D_{\Lambda/q}$ are the transversity and unpolarized FFs of the Λ baryon, and N_q^H is the fitted parameter. We also follow the assumptions made in [42, 106] and demand:

$$D_{\Lambda/q} = D_{\bar{\Lambda}/q} = \frac{1}{2} D_{\Lambda/\bar{\Lambda} \leftarrow q}, \quad (4.23)$$

as for the unpolarized Λ baryon FFs that appear in the denominator of $A_{TU,T}^{\cos(\phi_S - \hat{\phi}_{S_h})}$, we use the AKK parametrization [107]. For both the transversity PDFs and transversity FFs, we also vary their fitted parameters according to the extracted uncertainties, weighted by Gaussian random number with a mean of 0 and variance of 1.

Using the above setup, we now present the first prediction for the spin asymmetry $A_{TU,T}^{\cos(\phi_S - \hat{\phi}_{S_h})}$. We choose the jet kinematics consistent with the available data from STAR [102], with the center of mass energy at $\sqrt{s} = 200$ GeV, rapidity ranges $\eta \in (0, 0.9)$ and $\eta \in (-0.9, 0)$. The jets are reconstructed using the anti- k_T algorithm with radius $R = 0.6$. The numerical implementation is very similar to that used in the longitudinal momentum distribution of hadrons inside jets [21], with the numerical DGLAP evolution tool developed in PEGASUS [108]. The RG evolution of the various parts of the cross sections is performed as outlined in [23].

In Fig. 6, the prediction to $A_{TU,T}^{\cos(\phi_S - \hat{\phi}_{S_h})}$ for the jet(Λ) production at RHIC kinematics is presented. The blue band is obtained by varying the fitted parameters of both transversity PDFs and transversity FFs, while the yellow band is obtained by varying the parameters of transversity PDFs only (with parameters for transversity FFs fixed at central values). We can therefore deduce that the uncertainty of theoretical prediction for the observable $A_{TU,T}^{\cos(\phi_S - \hat{\phi}_{S_h})}$ comes largely from the transversity FFs, *i.e.*, variation of N_q^H in Eq. (4.22). Given the large uncertainty resulting from the currently available extraction of the transversity FFs for Λ baryon, this observable, when measured in the future, can be used to constrain the uncertainty on the Λ transversity FFs. In Fig. 7, the same predictions are presented but with a negative rapidity range. Similar patterns occur as in Fig. 6, but with a much smaller

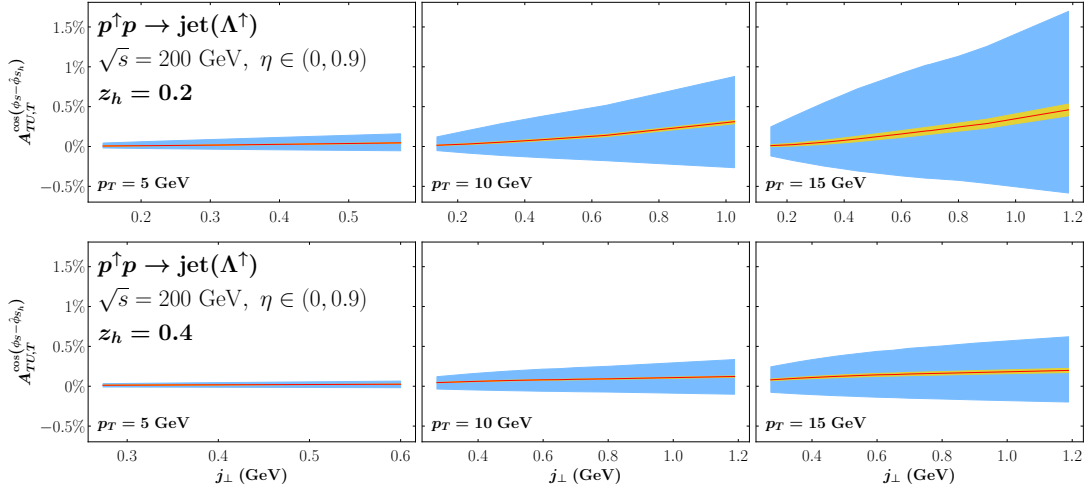


Figure 6: Hadron j_1 -distribution within jets in pp collisions at $\sqrt{s} = 200$ GeV. Jets are detected in the rapidity interval $\eta \in (0, 0.9)$ (*i.e.*, the jet is scattered forward relative to the polarized beam), and are reconstructed using the anti- k_T algorithm with $R = 0.6$. We vary the jet transverse momentum from 5 to 15 GeV, and choose average z_h at 0.2 (top row) and 0.4 (bottom row), which is within the typical kinematic region according to [102]. The blue band is obtained by varying the parameters for transversity PDFs and transversity FFs within their fitted uncertainties. While the yellow band is obtained by keeping the fitted parameters of transversity FFs fixed at their central values and varying only the parameters of transversity PDFs. The red lines show the theory obtained from the central of the fitted parameters.

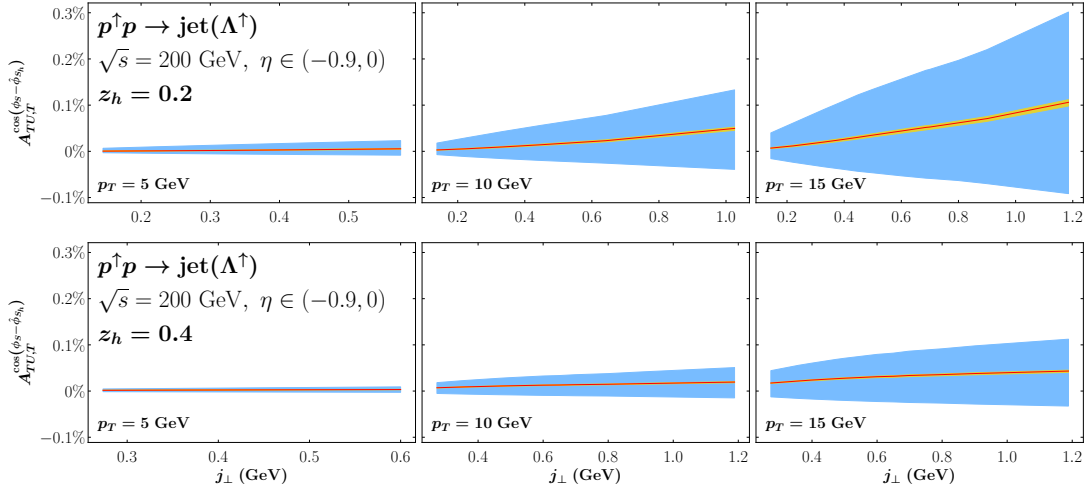


Figure 7: Same plot as Fig. 6, but with jet scattered backward relative to the polarized beam.

magnitude, indicating a much smaller probability of producing polarized final particles in the opposite direction of the polarized beam.

Overall, in proton-proton collisions for Λ -in-jet production, where one of the proton beams is transversely polarized, and the resulting Lambda particles in the jet also exhibit transverse polarization, a distinct observation emerges. Specifically, in the forward region (positive rapidity), a moderate spin asymmetry $A_{TU,T}^{\cos(\phi_S-\hat{\phi}_{S_h})} \sim 1.5\%$ can be observed at RHIC kinematics, while in the backward region (negative rapidity), the spin asymmetry $A_{TU,T}^{\cos(\phi_S-\hat{\phi}_{S_h})}$ appears to be very small. This is largely due to the probing x range for the transversity PDF $h_1(x, \mu)$: in the forward rapidity region $x \sim 0.2$ at $p_T \sim 15$ GeV where $h_1(x, \mu)$ is sizable [104]; in the backward rapidity region $x \sim 0.05$ for $p_T \sim 15$ GeV where $h_1(x, \mu)$ is very small.

4.2 Back-to-back electron-jet production with longitudinally polarized Λ in jet

For exclusive jet production, we choose to study back-to-back electron-jet production in deep inelastic ep scattering:

$$e(\ell, \lambda_e) + p(P, S) \rightarrow e(\ell') + [\text{jet}(p_J)h(z_h, \mathbf{j}_\perp, S_h)] + X, \quad (4.24)$$

where ℓ and ℓ' are the momenta of the incident and scattered lepton respectively. The incident electron could carry a helicity λ_e and the scattered lepton is assumed to be unpolarized but with a transverse momentum ℓ'_T . Here we use P and S to represent the momentum and polarization of the incoming proton, and the jet has a momentum p_J with transverse component \mathbf{p}_T . The hadron inside the jet has a transverse momentum \mathbf{j}_\perp with respect to the jet axis and collinear momentum fraction z_h of the jet, as well as a polarization S_h with respect to the jet axis. The kinematics is shown in Fig. 8. In the back-to-back region where $|\mathbf{q}_T| \ll |\mathbf{p}_T|$ with the transverse momentum imbalance $\mathbf{q}_T \equiv \ell'_T + \mathbf{p}_T$, TMD factorization formalism for the full differential cross section has been given in the previous publication [41], where various structure functions were defined and studied. For example, the structure function $F_{UU,U}^{\cos(\phi_q-\hat{\phi}_h)}$ for π^\pm -in-jet production is sensitive to Boer-Mulder function and Collins function, while $F_{UU,T}^{\cos(\hat{\phi}_h-\hat{\phi}_{S_h})}$ from Λ -in-jet production has the sensitivity to the polarizing TMD FFs D_{1T}^\perp . At the same time, in [93], the structure function $F_{TU,U}^{\sin(\phi_S-\hat{\phi}_h)}$ is computed for $\pi^{+/-}$ -in-jet production, and is found to be able to further constrain the Collins FFs.

In this section, we studied yet another observable - the spin asymmetry $A_{TU,L}^{\cos(\phi_q-\phi_S)}$ defined as

$$A_{TU,L}^{\cos(\phi_q-\phi_S)} \equiv \frac{F_{TU,L}^{\cos(\phi_q-\phi_S)}}{F_{UU,U}}, \quad (4.25)$$

where the structure $F_{TU,L}^{\cos(\phi_q-\phi_S)}$ in the numerator denotes the spin-dependent structure functions, with T , U and L being the polarization of incoming proton, incoming electron, and the final-state hadron inside the jet, respectively. Here, ϕ_S is the angle between the transverse spin of the incoming proton \mathbf{S}_T and the x -axis, while ϕ_q is the azimuthal angle between the transverse momentum imbalance \mathbf{q}_T and the x -axis, see Fig. 8. Following [41],

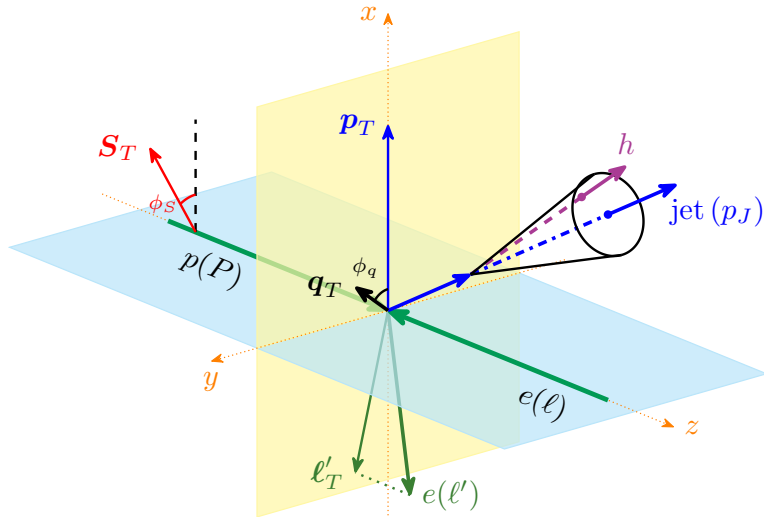


Figure 8: Illustration for the distribution of hadrons inside jets in the collisions of a polarized proton and an unpolarized lepton. For a detailed illustration of jet and hadron kinematics, please see Fig. 3.

this structure function can be factorized as follows:

$$F_{TU,L}^{\cos(\phi_q - \phi_s)}(z_h, j_\perp) = \hat{\sigma}_0 H(Q, \mu) \sum_q e_q^2 \mathcal{G}_{1L}^{h/q}(z_h, \mathbf{j}_\perp, p_T R, \mu, \zeta_J) \times \int \frac{b^2 db}{2\pi} J_1(q_T b) x M \tilde{g}_{1T}^{(1)q}(x, \mathbf{b}, \mu, \zeta) \bar{S}_{\text{global}}(b^2, \mu) \bar{S}_{\text{cs}}(b^2, R, \mu), \quad (4.26)$$

where the global soft function \bar{S}_{global} and the collinear-soft function \bar{S}_{cs} are given in [41]. The bar in $\bar{S}_{\text{global/cs}}$ indicates that their dependence on azimuthal angle is averaged. $\hat{\sigma}_0$ is the partonic cross section of electron-quark scattering:

$$\hat{\sigma}_0 = \frac{\alpha_{\text{em}} \alpha_s}{\hat{s} Q^2} \frac{2(\hat{u}^2 + \hat{s}^2)}{\hat{t}^2}, \quad (4.27)$$

with the Mandelstam variables $\hat{s} \equiv (xP + \ell)^2$, $\hat{t} \equiv (\ell - \ell')^2$ and $\hat{u} \equiv (xP - \ell')^2$, where x is the fraction of collinear momentum carried by the parton inside the incoming proton. The electromagnetic and strong coupling constants are denoted as α_{em} and α_s , and the virtuality of the exchanged photon is defined as $Q^2 \equiv -(\ell - \ell')^2 = -\hat{t}$.

It is evident from Eq. (4.26) that this spin asymmetry $A_{TU,L}^{\cos(\phi_q - \phi_s)}$ has sensitivity on both “worm-gear” TMD PDFs $\tilde{g}_{1T}^q(x, \mathbf{b}, \mu, \zeta)$, as well as the longitudinally polarized exclusive TMD FJFs $\mathcal{G}_{1L}(z_h, \mathbf{j}_\perp, p_T R, \mu, \zeta_J)$ in Eq. (3.76), which is connected to the helicity TMD FFs $G_{1L}^{h/q}$. The observable describes the following scattering process: a longitudinally polarized quark inside the transversely polarized proton (as denoted by the TMD PDFs g_{1T}^q) scatters with an unpolarized electron and then initiates a jet in which a longitudinally polarized hadron is observed. To generate a prediction, for the first moment of “worm-gear” distribution $\tilde{g}_{1T}^{(1)q}$, we adopt its parameterization in \mathbf{k}_\perp -space from [109], and Fourier

transform it to the conjugate \mathbf{b} -space:

$$\tilde{g}_{1T}^{(1)q}(x, \mathbf{b}, \mu, \zeta) = \frac{2\pi}{M^2} \int dk_{\perp} \frac{k_{\perp}^2}{b} J_1(k_{\perp} b) g_{1T}^q(x, \mathbf{k}_{\perp}^2) = g_{1T}^{(1)q}(x) \exp\left(-\frac{1}{4} b^2 \langle k_{\perp}^2 \rangle_{g_{1T}^q}\right), \quad (4.28)$$

where $M \approx 938.272$ MeV is the proton mass and $g_{1T}^{(1)q}(x)$ is the collinear function that is parameterized at $Q_0 = 2$ GeV [109]. Note that this is a simple parton model extraction without TMD evolution, we thus also do not take into account TMD evolution for \tilde{g}_{1T}^q . Since CT10 PDFs [110] are used in the extraction of \tilde{g}_{1T}^q , we will use them in the computation of $F_{UU,U}$ as well. For the final-state hadron, we observe the longitudinally polarized $\Lambda/\bar{\Lambda}$ production. The corresponding helicity TMD FFs is given by:

$$\tilde{G}_{1L}^{\Lambda/q}(z_h, \mathbf{b}, \mu, \zeta_J) = G_{1L}^{\Lambda/q}(z_h, \mu_{b_*}) \exp\left[\int_{\mu_{b_*}}^{\mu} \frac{d\mu'}{\mu'} \gamma_{\mu}^i[\alpha_s(\mu), \zeta_J/\mu^2]\right] S_{NP}^q(b, Q_0, \sqrt{\zeta_J}), \quad (4.29)$$

where we use the TMD evolution in Eq. (3.34) and we assume the non-perturbative Sudakov is the same as the unpolarized case in Eq. (4.2) [111]. For the collinear helicity FFs for $\Lambda/\bar{\Lambda}$, we take the parameterizations from [112], in which three scenarios are provided, each with a different assumption for the source of contribution to Λ longitudinal polarization. Specifically,

- Scenario 1: only polarized s quark contributes;
- Scenario 2: u and d quarks have equal contributions, while the distribution of s quark has an opposite sign relative to u and d quarks; u and d helicity FFs are negative
- Scenario 3: u , d , and s quarks have the same distribution functions, which are all positive.

With the above setup, we are able to make predictions for the exclusive process $ep \rightarrow e + \text{jet}(\Lambda/\bar{\Lambda}) + X$, in which we measure the longitudinal polarization of the final state $\Lambda/\bar{\Lambda}$ inside the jet. In Fig. 9, we plot the spin asymmetry $A_{TU,L}^{\cos(\phi_q - \phi_S)}$ defined in Eq. (4.25) with EIC kinematics, where $\sqrt{s} = 105$ GeV, jet transverse momentum $p_T \in (10, 15)$ GeV, and jet radius parameter $R = 0.6$. We also introduce the quantity event inelasticity $y = 1 - \frac{\ell'_T}{\sqrt{s}} e^{-y_e} \in (0.1, 0.9)$, where ℓ'_T and y_e are the measured transverse momentum and rapidity of the scattered electron. Constraining the event inelasticity ensures that our calculation stays in the region with reasonable resolution on x and Q^2 , as well as avoiding the phase where QED radiative corrections are important [93]. On the left panel, we plot $A_{TU,L}^{\cos(\phi_q - \phi_S)}$ as a function of hadron transverse momentum j_{\perp} , while on the right panel, we plot the same spin asymmetry as a function of the electron-jet transverse momentum imbalance q_T . For the j_{\perp} -distribution (left), q_T is chosen to be 0.5 GeV, while for the q_T -distribution (right), j_{\perp} is chosen to be 0.5 GeV. The uncertainty band is obtained by computing the $1\text{-}\sigma$ band of the fitted parameters for the ‘‘worm-gear’’ PDFs g_{1T} , and the three scenarios for the helicity fragmentation functions of $\Lambda/\bar{\Lambda}$ are shown by blue (scenario 1), red (scenario 2) and green (scenario 3). We collectively denote $\Lambda/\bar{\Lambda}$ as Λ .

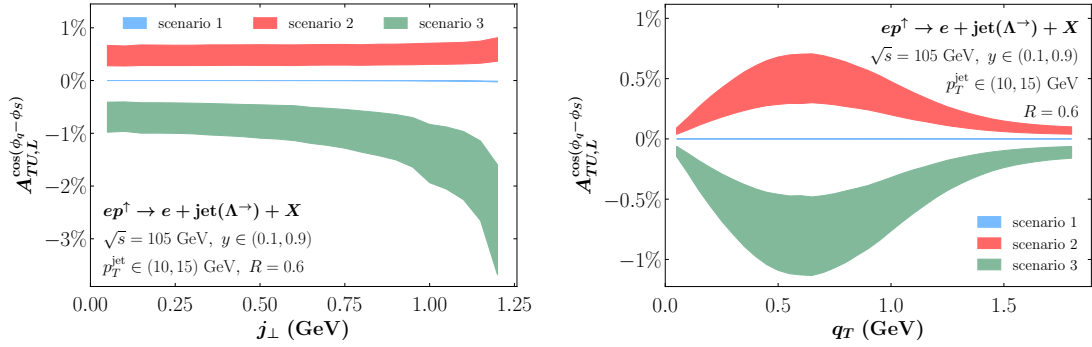


Figure 9: Longitudinally polarized hadron j_{\perp} -distribution (left) and q_T -distribution (right) within jets in ep collisions at $\sqrt{s} = 105$ GeV. The event inelasticity y is constrained within $(0.1, 0.9)$. Jets are detected with transverse momentum $p_T \in (10, 15)$ GeV, and are reconstructed using the anti- k_T algorithm with $R = 0.6$. For the j_{\perp} -distribution, q_T is chosen to be 0.5 GeV, while for the q_T -distribution, j_{\perp} is chosen to be 0.5 GeV. The uncertainty band is obtained by computing the $1\text{-}\sigma$ band of the fitted parameters for the “worm-gear” PDFs g_{1T} , and the three scenarios for $\Lambda/\bar{\Lambda}$ are shown by blue (scenario 1), red (scenario 2) and green (scenario 3). We collectively denote $\Lambda/\bar{\Lambda}$ as Λ . Scenario 1 is consistent with zero because the current extraction of the strange quark worm-gear function is zero.

As can be inferred from Fig. 9, the different scenarios for helicity FFs provided in [112] can result in drastically different values in $A_{TU,L}^{\cos(\phi_q - \phi_s)}$. Notably, Scenario 1 is consistent with zero because only the s quark helicity FFs contribute in this scenario. However, the current extraction of the “worm-gear” function $g_{1T}^{(1)q}(x)$ of the incident proton receives contributions solely from u and d quarks, and the s quark worm-gear function vanish [109]. As for Scenarios 2 and 3, distinct measurable asymmetries emerge with different signs, simply because in Scenario 2, both u and d helicity FFs are both negative, while they are positive in Scenario 3. This observable thus enables the discrimination of previously indistinguishable helicity fragmentation functions for $\Lambda/\bar{\Lambda}$ from different quark flavors.

5 Conclusion

The study of fragmenting jet functions (FJFs) has become a topic of paramount importance in high-energy physics, particularly at the LHC and RHIC, where measurements have been made for a broad range of identified particles within jets. These studies not only provide crucial information at the LHC and RHIC, but also hold the potential to yield novel insights at the upcoming Electron-Ion Collider (EIC).

It is thus important to study both longitudinal and transverse momentum distribution of hadrons inside the jet, which are characterized by the so-called semi-inclusive fragmenting jet functions and exclusive fragmenting jet functions. They are critical ingredients in the factorization theorems. The semi-inclusive fragmenting jet functions arise in the situation *e.g.*, single inclusive jet production in proton-proton or electron-proton collisions, while the exclusive fragmenting jet functions appear in the situation *e.g.*, back-to-back electron-jet

production in electron-proton collisions. There have been partial results available in previous publications, but never the complete full results, which we set up to do in this paper. In this work, we have studied the hadron longitudinal momentum fraction z_h distribution, as well as the hadron transverse momentum j_\perp distribution within jets, for both semi-inclusive and exclusive fragmenting jet functions. We set up factorization formalism within SCET framework that allows for the systematic determination of these distributions. We first calculated all the components of the factorization theorem up to NLO, then we resummed all the associated large logarithms $\ln R$ and $\ln(p_T R/j_\perp)$.

In the phenomenology for semi-inclusive process, we study the transverse polarization of Lambda hyperons inside the jet produced in transversely polarized proton-proton collisions, which is sensitive to the elusive TMD transversity fragmentation functions. Our numerical estimate shows that this observable is promising at the RHIC. For the exclusive jet production process, we study the longitudinal polarization of Lambda hyperon inside the jet, in the back-to-back electron-jet production in electron-proton collisions where the proton is transversely polarized. We find that this observable is sensitive to the ‘‘worm-gear’’ TMD PDF g_{1T} and the TMD helicity fragmentation functions and its measurement is promising at the future EIC. With the various applications for probing the 3D QCD structures, the future for fragmenting jet observables is promising with all the planned measurements at the RHIC and the EIC.

Acknowledgments

We thank Y. He, H. Wang and S. Yang for useful discussions. H.X. and Y.Z. are supported by the Guangdong Major Project of Basic and Applied Basic Research No. 2020B0301030008, No. 2022A1515010683, the National Natural Science Foundation of China under Grants No. 12022512, No. 12035007. Z.K. is supported by the National Science Foundation under Grant No. PHY-1945471. F.Z. is supported by U.S. Department of Energy, Office of Science, Office of Nuclear Physics under grant Contract Number DESC0011090 and U.S. Department of Energy, Office of Science, National Quantum Information Science Research Centers, Co-design Center for Quantum Advantage (C2QA) under Contract No. DESC0012704.

A Perturbative NLO semi-inclusive FJFs

As defined in Section 2.1.1, we have the leading order and one-loop bare semi-inclusive FJFs for longitudinally and transversely polarized quarks and gluons. To get the final expression as given in Eqs. (2.22) to (2.25) and (2.27), we first perform the q_\perp integral:

$$\int \frac{dq_\perp^2}{(q_\perp^2)^{1+\epsilon}} \Theta_{\text{both}}^{\text{anti-}k_T}(q_\perp) = \frac{-1}{\epsilon} \left(\omega_J^2 \tan^2\left(\frac{\mathcal{R}}{2}\right) \right)^{-\epsilon} z_h^{-2\epsilon} (1-z_h)^{-2\epsilon}, \quad (\text{A.1})$$

$$\int \frac{dq_\perp^2}{(q_\perp^2)^{1+\epsilon}} \Theta_j^{\text{anti-}k_T}(q_\perp) = \frac{1}{\epsilon} \left(\omega_J^2 \tan^2\left(\frac{\mathcal{R}}{2}\right) \right)^{-\epsilon} (1-z)^{-2\epsilon}, \quad (\text{A.2})$$

then apply the following expansions as $\epsilon \rightarrow 0$:

$$\frac{1}{(1-z)^{1+2\epsilon}} = \frac{-1}{2\epsilon} \delta(1-z) + \frac{1}{(1-z)_+} - 2\epsilon \left(\frac{\ln(1-z)}{(1-z)} \right)_+ + \mathcal{O}(\epsilon^2), \quad (\text{A.3})$$

$$\frac{1}{z^{2\epsilon}} = 1 - 2\epsilon \ln(z) + \mathcal{O}(\epsilon^2), \quad (\text{A.4})$$

$$\left(\frac{e^{\gamma_E} \mu^2}{\omega_J^2 \tan^2\left(\frac{\mathcal{R}}{2}\right)} \right)^\epsilon \frac{1}{\Gamma(1-\epsilon)} = 1 + L\epsilon + \frac{1}{12}(6L^2 - \pi^2)\epsilon^2 + \mathcal{O}(\epsilon^3), \quad (\text{A.5})$$

where $L \equiv \ln\left(\frac{\mu^2}{\omega_J^2 \tan^2\left(\frac{\mathcal{R}}{2}\right)}\right) = \ln\left(\frac{\mu^2}{(p_T R)^2}\right)$.

B Calculation of collinear exclusive FJFs

In this section, we provide the derivation for the matching coefficients $\Delta_{(T)} \mathcal{J}_{ij}$ of the exclusive fragmenting jet functions $\Delta_{(T)} \mathcal{G}_i^h(z_h, p_T R, \mu)$ to the collinear fragmentation function $\Delta_{(T)} D_i^h(z_h, \mu)$ for anti- k_T jets. The unpolarized results were first written down in the appendix of [72]. We start by specifying the phase space constraint from the jet algorithm, which was nicely outlined in [64]. Consider a parton splitting process, $i(\ell) \rightarrow j(q) + k(\ell - q)$, where an incoming parton i with momentum ℓ splits into a parton j with momentum q and a parton k with momentum $\ell - q$. The four-vector ℓ^μ can be decomposed in light-cone coordinates as $\ell^\mu = (\ell^+, \ell^- = \omega, 0_\perp)$ where $\ell^\pm = \ell^0 \mp \ell^z$. The constraint for anti- k_T algorithm with radius R is given by:

$$\Theta^{\text{anti-}k_T} = \theta\left(\tan^2\left(\frac{\mathcal{R}}{2}\right) - \frac{q^+ \omega^2}{q^-(\omega - \ell^-)^2}\right). \quad (\text{B.1})$$

For fragmenting jet functions, the above constraint leads to a constraint on the jet invariant mass $m_J^2 = \omega \ell^+$ [74], which is derived and listed as follows:

$$\delta_{\text{anti-}k_T} = \theta\left(z_h(1-z_h)\omega^2 \tan^2\left(\frac{\mathcal{R}}{2}\right) - m_J^2\right) \theta(m_J^2), \quad (\text{B.2})$$

where $z_h = \omega_h/\omega_J = \omega_h/\omega$, ω_h is the large light-cone momentum of the final hadron, and $\omega = \omega_J$ since both partons are in the jet (see Fig. 2 (A)).

The exclusive FJFs $\Delta_{(T)} \mathcal{G}_i^h(z_h, p_T R, \mu)$ can be matched onto corresponding fragmentation functions $\Delta_{(T)} D_i^h(z_h, \mu)$ as listed in Table 3:

$$\begin{aligned} \Delta_{(T)} \mathcal{G}_i^h(z_h, p_T R, \mu) &= \sum_j \int_{z_h}^1 \frac{dz'_h}{z'_h} \Delta_{(T)} \mathcal{J}_{ij}(z'_h, p_T R, \mu) \Delta_{(T)} D_{h/j}\left(\frac{z_h}{z'_h}, \mu\right) \\ &+ \mathcal{O}\left(\frac{\Lambda_{\text{QCD}}^2}{(p_T R)^2}\right), \end{aligned} \quad (\text{B.3})$$

where $\Delta_{(T)} \mathcal{J}_{ij}$ are the matching coefficients. The exclusive FJFs $\Delta_{(T)} \mathcal{G}_i^j(z_h, m_J^2, \mu)$ with $i, j \in \{q, g\}$ has been extensively studied in [31, 113]. Using pure dimensional regularization

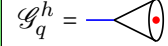

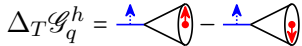
		Quark polarization		
		U	L	T
Hadron pol.	U	$\mathcal{G}_q^h =$ 		
	L		$\Delta \mathcal{G}_q^h =$ 	
	T			$\Delta_T \mathcal{G}_q^h =$ 

Table 3: Summary of the exclusive collinear FJFs. The header row represents the polarization of the quark (indicated by the blue line) that initiates the jet, while the header column indicates the corresponding polarizations of produced hadrons (indicated by the red arrow from the red dot). Shown here is for quark FJFs, with U , L , T representing the unpolarized case, and longitudinal and transverse polarization. For gluon FJFs, one would interpret L , T , as circular and linear polarization.

with $4 - 2\epsilon$ dimensions in the $\overline{\text{MS}}$ scheme, the bare results at $\mathcal{O}(\alpha_s)$ can be written in the following compact form [33, 113, 114]:

$$\Delta_{(T)\mathcal{G}_{i,\text{bare}}^j}(z_h, m_J^2) = \frac{\alpha_s (e^{\gamma_E} \mu^2)^\epsilon}{2\pi \Gamma(1-\epsilon)} \Delta_{(T)\hat{P}_{ji}}(z_h, \epsilon) z_h^{-\epsilon} (1-z_h)^{-\epsilon} (m_J^2)^{-1-\epsilon}. \quad (\text{B.4})$$

Generalized from [33], $\Delta_{(T)\mathcal{G}_{i,\text{bare}}^j}(z_h, m_J^2, \mu)$ is related to $\Delta_{(T)\mathcal{G}_{i,\text{bare}}^h}(z_h, p_T R, \mu)$ by:

$$\Delta_{(T)\mathcal{G}_{i,\text{bare}}^h}(z_h, p_T R) = \int dm_J^2 \Delta_{(T)\mathcal{G}_{i,\text{bare}}^h}(z_h, m_J^2) \delta_{\text{anti-}k_T}, \quad (\text{B.5})$$

notice that we reinstated hadronic FJFs. The splitting functions $\Delta_{(T)\hat{P}_{ji}}(z_h, \epsilon)$ are given in Eqs. (2.17) to (2.21). By performing the integration over m_J^2 with the constraints imposed by the jet algorithm $\delta_{\text{anti-}k_T}$, one obtains the bare exclusive FJFs $\Delta_{(T)\mathcal{G}_{i,\text{bare}}^j}(z_h, p_T R)$. We present the results for anti- k_T jets here, as their explicit expressions are not available in the literature:

$$\begin{aligned} \Delta_{\mathcal{G}_{q,\text{bare}}^q}(z_h, p_T R) &= \frac{\alpha_s}{2\pi} \left\{ C_F \left(\frac{1}{\epsilon^2} + \frac{3}{2\epsilon} + \frac{L}{\epsilon} \right) \delta(1-z_h) - \frac{1}{\epsilon} \Delta P_{qq}(z_h) + C_F(1-z_h) \right. \\ &\quad + C_F \delta(1-z_h) \left(\frac{L^2}{2} - \frac{\pi^2}{12} \right) + \Delta P_{qq}(z_h) (2 \ln(z_h) - L) \\ &\quad \left. + \frac{3C_F L}{2} \delta(1-z_h) + 2C_F (1+z_h^2) \left(\frac{\ln(1-z_h)}{1-z_h} \right)_+ \right\}, \end{aligned} \quad (\text{B.6})$$

$$\Delta_{\mathcal{G}_{q,\text{bare}}^g}(z_h, p_T R) = \frac{\alpha_s}{2\pi} \left\{ \frac{-1}{\epsilon} \Delta P_{gq}(z_h) + \Delta P_{gq}(z_h) \left[2 \ln(z_h(1-z_h)) - L \right] - 2C_F(1-z_h) \right\}, \quad (\text{B.7})$$

$$\Delta_{g,\text{bare}}^{\mathcal{G}^q}(z_h, p_T R) = \frac{\alpha_s}{2\pi} \left\{ \frac{-1}{\epsilon} \Delta P_{qg}(z_h) + \Delta P_{qg}(z_h) [2 \ln(z_h(1-z_h)) - L] + 2T_F(1-z_h) \right\}, \quad (\text{B.8})$$

$$\begin{aligned} \Delta_{g,\text{bare}}^{\mathcal{G}^g}(z_h, p_T R) &= \frac{\alpha_s}{2\pi} \left\{ C_A \left(\frac{1}{\epsilon^2} + \frac{1}{\epsilon} \frac{\beta_0}{2C_A} + \frac{L}{\epsilon} \right) \delta(1-z_h) - \frac{1}{\epsilon} \Delta P_{gg}(z_h) \right. \\ &\quad + C_A \delta(1-z_h) \left(\frac{L^2}{2} - \frac{\pi^2}{12} \right) + \Delta P_{gg}(z_h) (2 \ln(z_h) - L) + \frac{\beta_0 L}{2} \delta(1-z_h) \\ &\quad \left. - 4C_A(1-z_h) + 4C_A [2(1-z_h)^2 + z_h] \left(\frac{\ln(1-z_h)}{1-z_h} \right)_+ \right\}, \quad (\text{B.9}) \end{aligned}$$

$$\begin{aligned} \Delta_{Tq,\text{bare}}^{\mathcal{G}^q}(z_h, p_T R) &= \frac{\alpha_s}{2\pi} \left\{ C_F \left(\frac{1}{\epsilon^2} + \frac{3}{2\epsilon} + \frac{L}{\epsilon} \right) \delta(1-z_h) - \frac{1}{\epsilon} \Delta_T P_{qq}(z_h) \right. \\ &\quad + C_F \delta(1-z_h) \left(\frac{L^2}{2} - \frac{\pi^2}{12} \right) + \Delta_T P_{qq}(z_h) (2 \ln(z_h) - L) \\ &\quad \left. + \frac{3C_F L}{2} \delta(1-z_h) + 4C_F z_h \left(\frac{\ln(1-z_h)}{1-z_h} \right)_+ \right\}, \quad (\text{B.10}) \end{aligned}$$

where, as given in the main text, β_0 is defined as:

$$\beta_0 \equiv \frac{11}{3} C_A - \frac{4}{3} T_F n_f \quad (\text{B.11})$$

and $\Delta_{(T)P_{ji}}(z_h)$ are given in Eqs. (2.28) to (2.32). It is instructive to point out that the ϵ poles in the first term of Eqs. (B.6), (B.9) and (B.10) correspond to ultraviolet (UV) divergences, and they are related to the renormalization of the FJFs $\Delta_{(T)\mathcal{G}_{i,\text{bare}}^j}(z_h, p_T R)$. All the remaining ϵ poles in Eqs. (B.6) to (B.10) are infrared (IR) poles, and they match exactly with those in the fragmentation functions $\Delta_{(T)D_{j/i}}(z_h, \mu)$, which we will show below. $\Delta_{(T)\mathcal{G}_{i,\text{bare}}^h}(z_h, p_T R)$ is renormalized by:

$$\Delta_{(T)\mathcal{G}_{i,\text{bare}}^h}(z_h, p_T R) = \mathcal{Z}_{\mathcal{G}}^i(\mu) \Delta_{(T)\mathcal{G}_i^h}(z_h, p_T R, \mu), \quad (\text{B.12})$$

where i is not summed over in the above equation. The corresponding renormalization group (RG) equation is:

$$\mu \frac{d}{d\mu} \Delta_{(T)\mathcal{G}_i^h}(z_h, p_T R, \mu) = \gamma_{\mathcal{G}}^i(\mu) \Delta_{(T)\mathcal{G}_i^h}(z_h, p_T R, \mu), \quad (\text{B.13})$$

where the anomalous dimension $\gamma_{\mathcal{G}}^i(\mu)$ is:

$$\gamma_{\mathcal{G}}^i(\mu) = -(\mathcal{Z}_{\mathcal{G}}^i(\mu))^{-1} \mu \frac{d}{d\mu} \mathcal{Z}_{\mathcal{G}}^i(\mu). \quad (\text{B.14})$$

The solution to Eq. (B.14) is then:

$$\Delta_{(T)\mathcal{G}_i^h}(z_h, p_T R, \mu) = \Delta_{(T)\mathcal{G}_i^h}(z_h, p_T R, \mu_{\mathcal{G}}) \exp\left(\int_{\mu_{\mathcal{G}}}^{\mu} \frac{d\mu'}{\mu'} \gamma_{\mathcal{G}}^i(\mu') \right), \quad (\text{B.15})$$

where the scale $\mu_{\mathcal{G}}$ should be the characteristic scale chosen such that large logarithms in the fixed-order calculation vanish. The counter terms $\mathcal{Z}_{\mathcal{G}}^i(\mu)$ are given by⁵:

$$\mathcal{Z}_{\mathcal{G}}^q(\mu) = 1 + \frac{\alpha_s}{2\pi} C_F \left[\frac{1}{\epsilon^2} + \frac{3}{2\epsilon} + \frac{L}{\epsilon} \right], \quad (\text{B.16})$$

$$\mathcal{Z}_{\mathcal{G}}^g(\mu) = 1 + \frac{\alpha_s}{2\pi} C_A \left[\frac{1}{\epsilon^2} + \frac{1}{\epsilon} \frac{\beta_0}{2C_A} + \frac{L}{\epsilon} \right]. \quad (\text{B.17})$$

From these results we obtain the anomalous dimension $\gamma_{\mathcal{G}}^i(\mu)$ with the following form:

$$\gamma_{\mathcal{G}}^i(\mu) = \Gamma_{\text{cusp}}^i(\alpha_s) \ln \left(\frac{\mu^2}{(p_T R)^2} \right) + \gamma^i(\alpha_s), \quad (\text{B.18})$$

where $\Gamma_{\text{cusp}}^i = \sum_n \Gamma_{n-1}^i \left(\frac{\alpha_s}{4\pi} \right)^n$ and $\gamma^i = \sum_n \gamma_{n-1}^i \left(\frac{\alpha_s}{4\pi} \right)^n$. The lowest-order coefficients can be extracted from the above calculations:

$$\Gamma_0^q = 4C_F, \quad \gamma_0^q = 6C_F, \quad (\text{B.19})$$

$$\Gamma_0^g = 4C_A, \quad \gamma_0^g = 2\beta_0, \quad (\text{B.20})$$

and higher-order results can be found in [31, 86, 115–117]. After the subtraction of the UV counter terms in Eqs. (B.16) and (B.17), the renormalized FJFs $\Delta_{(T)} \mathcal{G}_i^j(\omega, R, z_h, \mu)$ are given by:

$$\begin{aligned} \Delta \mathcal{G}_q^q(z_h, p_T R, \mu) &= \frac{\alpha_s}{2\pi} \left\{ \frac{-1}{\epsilon} \Delta P_{qq}(z_h) + C_F \delta(1-z_h) \left(\frac{L^2}{2} - \frac{\pi^2}{12} \right) + C_F(1-z_h) \right. \\ &\quad \left. + \Delta P_{qq}(z_h)(2 \ln(z_h) - L) + \frac{3C_F L}{2} \delta(1-z_h) \right. \\ &\quad \left. + 2C_F(1+z_h^2) \left(\frac{\ln(1-z_h)}{1-z_h} \right)_+ \right\}, \end{aligned} \quad (\text{B.21})$$

$$\Delta \mathcal{G}_q^g(z_h, p_T R, \mu) = \frac{\alpha_s}{2\pi} \left\{ \frac{-1}{\epsilon} \Delta P_{gq}(z_h) + \Delta P_{gq}(z_h) \left[2 \ln(z_h(1-z_h)) - L \right] - 2C_F(1-z_h) \right\}, \quad (\text{B.22})$$

$$\Delta \mathcal{G}_g^q(z_h, p_T R, \mu) = \frac{\alpha_s}{2\pi} \left\{ \frac{-1}{\epsilon} \Delta P_{qg}(z_h) + \Delta P_{qg}(z_h) \left[2 \ln(z_h(1-z_h)) - L \right] + 2T_F(1-z_h) \right\}, \quad (\text{B.23})$$

$$\begin{aligned} \Delta \mathcal{G}_g^g(z_h, p_T R, \mu) &= \frac{\alpha_s}{2\pi} \left\{ \frac{-1}{\epsilon} \Delta P_{gg}(z_h) + C_A \delta(1-z_h) \left(\frac{L^2}{2} - \frac{\pi^2}{12} \right) \right. \\ &\quad \left. + \Delta P_{gg}(z_h)(2 \ln(z_h) - L) + \frac{\beta_0 L}{2} \delta(1-z_h) - 4C_A(1-z_h) \right. \\ &\quad \left. + 4C_A \left[2(1-z_h)^2 + z_h \right] \left(\frac{\ln(1-z_h)}{1-z_h} \right)_+ \right\}, \end{aligned} \quad (\text{B.24})$$

$$\Delta_T \mathcal{G}_q^q(z_h, p_T R, \mu) = \frac{\alpha_s}{2\pi} \left\{ \frac{-1}{\epsilon} \Delta_T P_{qq}(z_h) + C_F \delta(1-z_h) \left(\frac{L^2}{2} - \frac{\pi^2}{12} \right) + \frac{3C_F L}{2} \delta(1-z_h) \right\}$$

⁵Note here the counter terms for polarized quark and gluon FJFs are the same as those of the unpolarized ones as shown in [33]. For explanation, see the main text in Section 2.2.

$$+ \Delta_T P_{qq}(z_h)(2 \ln(z_h) - L) + 4C_F z_h \left(\frac{\ln(1-z_h)}{1-z_h} \right)_+ \Big\}, \quad (\text{B.25})$$

where we can eliminate all large logarithms L by choosing $\mu \sim p_T R$. At the intermediate scale $\mu_g \gg \Lambda_{\text{QCD}}$, one can match the FJFs $\Delta_{(T)} \mathcal{G}_i^h(z_h, p_T R, \mu)$ onto the longitudinally (transversely) polarized fragmentation functions $\Delta_{(T)} D_{h/j}(z_h, \mu)$ as in Eq. (B.3). In order to perform the matching calculation and determine the coefficients \mathcal{J}_{ij} , we simply need the perturbative results of the fragmentation functions $\Delta_{(T)} D_{j/i}(z_h, \mu)$ for a parton i fragmenting into a parton j . The renormalized $\Delta_{(T)} D_{j/i}(z_h, \mu)$ at $\mathcal{O}(\alpha_s)$ using pure dimensional regularization are given by:

$$\Delta D_q^q(z_h, \mu) = \delta(1-z_h) + \frac{\alpha_s C_F}{2\pi} \left(-\frac{1}{\epsilon} \right) \Delta P_{qq}(z_h), \quad (\text{B.26})$$

$$\Delta D_q^g(z_h, \mu) = \frac{\alpha_s C_F}{2\pi} \left(-\frac{1}{\epsilon} \right) \Delta P_{gq}(z_h), \quad (\text{B.27})$$

$$\Delta D_g^q(z_h, \mu) = \frac{\alpha_s T_F}{2\pi} \left(-\frac{1}{\epsilon} \right) \Delta P_{qg}(z_h), \quad (\text{B.28})$$

$$\Delta D_g^g(z_h, \mu) = \delta(1-z_h) + \frac{\alpha_s C_A}{2\pi} \left(-\frac{1}{\epsilon} \right) \Delta P_{gg}(z_h), \quad (\text{B.29})$$

$$\Delta_T D_q^q(z_h, \mu) = \delta(1-z_h) + \frac{\alpha_s C_F}{2\pi} \left(-\frac{1}{\epsilon} \right) \Delta_T P_{qq}(z_h). \quad (\text{B.30})$$

Using the results for $\Delta_{(T)} \mathcal{G}_i^j(z_h, p_T R, \mu)$ and $\Delta_{(T)} D_{j/i}(z_h, \mu)$, we obtain the following matching coefficients:

$$\begin{aligned} \Delta \mathcal{J}_{qq}(z_h, p_T R, \mu) = & \delta(1-z_h) + \frac{\alpha_s}{2\pi} \left[C_F \delta(1-z_h) \left(\frac{L^2}{2} - \frac{\pi^2}{12} \right) + C_F(1-z_h) - \Delta P_{qq}(z_h)L \right. \\ & \left. + \frac{3C_F L}{2} \delta(1-z_h) + \Delta \hat{\mathcal{J}}_{qq}^{\text{anti-}k_T}(z_h) \right], \end{aligned} \quad (\text{B.31})$$

$$\Delta \mathcal{J}_{qg}(z_h, p_T R, \mu) = \frac{\alpha_s}{2\pi} \left[-\Delta P_{gq}(z_h)L - 2C_F(1-z_h) + \Delta \hat{\mathcal{J}}_{qg}^{\text{anti-}k_T}(z_h) \right], \quad (\text{B.32})$$

$$\Delta \mathcal{J}_{gq}(z_h, p_T R, \mu) = \frac{\alpha_s}{2\pi} \left[-\Delta P_{qg}(z_h)L + 2T_F(1-z_h) + \Delta \hat{\mathcal{J}}_{gq}^{\text{anti-}k_T}(z_h) \right], \quad (\text{B.33})$$

$$\begin{aligned} \Delta \mathcal{J}_{gg}(z_h, p_T R, \mu) = & \delta(1-z_h) + \frac{\alpha_s}{2\pi} \left[C_A \delta(1-z_h) \left(\frac{L^2}{2} - \frac{\pi^2}{12} \right) - 4C_A(1-z_h) - \Delta P_{gg}(z_h)L \right. \\ & \left. + \frac{\beta_0 L}{2} \delta(1-z_h) + \Delta \hat{\mathcal{J}}_{gg}^{\text{anti-}k_T}(z_h) \right], \end{aligned} \quad (\text{B.34})$$

$$\begin{aligned} \Delta_T \mathcal{J}_{qq}(z_h, p_T R, \mu) = & \delta(1-z_h) + \frac{\alpha_s}{2\pi} \left[C_F \delta(1-z_h) \left(\frac{L^2}{2} - \frac{\pi^2}{12} \right) - \Delta_T P_{qq}(z_h)L \right. \\ & \left. + \frac{3C_F L}{2} \delta(1-z_h) + \Delta_T \hat{\mathcal{J}}_q^{\text{anti-}k_T} \right], \end{aligned} \quad (\text{B.35})$$

where $\Delta_{(T)} \hat{\mathcal{J}}_{ij}^{\text{anti-}k_T}(z_h)$ are jet-algorithm dependent. For anti- k_T jets, we have:

$$\Delta \hat{\mathcal{J}}_{qq}^{\text{anti-}k_T}(z_h) = 2\Delta P_{qq}(z_h) \ln(z_h) + 2C_F(1+z_h^2) \left(\frac{\ln(1-z_h)}{1-z_h} \right)_+, \quad (\text{B.36})$$

$$\Delta \hat{\mathcal{J}}_{gq}^{\text{anti-}k_T}(z_h) = 2\Delta P_{gq}(z_h) \left[\ln(z_h(1-z_h)) \right], \quad (\text{B.37})$$

$$\Delta \hat{\mathcal{J}}_{gq}^{\text{anti-}k_T}(z_h) = 2\Delta P_{gq}(z_h) \left[\ln(z_h(1-z_h)) \right], \quad (\text{B.38})$$

$$\Delta \hat{\mathcal{J}}_{gg}^{\text{anti-}k_T}(z_h) = 2\Delta P_{gg}(z_h) \ln(z_h) + 4C_A \left[2(1-z_h)^2 + z_h \right] \left(\frac{\ln(1-z_h)}{1-z_h} \right)_+, \quad (\text{B.39})$$

$$\Delta_T \hat{\mathcal{J}}_{qq}^{\text{anti-}k_T}(z_h) = 2\Delta_T P_{qq}(z_h) \ln(z_h) + 4C_F z_h \left(\frac{\ln(1-z_h)}{1-z_h} \right)_+. \quad (\text{B.40})$$

Substituting the matching coefficients $\Delta_{(T)} \mathcal{J}_{ij}$ into Eq. (B.3), and writing out explicitly the plus functions, one obtains:

$$\Delta_{(T)} \mathcal{G}_q^h(z_h, p_T R, \mu) = \left\{ 1 + \frac{\alpha_s}{2\pi} C_F \left[2 \ln^2 \left(\frac{p_T R(1-z_h)}{\mu} \right) - \frac{\pi^2}{12} \right] \right\} \Delta_{(T)} D_q^h(z_h, \mu) + \dots, \quad (\text{B.41})$$

$$\Delta \mathcal{G}_g^h(z_h, p_T R, \mu) = \left\{ 1 + \frac{\alpha_s}{2\pi} C_A \left[2 \ln^2 \left(\frac{p_T R(1-z_h)}{\mu} \right) - \frac{\pi^2}{12} \right] \right\} \Delta D_g^h(z_h, \mu) + \dots. \quad (\text{B.42})$$

Here the ellipses represent terms that are regular as $z_h \rightarrow 1$. Under the large z_h limit, one can find additional logarithms $\sim \ln(1-z_h)$. By choosing the scale $\mu = p_T R(1-z_h)$, we can simultaneously resum both logarithms of R and $(1-z_h)$ [74]. A more rigorous resummation at the threshold limit is given by [118].

C Separation of hard matching functions

In this work we follow the methodology outlined in [23] and separately evolve the hard matching functions. Doing this have the benefit of simplifying the final evolution of the TMD FJFs, for more details, please refer to [23]. In this section, we will only provide the result of such separation. We start by noticing that the anomalous dimensions $\gamma_{ij}^{L(T)}(z, p_T R, \mu)$ in Eqs. (3.65) to (3.69) include a purely diagonal piece $\delta_{ij} \delta(1-z) \Gamma_i(p_T R, \mu)$ and an off-diagonal Altarelli-Parisi splitting function $\Delta_{(T)} P_{ji}(z)$ that has polarization dependence. Therefore following the approach in [23], we can separate these two contributions by rewriting the functions $\hat{H}_{i \rightarrow j}^{U(L,T)}$ into two parts that follow different evolution equations:

$$\hat{H}_{i \rightarrow j}^{U(L,T)}(z, p_T R, \mu) = \mathcal{E}_i(p_T R, \mu) \hat{\mathcal{C}}_{i \rightarrow j}^{U(L,T)}(z, p_T R, \mu). \quad (\text{C.1})$$

The coefficients $\hat{\mathcal{C}}_{i \rightarrow j}^{U(L,T)}(z, p_T R, \mu)$ follow the evolution equations governed by the Altarelli-Parisi splitting functions:

$$\mu \frac{d}{d\mu} \hat{\mathcal{C}}_{i \rightarrow j}^U(z, p_T R, \mu) = \frac{\alpha_s}{2\pi} \sum_k \int_z^1 \frac{dz'}{z'} P_{ki} \left(\frac{z}{z'} \right) \hat{\mathcal{C}}_{k \rightarrow j}^U(z', p_T R, \mu), \quad (\text{C.2})$$

$$\mu \frac{d}{d\mu} \hat{\mathcal{C}}_{i \rightarrow j}^{L(T)}(z, p_T R, \mu) = \frac{\alpha_s}{2\pi} \sum_k \int_z^1 \frac{dz'}{z'} \Delta_{(T)} P_{ki} \left(\frac{z}{z'} \right) \hat{\mathcal{C}}_{k \rightarrow j}^{L(T)}(z', p_T R, \mu), \quad (\text{C.3})$$

and as pointed out in [23], although the above evolution equations look like DGLAP equations, it is only the combined TMD FJFs that will satisfy the standard timelike DGLAP

evolution equations. As for the functions $\mathcal{E}_i(p_T R, \mu)$, they follow the multiplicative RG equations:

$$\mu \frac{d}{d\mu} \ln \mathcal{E}_i(p_T R, \mu) = \Gamma_i(p_T R, \mu), \quad (\text{C.4})$$

with Γ_i given in Eq. (3.71) and their solutions are:

$$\mathcal{E}_i(p_T R, \mu) = \mathcal{E}_i(p_T R, \mu_J) \exp\left(\int_{\mu_J}^{\mu} \frac{d\mu'}{\mu'} \Gamma_i(p_T R, \mu')\right), \quad (\text{C.5})$$

with the fixed-order results provided in [23]. By choosing $\mu_J = p_T R$, we obtain the initial condition $\mathcal{E}_i(p_T R, \mu_J) = 1$ for the evolution given in Eq. (C.4).

Collecting the results, for unpolarized hard matching function $\hat{H}_{i \rightarrow j}^U(z', p_T R, \mu)$, one find the coefficients $\hat{\mathcal{C}}_{i \rightarrow j}^U(z, p_T R, \mu)$ in Eq. (C.1) to be the same as in [23], here we list the results for completeness:

$$\hat{\mathcal{C}}_{q \rightarrow q'}^U(z, p_T R, \mu) = \delta_{qq'} \delta(1-z) + \delta_{qq'} \frac{\alpha_s}{2\pi} \left[C_F \delta(1-z) \frac{\pi^2}{12} + P_{qq}(z) L - 2C_F(1+z^2) \left(\frac{\ln(1-z)}{1-z} \right)_+ - C_F(1-z) \right], \quad (\text{C.6})$$

$$\hat{\mathcal{C}}_{q \rightarrow g}^U(z, p_T R, \mu) = \frac{\alpha_s}{2\pi} [(L - 2 \ln(1-z)) P_{gq}(z) - C_F z], \quad (\text{C.7})$$

$$\hat{\mathcal{C}}_{g \rightarrow g}^U(z, p_T R, \mu) = \delta(1-z) + \frac{\alpha_s}{2\pi} \left[\delta(1-z) \frac{\pi^2}{12} + P_{gg}(z) L - \frac{4C_A(1-z+z^2)^2}{z} \left(\frac{\ln(1-z)}{1-z} \right)_+ \right], \quad (\text{C.8})$$

$$\hat{\mathcal{C}}_{g \rightarrow q}^U(z, p_T R, \mu) = \frac{\alpha_s}{2\pi} [(L - 2 \ln(1-z)) P_{gq}(z) - 2T_F z(1-z)]. \quad (\text{C.9})$$

As for the coefficients of polarized functions $\hat{H}_{i \rightarrow j}^{L(T)}(z, p_T R, \mu)$, given that $\mathcal{E}_i(p_T R, \mu)$ follow the same evolution as in Eq. (C.4), we can write Eq. (C.1) as:

$$\hat{H}_{i \rightarrow j}^{L(T)}(z, p_T R, \mu) = \exp\left(\int_{\mu_J}^{\mu} \frac{d\mu'}{\mu'} \Gamma_i(p_T R, \mu')\right) \hat{\mathcal{C}}_{i \rightarrow j}^{L(T)}(z, p_T R, \mu). \quad (\text{C.10})$$

And we therefore only need to evolve the functions $\hat{\mathcal{C}}_{i \rightarrow j}^{L(T)}(z, p_T R, \mu)$ from scale $\mu \sim \mu_J = p_T R$ to $\mu \sim p_T$ following Eq. (C.3). In particular, the fixed-order results are:

$$\hat{\mathcal{C}}_{q \rightarrow q'}^L(z, p_T R, \mu) = \delta_{qq'} \delta(1-z) + \delta_{qq'} \frac{\alpha_s}{2\pi} \left[C_F \delta(1-z) \frac{\pi^2}{12} + \Delta P_{qq}(z) L - 2C_F(1+z^2) \left(\frac{\ln(1-z)}{1-z} \right)_+ - C_F(1-z) \right], \quad (\text{C.11})$$

$$\hat{\mathcal{C}}_{q \rightarrow g}^L(z, p_T R, \mu) = \frac{\alpha_s}{2\pi} [(L - 2 \ln(1-z)) \Delta P_{gq}(z) + 2C_F(1-z)], \quad (\text{C.12})$$

$$\hat{\mathcal{C}}_{g \rightarrow q}^L(z, p_T R, \mu) = \frac{\alpha_s}{2\pi} [(L - 2 \ln(1-z)) \Delta P_{gq}(z) - 2T_F(1-z)], \quad (\text{C.13})$$

$$\hat{\mathcal{C}}_{g \rightarrow g}^L(z, p_T R, \mu) = \delta(1-z) + \frac{\alpha_s}{2\pi} \left[C_A \delta(1-z) \frac{\pi^2}{12} + \Delta P_{gg}(z) L \right]$$

$$+ 4C_A(1-z) - 4C_A(2(1-z)^2 + z) \left(\frac{\ln(1-z)}{1-z} \right)_+ \Big], \quad (\text{C.14})$$

$$\begin{aligned} \hat{\mathcal{C}}_{q \rightarrow q'}^T(z, p_T R, \mu) &= \delta_{qq'} \delta(1-z) \\ &+ \delta_{qq'} \frac{\alpha_s}{2\pi} \left\{ \Delta_T P_{qq}(z) L + C_F \left[-4z \left(\frac{\ln(1-z)}{1-z} \right)_+ + \frac{\pi^2}{12} \delta(1-z) \right] \right\}. \quad (\text{C.15}) \end{aligned}$$

So far, we have presented the perturbative expressions for polarized hard matching functions in Eq. (C.10) up to NLO.

References

- [1] J. M. Butterworth, A. R. Davison, M. Rubin, and G. P. Salam, *Jet substructure as a new Higgs search channel at the LHC*, *Phys. Rev. Lett.* **100** (2008) 242001, [[arXiv:0802.2470](#)].
- [2] P. Newman and M. Wing, *The Hadronic Final State at HERA*, *Rev. Mod. Phys.* **86** (2014), no. 3 1037, [[arXiv:1308.3368](#)].
- [3] R. Kogler et al., *Jet Substructure at the Large Hadron Collider: Experimental Review*, *Rev. Mod. Phys.* **91** (2019), no. 4 045003, [[arXiv:1803.06991](#)].
- [4] A. J. Larkoski, I. Moult, and B. Nachman, *Jet Substructure at the Large Hadron Collider: A Review of Recent Advances in Theory and Machine Learning*, *Phys. Rept.* **841** (2020) 1–63, [[arXiv:1709.04464](#)].
- [5] M. Connors, C. Nattrass, R. Reed, and S. Salur, *Jet measurements in heavy ion physics*, *Rev. Mod. Phys.* **90** (2018) 025005, [[arXiv:1705.01974](#)].
- [6] L. Cunqueiro and A. M. Sickles, *Studying the QGP with Jets at the LHC and RHIC*, *Prog. Part. Nucl. Phys.* **124** (2022) 103940, [[arXiv:2110.14490](#)].
- [7] R. Belmont et al., *Predictions for the sPHENIX physics program*, in *RBRC Workshop: Predictions for sPHENIX*, 5, 2023. [[arXiv:2305.15491](#)].
- [8] R. Abdul Khalek et al., *Science Requirements and Detector Concepts for the Electron-Ion Collider: EIC Yellow Report*, *Nucl. Phys. A* **1026** (2022) 122447, [[arXiv:2103.05419](#)].
- [9] R. Abdul Khalek et al., *Snowmass 2021 White Paper: Electron Ion Collider for High Energy Physics*, [[arXiv:2203.13199](#)].
- [10] E. C. Aschenauer, I. Borsa, R. Sassot, and C. Van Hulse, *Semi-inclusive Deep-Inelastic Scattering, Parton Distributions and Fragmentation Functions at a Future Electron-Ion Collider*, *Phys. Rev. D* **99** (2019), no. 9 094004, [[arXiv:1902.10663](#)].
- [11] B. Wang, J. O. Gonzalez-Hernandez, T. C. Rogers, and N. Sato, *Large Transverse Momentum in Semi-Inclusive Deeply Inelastic Scattering Beyond Lowest Order*, *Phys. Rev. D* **99** (2019), no. 9 094029, [[arXiv:1903.01529](#)].
- [12] **Jefferson Lab Angular Momentum (JAM) Collaboration**, R. M. Whitehill, Y. Zhou, N. Sato, and W. Melnitchouk, *Accessing gluon polarization with high-PT hadrons in SIDIS*, *Phys. Rev. D* **107** (2023), no. 3 034033, [[arXiv:2210.12295](#)].
- [13] R. Boussarie et al., *TMD Handbook*, [[arXiv:2304.03302](#)].
- [14] **LHCb Collaboration**, *Multidifferential study of identified charged hadron distributions in Z-tagged jets in proton-proton collisions at $\sqrt{s}=13$ TeV*, [[arXiv:2208.11691](#)].

- [15] **ATLAS** Collaboration, M. Aaboud et al., *Measurement of jet fragmentation in 5.02 TeV proton-lead and proton-proton collisions with the ATLAS detector*, *Nucl. Phys. A* **978** (2018) 65, [[arXiv:1706.02859](#)].
- [16] **ATLAS** Collaboration, M. Aaboud et al., *Comparison of Fragmentation Functions for Jets Dominated by Light Quarks and Gluons from pp and Pb+Pb Collisions in ATLAS*, *Phys. Rev. Lett.* **123** (2019), no. 4 042001, [[arXiv:1902.10007](#)].
- [17] **ATLAS** Collaboration, G. Aad et al., *Measurement of the jet fragmentation function and transverse profile in proton-proton collisions at a center-of-mass energy of 7 TeV with the ATLAS detector*, *Eur. Phys. J. C* **71** (2011) 1795, [[arXiv:1109.5816](#)].
- [18] **CMS** Collaboration, S. Chatrchyan et al., *Measurement of Jet Fragmentation in PbPb and pp Collisions at $\sqrt{s_{NN}} = 2.76$ TeV*, *Phys. Rev. C* **90** (2014), no. 2 024908, [[arXiv:1406.0932](#)].
- [19] **ALICE** Collaboration, *Exploring the non-universality of charm hadronisation through the measurement of the fraction of jet longitudinal momentum carried by Λ_c^+ baryons in pp collisions*, [[arXiv:2301.13798](#)].
- [20] J. Collins, *Foundations of perturbative QCD*, vol. 32. Cambridge University Press, 11, 2013.
- [21] Z.-B. Kang, F. Ringer, and I. Vitev, *Jet substructure using semi-inclusive jet functions in SCET*, *JHEP* **11** (2016) 155, [[arXiv:1606.07063](#)].
- [22] D. P. Anderle, T. Kaufmann, M. Stratmann, F. Ringer, and I. Vitev, *Using hadron-in-jet data in a global analysis of D^* fragmentation functions*, *Phys. Rev. D* **96** (2017), no. 3 034028, [[arXiv:1706.09857](#)].
- [23] Z.-B. Kang, X. Liu, F. Ringer, and H. Xing, *The transverse momentum distribution of hadrons within jets*, *JHEP* **11** (2017) 068, [[arXiv:1705.08443](#)].
- [24] F. Arleo, M. Fontannaz, J.-P. Guillet, and C. L. Nguyen, *Probing fragmentation functions from same-side hadron-jet momentum correlations in p-p collisions*, *JHEP* **04** (2014) 147, [[arXiv:1311.7356](#)].
- [25] T. Kaufmann, A. Mukherjee, and W. Vogelsang, *Hadron Fragmentation Inside Jets in Hadronic Collisions*, *Phys. Rev. D* **92** (2015), no. 5 054015, [[arXiv:1506.01415](#)]. [Erratum: *Phys.Rev.D* 101, 079901 (2020)].
- [26] L. Dai, C. Kim, and A. K. Leibovich, *Fragmentation of a Jet with Small Radius*, *Phys. Rev. D* **94** (2016), no. 11 114023, [[arXiv:1606.07411](#)].
- [27] Z.-B. Kang, K. Lee, J. Terry, and H. Xing, *Jet fragmentation functions for Z-tagged jets*, *Phys. Lett. B* **798** (2019) 134978, [[arXiv:1906.07187](#)].
- [28] S.-L. Zhang, H. Xing, and B.-W. Zhang, *Hadron productions and jet substructures associated with Z^0/γ in Pb+Pb collisions at the LHC*, [[arXiv:2209.15336](#)].
- [29] C. Liu, X. Shen, B. Zhou, and J. Gao, *Automated calculation of jet fragmentation at NLO in QCD*, *JHEP* **09** (2023) 108, [[arXiv:2305.14620](#)].
- [30] M. Procura and I. W. Stewart, *Quark Fragmentation within an Identified Jet*, *Phys. Rev. D* **81** (2010) 074009, [[arXiv:0911.4980](#)]. [Erratum: *Phys.Rev.D* 83, 039902 (2011)].
- [31] A. Jain, M. Procura, and W. J. Waalewijn, *Parton Fragmentation within an Identified Jet at NNLL*, *JHEP* **05** (2011) 035, [[arXiv:1101.4953](#)].

- [32] A. Jain, M. Procura, and W. J. Waalewijn, *Fully-Unintegrated Parton Distribution and Fragmentation Functions at Perturbative k_T* , *JHEP* **04** (2012) 132, [[arXiv:1110.0839](#)].
- [33] Y.-T. Chien, Z.-B. Kang, F. Ringer, I. Vitev, and H. Xing, *Jet fragmentation functions in proton-proton collisions using soft-collinear effective theory*, *JHEP* **05** (2016) 125, [[arXiv:1512.06851](#)].
- [34] Z.-B. Kang, K. Lee, and F. Zhao, *Polarized jet fragmentation functions*, *Phys. Lett. B* **809** (2020) 135756, [[arXiv:2005.02398](#)].
- [35] R. Bain, Y. Makris, and T. Mehen, *Transverse Momentum Dependent Fragmenting Jet Functions with Applications to Quarkonium Production*, *JHEP* **11** (2016) 144, [[arXiv:1610.06508](#)].
- [36] Y. Makris, D. Neill, and V. Vaidya, *Probing Transverse-Momentum Dependent Evolution With Groomed Jets*, *JHEP* **07** (2018) 167, [[arXiv:1712.07653](#)].
- [37] D. Neill, A. Papaefstathiou, W. J. Waalewijn, and L. Zoppi, *Phenomenology with a recoil-free jet axis: TMD fragmentation and the jet shape*, *JHEP* **01** (2019) 067, [[arXiv:1810.12915](#)].
- [38] A. Bacchetta and P. J. Mulders, *Deep inelastic leptonproduction of spin-one hadrons*, *Phys. Rev. D* **62** (2000) 114004, [[hep-ph/0007120](#)].
- [39] P. J. Mulders and J. Rodrigues, *Transverse momentum dependence in gluon distribution and fragmentation functions*, *Phys. Rev. D* **63** (2001) 094021, [[hep-ph/0009343](#)].
- [40] A. Metz and A. Vossen, *Parton Fragmentation Functions*, *Prog. Part. Nucl. Phys.* **91** (2016) 136–202, [[arXiv:1607.02521](#)].
- [41] Z.-B. Kang, K. Lee, D. Y. Shao, and F. Zhao, *Spin asymmetries in electron-jet production at the future electron ion collider*, *JHEP* **11** (2021) 005, [[arXiv:2106.15624](#)].
- [42] Z.-B. Kang, J. Terry, A. Vossen, Q. Xu, and J. Zhang, *Transverse Lambda production at the future Electron-Ion Collider*, *Phys. Rev. D* **105** (2022), no. 9 094033, [[arXiv:2108.05383](#)].
- [43] F. Zhao, *3D Imaging via Polarized Jet Fragmentation Functions and Quantum Simulation of the QCD Phase Diagram*, other thesis, 9, 2023.
- [44] A. Bacchetta, M. Radici, and L. Rossi, *Analogies between hadron-in-jet and dihadron fragmentation*, *Phys. Rev. D* **108** (2023), no. 1 014005, [[arXiv:2303.04314](#)].
- [45] Y.-T. Chien, A. Deshpande, M. M. Mondal, and G. Sterman, *Probing hadronization with flavor correlations of leading particles in jets*, *Phys. Rev. D* **105** (2022), no. 5 L051502, [[arXiv:2109.15318](#)].
- [46] D. Neill, I. Scimemi, and W. J. Waalewijn, *Jet axes and universal transverse-momentum-dependent fragmentation*, *JHEP* **04** (2017) 020, [[arXiv:1612.04817](#)].
- [47] D. Gutierrez-Reyes, I. Scimemi, W. J. Waalewijn, and L. Zoppi, *Transverse momentum dependent distributions in e^+e^- and semi-inclusive deep-inelastic scattering using jets*, *JHEP* **10** (2019) 031, [[arXiv:1904.04259](#)].
- [48] Y. Makris, *Revisiting the role of grooming in DIS*, *Phys. Rev. D* **103** (2021), no. 5 054005, [[arXiv:2101.02708](#)].
- [49] Y. Makris and V. Vaidya, *Transverse Momentum Spectra at Threshold for Groomed Heavy Quark Jets*, *JHEP* **10** (2018) 019, [[arXiv:1807.09805](#)].

- [50] D. Gutierrez-Reyes, Y. Makris, V. Vaidya, I. Scimemi, and L. Zoppi, *Probing Transverse-Momentum Distributions With Groomed Jets*, *JHEP* **08** (2019) 161, [[arXiv:1907.05896](#)].
- [51] A. Gao, H. T. Li, I. Moulton, and H. X. Zhu, *Precision QCD Event Shapes at Hadron Colliders: The Transverse Energy-Energy Correlator in the Back-to-Back Limit*, *Phys. Rev. Lett.* **123** (2019), no. 6 062001, [[arXiv:1901.04497](#)].
- [52] H. T. Li, I. Vitev, and Y. J. Zhu, *Transverse-Energy-Energy Correlations in Deep Inelastic Scattering*, *JHEP* **11** (2020) 051, [[arXiv:2006.02437](#)].
- [53] Z.-B. Kang, K. Lee, D. Y. Shao, and F. Zhao, *Probing Transverse Momentum Dependent Structures with Azimuthal Dependence of Energy Correlators*, [arXiv:2310.15159](#).
- [54] C. W. Bauer, S. Fleming, and M. E. Luke, *Summing Sudakov logarithms in $B \rightarrow X_s \gamma$ in effective field theory*, *Phys. Rev. D* **63** (2000) 014006, [[hep-ph/0005275](#)].
- [55] C. W. Bauer, S. Fleming, D. Pirjol, and I. W. Stewart, *An Effective field theory for collinear and soft gluons: Heavy to light decays*, *Phys. Rev. D* **63** (2001) 114020, [[hep-ph/0011336](#)].
- [56] C. W. Bauer and I. W. Stewart, *Invariant operators in collinear effective theory*, *Phys. Lett. B* **516** (2001) 134–142, [[hep-ph/0107001](#)].
- [57] C. W. Bauer, D. Pirjol, and I. W. Stewart, *Soft collinear factorization in effective field theory*, *Phys. Rev. D* **65** (2002) 054022, [[hep-ph/0109045](#)].
- [58] C. W. Bauer, S. Fleming, D. Pirjol, I. Z. Rothstein, and I. W. Stewart, *Hard scattering factorization from effective field theory*, *Phys. Rev. D* **66** (2002) 014017, [[hep-ph/0202088](#)].
- [59] Z.-B. Kang, F. Ringer, and I. Vitev, *The semi-inclusive jet function in SCET and small radius resummation for inclusive jet production*, *JHEP* **10** (2016) 125, [[arXiv:1606.06732](#)].
- [60] R. von Kuk, J. K. L. Michel, and Z. Sun, *Transverse momentum distributions of heavy hadrons and polarized heavy quarks*, *JHEP* **09** (2023) 205, [[arXiv:2305.15461](#)].
- [61] L. Dai, C. Kim, and A. K. Leibovich, *Heavy Quark Jet Fragmentation*, *JHEP* **09** (2018) 109, [[arXiv:1805.06014](#)].
- [62] M. Cacciari, G. P. Salam, and G. Soyez, *The anti- k_t jet clustering algorithm*, *JHEP* **04** (2008) 063, [[arXiv:0802.1189](#)].
- [63] V. Barone and P. G. Ratcliffe, *Transverse spin physics*. 2003.
- [64] S. D. Ellis, C. K. Vermilion, J. R. Walsh, A. Hornig, and C. Lee, *Jet Shapes and Jet Algorithms in SCET*, *JHEP* **11** (2010) 101, [[arXiv:1001.0014](#)].
- [65] Z.-B. Kang, F. Ringer, and W. J. Waalewijn, *The Energy Distribution of Subjets and the Jet Shape*, *JHEP* **07** (2017) 064, [[arXiv:1705.05375](#)].
- [66] W. Vogelsang, *The Spin dependent two loop splitting functions*, *Nucl. Phys. B* **475** (1996) 47–72, [[hep-ph/9603366](#)].
- [67] W. Vogelsang, *Next-to-leading order evolution of transversity distributions and Soffer’s inequality*, *Phys. Rev. D* **57** (1998) 1886–1894, [[hep-ph/9706511](#)].
- [68] G. Altarelli and G. Parisi, *Asymptotic Freedom in Parton Language*, *Nucl. Phys. B* **126** (1977) 298–318.
- [69] Z.-B. Kang, K. Lee, D. Y. Shao, and J. Terry, *The Sivers Asymmetry in Hadronic Dijet Production*, *JHEP* **02** (2021) 066, [[arXiv:2008.05470](#)].

- [70] M.-S. Gao, Z.-B. Kang, D. Y. Shao, J. Terry, and C. Zhang, *QCD resummation of dijet azimuthal decorrelations in pp and pA collisions*, *JHEP* **10** (2023) 013, [[arXiv:2306.09317](#)].
- [71] X. Liu, F. Ringer, W. Vogelsang, and F. Yuan, *Lepton-jet Correlations in Deep Inelastic Scattering at the Electron-Ion Collider*, *Phys. Rev. Lett.* **122** (2019), no. 19 192003, [[arXiv:1812.08077](#)].
- [72] W. J. Waalewijn, *Calculating the Charge of a Jet*, *Phys. Rev. D* **86** (2012) 094030, [[arXiv:1209.3019](#)].
- [73] M. Baumgart, A. K. Leibovich, T. Mehen, and I. Z. Rothstein, *Probing Quarkonium Production Mechanisms with Jet Substructure*, *JHEP* **11** (2014) 003, [[arXiv:1406.2295](#)].
- [74] M. Procura and W. J. Waalewijn, *Fragmentation in Jets: Cone and Threshold Effects*, *Phys. Rev. D* **85** (2012) 114041, [[arXiv:1111.6605](#)].
- [75] J.-y. Chiu, A. Jain, D. Neill, and I. Z. Rothstein, *The Rapidity Renormalization Group*, *Phys. Rev. Lett.* **108** (2012) 151601, [[arXiv:1104.0881](#)].
- [76] J.-Y. Chiu, A. Jain, D. Neill, and I. Z. Rothstein, *A Formalism for the Systematic Treatment of Rapidity Logarithms in Quantum Field Theory*, *JHEP* **05** (2012) 084, [[arXiv:1202.0814](#)].
- [77] M. G. A. Buffing, Z.-B. Kang, K. Lee, and X. Liu, *A transverse momentum dependent framework for back-to-back photon+jet production*, [[arXiv:1812.07549](#)].
- [78] M. A. Ebert, I. W. Stewart, and Y. Zhao, *Towards Quasi-Transverse Momentum Dependent PDFs Computable on the Lattice*, *JHEP* **09** (2019) 037, [[arXiv:1901.03685](#)].
- [79] I. Moutl, H. X. Zhu, and Y. J. Zhu, *The four loop QCD rapidity anomalous dimension*, *JHEP* **08** (2022) 280, [[arXiv:2205.02249](#)].
- [80] C. Duhr, B. Mistlberger, and G. Vita, *Four-Loop Rapidity Anomalous Dimension and Event Shapes to Fourth Logarithmic Order*, *Phys. Rev. Lett.* **129** (2022), no. 16 162001, [[arXiv:2205.02242](#)].
- [81] P. Shanahan, M. Wagman, and Y. Zhao, *Lattice QCD calculation of the Collins-Soper kernel from quasi-TMDPDFs*, *Phys. Rev. D* **104** (2021), no. 11 114502, [[arXiv:2107.11930](#)].
- [82] **LPC** Collaboration, M.-H. Chu et al., *Nonperturbative determination of the Collins-Soper kernel from quasitransverse-momentum-dependent wave functions*, *Phys. Rev. D* **106** (2022), no. 3 034509, [[arXiv:2204.00200](#)].
- [83] **Lattice Parton (LPC)** Collaboration, M.-H. Chu et al., *Lattice calculation of the intrinsic soft function and the Collins-Soper kernel*, *JHEP* **08** (2023) 172, [[arXiv:2306.06488](#)].
- [84] H.-T. Shu, M. Schlemmer, T. Sizmann, A. Vladimirov, L. Walter, M. Engelhardt, A. Schäfer, and Y.-B. Yang, *Universality of the Collins-Soper kernel in lattice calculations*, *Phys. Rev. D* **108** (2023), no. 7 074519, [[arXiv:2302.06502](#)].
- [85] A. Avkhadiev, P. Shanahan, M. Wagman, and Y. Zhao, *Collins-Soper kernel from lattice QCD at the physical pion mass*, [[arXiv:2307.12359](#)].
- [86] T. Becher, M. Neubert, and B. D. Pecjak, *Factorization and Momentum-Space Resummation in Deep-Inelastic Scattering*, *JHEP* **01** (2007) 076, [[hep-ph/0607228](#)].
- [87] M.-x. Luo, T.-Z. Yang, H. X. Zhu, and Y. J. Zhu, *Unpolarized quark and gluon TMD PDFs and FFs at N³LO*, *JHEP* **06** (2021) 115, [[arXiv:2012.03256](#)].

- [88] M. A. Ebert, B. Mistlberger, and G. Vita, *TMD fragmentation functions at $N^3\text{LO}$* , *JHEP* **07** (2021) 121, [[arXiv:2012.07853](#)].
- [89] D. Gutierrez-Reyes, I. Scimemi, and A. Vladimirov, *Transverse momentum dependent transversely polarized distributions at next-to-next-to-leading-order*, *JHEP* **07** (2018) 172, [[arXiv:1805.07243](#)].
- [90] P. Cal, F. Ringer, and W. J. Waalewijn, *The jet shape at NLL'*, *JHEP* **05** (2019) 143, [[arXiv:1901.06389](#)].
- [91] Z.-B. Kang, A. Prokudin, F. Ringer, and F. Yuan, *Collins azimuthal asymmetries of hadron production inside jets*, *Phys. Lett. B* **774** (2017) 635–642, [[arXiv:1707.00913](#)].
- [92] M. Arratia, Z.-B. Kang, S. J. Paul, A. Prokudin, F. Ringer, and F. Zhao, *Neutrino-tagged jets at the Electron-Ion Collider*, *Phys. Rev. D* **107** (2023), no. 9 094036, [[arXiv:2212.02432](#)].
- [93] M. Arratia, Z.-B. Kang, A. Prokudin, and F. Ringer, *Jet-based measurements of Sivers and Collins asymmetries at the future electron-ion collider*, *Phys. Rev. D* **102** (2020), no. 7 074015, [[arXiv:2007.07281](#)].
- [94] J. C. Collins, D. E. Soper, and G. F. Sterman, *Transverse Momentum Distribution in Drell-Yan Pair and W and Z Boson Production*, *Nucl. Phys. B* **250** (1985) 199–224.
- [95] A. Kulesza, G. F. Sterman, and W. Vogelsang, *Joint resummation in electroweak boson production*, *Phys. Rev. D* **66** (2002) 014011, [[hep-ph/0202251](#)].
- [96] J.-w. Qiu and X.-f. Zhang, *Role of the nonperturbative input in QCD resummed Drell-Yan Q_T distributions*, *Phys. Rev. D* **63** (2001) 114011, [[hep-ph/0012348](#)].
- [97] S. Catani, D. de Florian, G. Ferrera, and M. Grazzini, *Vector boson production at hadron colliders: transverse-momentum resummation and leptonic decay*, *JHEP* **12** (2015) 047, [[arXiv:1507.06937](#)].
- [98] M. A. Ebert and F. J. Tackmann, *Resummation of Transverse Momentum Distributions in Distribution Space*, *JHEP* **02** (2017) 110, [[arXiv:1611.08610](#)].
- [99] P. F. Monni, E. Re, and P. Torrielli, *Higgs Transverse-Momentum Resummation in Direct Space*, *Phys. Rev. Lett.* **116** (2016), no. 24 242001, [[arXiv:1604.02191](#)].
- [100] P. Sun, J. Isaacson, C. P. Yuan, and F. Yuan, *Nonperturbative functions for SIDIS and Drell-Yan processes*, *Int. J. Mod. Phys. A* **33** (2018), no. 11 1841006, [[arXiv:1406.3073](#)].
- [101] M. G. Echevarria, Z.-B. Kang, and J. Terry, *Global analysis of the Sivers functions at $N\text{LO}+\text{NNLL}$ in QCD*, *JHEP* **01** (2021) 126, [[arXiv:2009.10710](#)].
- [102] **STAR** Collaboration, M. Abdallah et al., *Azimuthal transverse single-spin asymmetries of inclusive jets and identified hadrons within jets from polarized pp collisions at $\sqrt{s} = 200$ GeV*, *Phys. Rev. D* **106** (2022), no. 7 072010, [[arXiv:2205.11800](#)].
- [103] **STAR** Collaboration, J. Adam et al., *Transverse spin transfer to Λ and $\bar{\Lambda}$ hyperons in polarized proton-proton collisions at $\sqrt{s} = 200$ GeV*, *Phys. Rev. D* **98** (2018), no. 9 091103, [[arXiv:1808.08000](#)].
- [104] Z.-B. Kang, A. Prokudin, P. Sun, and F. Yuan, *Extraction of Quark Transversity Distribution and Collins Fragmentation Functions with QCD Evolution*, *Phys. Rev. D* **93** (2016), no. 1 014009, [[arXiv:1505.05589](#)].

- [105] **Jefferson Lab Angular Momentum (JAM) Collaboration**, C. Cocuzza, W. Melnitchouk, A. Metz, and N. Sato, *Polarized antimatter in the proton from a global QCD analysis*, *Phys. Rev. D* **106** (2022), no. 3 L031502, [[arXiv:2202.03372](#)].
- [106] D. Callos, Z.-B. Kang, and J. Terry, *Extracting the transverse momentum dependent polarizing fragmentation functions*, *Phys. Rev. D* **102** (2020), no. 9 096007, [[arXiv:2003.04828](#)].
- [107] S. Albino, B. A. Kniehl, and G. Kramer, *Fragmentation functions for $K0(S)$ and Λ with complete quark flavor separation*, *Nucl. Phys. B* **734** (2006) 50–61, [[hep-ph/0510173](#)].
- [108] A. Vogt, *Efficient evolution of unpolarized and polarized parton distributions with QCD-PEGASUS*, *Comput. Phys. Commun.* **170** (2005) 65–92, [[hep-ph/0408244](#)].
- [109] S. Bhattacharya, Z.-B. Kang, A. Metz, G. Penn, and D. Pitonyak, *First global QCD analysis of the TMD $g1T$ from semi-inclusive DIS data*, *Phys. Rev. D* **105** (2022), no. 3 034007, [[arXiv:2110.10253](#)].
- [110] H.-L. Lai, M. Guzzi, J. Huston, Z. Li, P. M. Nadolsky, J. Pumplin, and C. P. Yuan, *New parton distributions for collider physics*, *Phys. Rev. D* **82** (2010) 074024, [[arXiv:1007.2241](#)].
- [111] Y. Koike, J. Nagashima, and W. Vogelsang, *Resummation for polarized semi-inclusive deep-inelastic scattering at small transverse momentum*, *Nucl. Phys. B* **744** (2006) 59–79, [[hep-ph/0602188](#)].
- [112] D. de Florian, M. Stratmann, and W. Vogelsang, *QCD analysis of unpolarized and polarized Λ baryon production in leading and next-to-leading order*, *Phys. Rev. D* **57** (1998) 5811–5824, [[hep-ph/9711387](#)].
- [113] M. Ritzmann and W. J. Waalewijn, *Fragmentation in Jets at NNLO*, *Phys. Rev. D* **90** (2014), no. 5 054029, [[arXiv:1407.3272](#)].
- [114] W. T. Giele and E. W. N. Glover, *Higher order corrections to jet cross-sections in e^+e^- annihilation*, *Phys. Rev. D* **46** (1992) 1980–2010.
- [115] T. Becher and M. D. Schwartz, *Direct photon production with effective field theory*, *JHEP* **02** (2010) 040, [[arXiv:0911.0681](#)].
- [116] M. G. Echevarria, A. Idilbi, A. Schäfer, and I. Scimemi, *Model-Independent Evolution of Transverse Momentum Dependent Distribution Functions (TMDs) at NNLL*, *Eur. Phys. J. C* **73** (2013), no. 12 2636, [[arXiv:1208.1281](#)].
- [117] S. Moch, J. A. M. Vermaseren, and A. Vogt, *The Three loop splitting functions in QCD: The Nonsinglet case*, *Nucl. Phys. B* **688** (2004) 101–134, [[hep-ph/0403192](#)].
- [118] T. Kaufmann, X. Liu, A. Mukherjee, F. Ringer, and W. Vogelsang, *Hadron-in-jet production at partonic threshold*, *JHEP* **02** (2020) 040, [[arXiv:1910.11746](#)].